ΕΘΝΙΚΟ ΚΑΙ ΚΑΠΟΔΙΣΤΡΙΑΚΟ ΠΑΝΕΠΙΣΤΗΜΙΟ ΑΘΗΝΩΝ

ΣΧΟΛΗ ΘΕΤΙΚΩΝ ΕΠΙΣΤΗΜΩΝ

ΤΜΗΜΑ ΓΕΩΛΟΓΙΑΣ & ΓΕΩΠΕΡΙΒΑΛΛΟΝΤΟΣ

MΕΤΑΠΤΥΧΙΑΚΟ ΠΡΟΓΡΑΜΜΑ ΣΠΟΥΔΩΝ

ΤΟΜΕΑΣ ΔΥΝΑΜΙΚΗΣ, ΤΕΚΤΟΝΙΚΗΣ & ΕΦΑΡΜΟΣΜΕΝΗΣ ΓΕΩΛΟΓΙΑΣ

ΔΙΠΛΩΜΑΤΙΚΗ ΕΡΓΑΣΙΑ

# "Morphotectonic analysis on the basis of active faulting and erosional processes in the southwestern Gulf of Corinth"

ΣΙΜΟΥ ΕΙΡΗΝΗ

Α.Μ. 21114

ΑΘΗΝΑ

ΜΑΙΟΣ 2014

NATIONAL AND KAPODISTRIAN UNIVERSITY OF ATHENS

SCHOOL OF SCIENCE

FACULTY OF GEOLOGY & GEOENVIRONMENT

"Morphotectonic analysis on the basis of active faulting and erosional processes in the southwestern Gulf of Corinth"
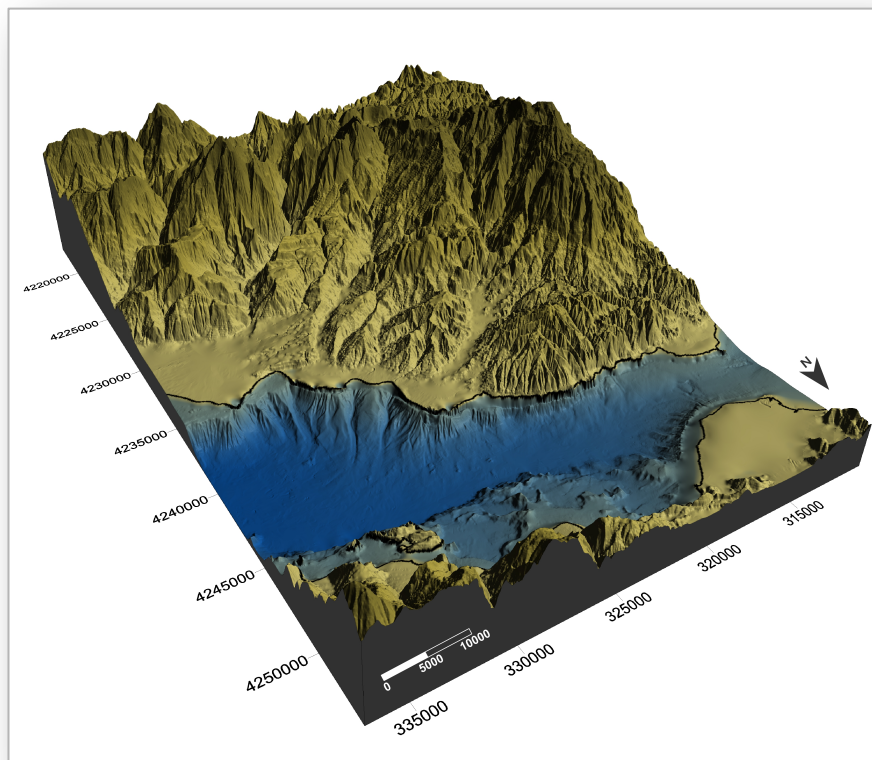
SIMOU EIRINI

Scientific Committee:

PAPANIKOLAOU DIMITRIOS (Professor NKUA, Supervisor)

LYKOUSIS VASILIOS (Researcher A, HCMR)

NOMIKOU PARASKEVI (Lecturer, NKUA)

Athens, May 2014

Preface

The tectonically active landscapes result from a complex interaction of crustal and vertical movements, which act simultaneously with erosional and depositional processes. The geodynamic and geomorphic implications of such active landforms, in combination with the rapid technological advancement (geodetic monitoring, satellite imagery, digital topography, GIS software) can offer valuable information in the understanding of the physical models which are related to surface processes.

High levels of extension, which characterize the rift systems, are mainly responsible for the tectonic control on a currently deforming landscape, such as the Gulf of Corinth. Intense neotectonic activity expressed by large-scale fault structures, analysed with regard to erosion and sediment transport, can lead to the development of a comprehensible conceptual and quantitative model.

The Gulf of Corinth, the northern and most active part of the present-day Corinth Rift, constitutes a natural laboratory for morphotectonic studies as it has been long identified as a site of major importance due to the continuous tectonic deformation. Enduring fault activity, high levels of concentrated seismicity and extensive erosion (often expressed through instabilities and landslide occurrence both in the marine and the terrestrial environment) indicate the active geodynamic regime evolving towards the coastal zone of NW Peloponnese.

As a special interest has been arisen nowadays concerning risk assessment and management, the results of this study could be further evaluated, not only from a geological, but from a geohazard perspective as well.

TABLE OF CONTENTS

1 Introduction

1.1 Continental rifting as a geodynamic process

Continental rifting, as a typical example of extensional tectonics occurring in a wide variety of geotectonic settings, corresponds to linear bands of localized crustal extension. The initial breakup of the continental crust is marked by the inception of a rift system, a tectonic structure that is gradually being transformed into a new ocean basin.

The rift zones, which are structural valleys bounded by extensional normal faults (Leeder, 1995), range in dimensions from a few up to several hundreds of km^2. The axis of the rift lays, more-or-less, perpendicular to the direction of the stress. The typical rift structures refer to down-faulted blocks accommodating central linear depression creating a graben, and up-faulted areas known as horsts. The bounding faults may be planar or listric, and if the displacement is greater on one side they form asymmetric basins referred as half-graben structures (Nichols, 2009). Uplift on the flanks of rifts due to the effect of relative movements on the rift-bounding faults preserves older rift features and creates local sediment sources for rift valleys (syn-rift sedimentation).

There can be several factors conducing to the formation of a rift (including the processes and the thermal structure of the mantle and the mechanical structure of the crust) and two models of rifting, which are known as active and passive rifting, depending on the controlling factor. Rifts created by rising hot mantle material characterize the active rifting model. On the contrary, in the passive rifting models, the formation of the rift is a result of far-field stresses related to plate tectonics.
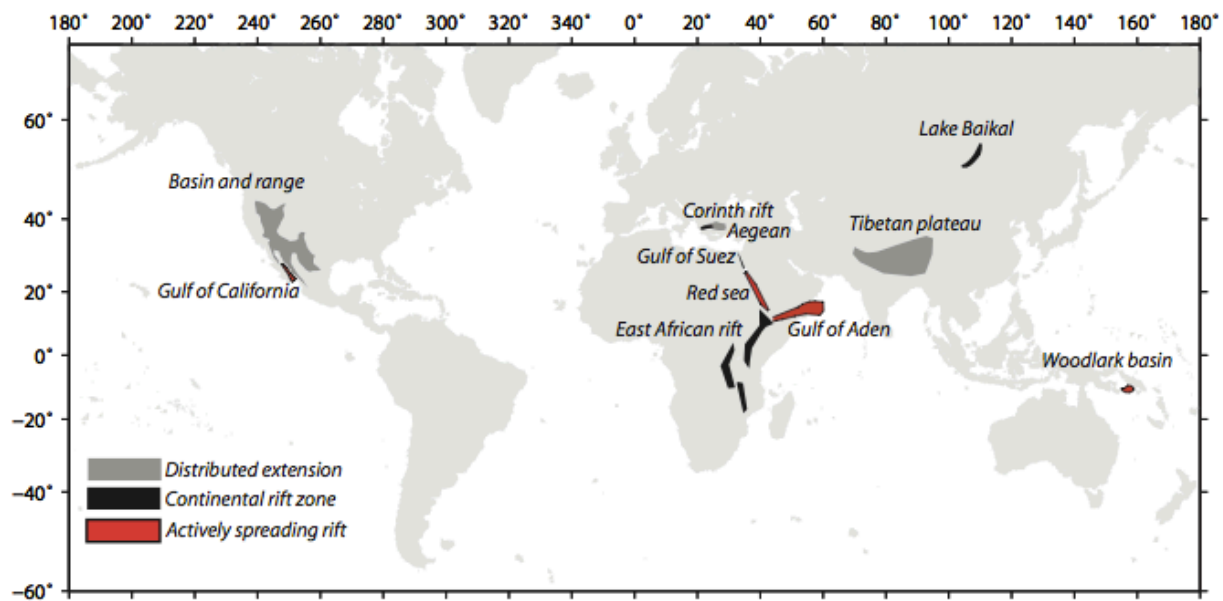
Figure 1.1 Global distribution of currently active continental lithosphere extension (Bell, 2008).

The extensional development of a rift generally follows McKenzie's (1978) 'stretching theory' for the formation of rifted basins. This theory consists of three main stages:

a. The **initial rifting stage** (rift initiation). The upper part of the lithosphere starts to extend and this early extension leads to large-scale, steep fractures, which may reach deep enough and lead to the development of isolated basins (Fig. 1.2a).

b. The **stretching phase** (mature rift stage), which comprises the main stage of the rifting development. During this stage and as the rift evolves, some of the individual fractures grow and become linked together forming major marginal normal faults which contribute to the vertical thinning of the crust and the lateral extension. The fault-related subsidence along the rift axis, as a result of mechanical stretching of the continental lithosphere, causes a significant uplift of the rift sides at this stage, strongly influencing the drainage pattern and the sedimentation in the rift basin (Fig. 1.2b).

c. The **post-rift subsidence and sedimentation stage**. Once rifting ceases, the crust beneath the rift cools and this phase is accompanied by a post-rift subsidence, as a consequence of isostatic balance (Fig. 1.2c).

Figure 1.2 The three stages of rift development:

(a) The early phase of crustal extension.

(b) The stretching phase.

(c) The post rift subsidence and sedimentation phase.

Pre-rift, syn-rift and post-rift sequences indicate the extensional development (Fossen, 2010).

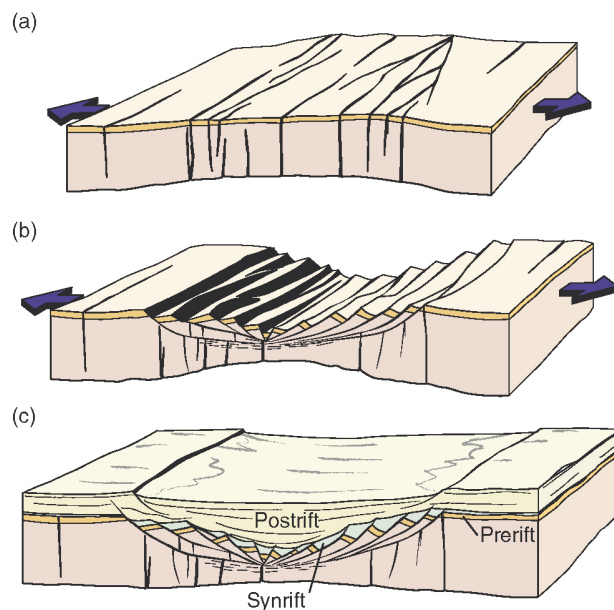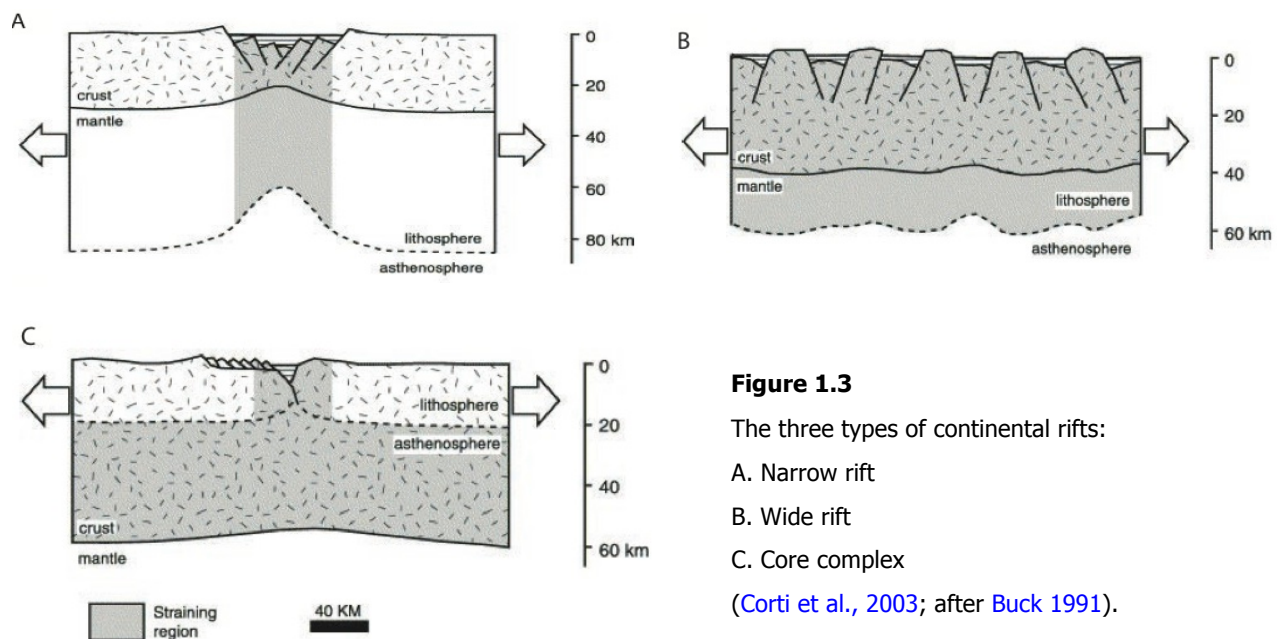The continental rifts can be developed according to three different fundamental types (Fig. 1.3). This classification depends on how the extension distributes in the wider rifting area:

- **Narrow rifts** (e.g. Gulf of Corinth), which are associated with extensive changes to the crustal topography as extension is concentrated in a band of less than 150km.

- **Wide rifts** (e.g. Aegean domain), which are related to extended terrains. In those cases the deformation is concentrated in many individual basins across the deformation field (e.g. Gulf of Corinth), covering a region up to thousands of meters wide.

- **Core complexes**, which characterize rifts related to slow spreading oceanic plate boundaries, which have a limited supply of upwelling magma. The extensional strain in those cases occurs along low-angle detachment faults.

The controls on sedimentation in rift systems are a combination of tectonic factors and climate. The tectonic factors determine the rift flank relief and hence availability of material, as well as the pathways of sediment into the basin while climate influences weathering, water availability for transport and facies in the rift basin (Nichols & Uttamo 2005). As a result, the rift growth is usually reflected by its sedimentary records. The pre-rift sediments refer to a sequence deposited before the onset of rifting, prior to the extension. The syn-rift deposits correspond to the sequences deposited during the main rifting stage. Syn-rift sequences display abrupt thickness changes across the normal faults, they have wedge shaped stratal geometries when suggesting deposition into half graben structures, and their lithofacies are controlled by the extensional marginal faults. Finally, the post-rift sediments, which are on the top of the rifting sequences, are controlled by the geometry of the fault blocks and the subsidence after cessation of the extension.

Figure 1.3

The three types of continental rifts:

A. Narrow rift

B. Wide rift

C. Core complex

(Corti et al., 2003; after Buck 1991).

It is of great importance to be mentioned that the rift zones do not generally constitute continuous tectonic structures influenced by one single fault but are instead controlled by multiple, often en-echelon shorter fault segments (Bell, 2008), indicating the variable mechanical properties of the crust. The fault segments interact and this interaction finally contributes to the rift propagation.

1.2   Introduction to the Corinth Rift; the study area

Continental rift zones, as a result of evolving extensional processes, mainly provide valuable information concerning the crustal deformation mechanisms, the landscape evolution (including all the geomorphic processes which interact with the landform changes) and the potential related natural geohazards (seismicity, landslide occurrence and tsunamis).

The back arc extension due to the subduction of the African plate at the Hellenic Trench (McKenzie 1972; 1978; Angelier 1978) in combination with the westward propagation of the North Anatolian fault across the mainland Greece (Taymaz et al. 1991; Armijo et al. 1996; Papanikolaou & Royden, 2007; Royden & Papanikolaou, 2011) and the gravitational collapse of lithosphere thickened during the Hellenides' orogeny (Jolivet 2001) are responsible for the widespread extension that has affected the whole Aegean region from central Greece to western Turkey since ~20 - 14 Ma (Seyitoglu & Scott 1996).

The deformation field of the Aegean has led to the formation of a high strain band in central Greece, the Gulf of Corinth, which is supposed to be a less than 5Myr rift basin that resulted from the main, most recent phase of currently evolving extension (Bell 2008). Its very young history in combination with the relatively well-studied depositional evolution and the structural setting, both in the onshore and the offshore environment, offer a good motive for further studies.

Western Gulf of Corinth

The western part of the Gulf of Corinth corresponds to the most active part of the rift structure as extensional deformation occurs in the highest levels, reaching approx. 14 ± 2 mm/yr, as documented by present-day GPS monitoring. The extremely high rates of seismicity, the continuous neotectonic activity, the well-preserved sedimentary sequences and the evidence of the intense geodynamic and geomorphological processes are only a few reasons for attempting a further, detailed morphotectonic study.

Consequently, the study area was chosen towards the south-western part of the Gulf of Corinth, between the Selianitika and Psathopyrgos settlements (Achaia, Greece) where the Psathopyrgos fault zone defines the south coast of the currently active part of the Corinth Rift. Further details are given in a following chapter (Ch. 4).
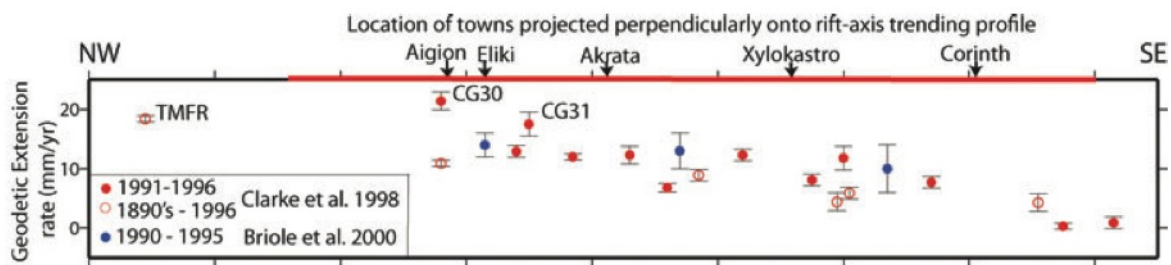

Figure 1.4 Representative geodetic 'horizontal extension rates' across the Corinth Rift, showing the higher levels towards west (Briole et al. 2000, blue circles; Clarke et al. 1998, red circles are estimates for the period 1991–1996, and white circles 1890s–1996). TMFR, CG30 and CG31 are site names from Clarke et al. (1998); after Bell et al., 2011.

1.3 Aims and objectives

The formation, growth and migration northwards of the prevailing fault systems, which evolve simultaneously with the intense morphogenetic processes, are overprinted in the age, facies and thickness of the Plio-Pleistocene sequences constructing the south margin of the western Gulf of Corinth. The dominant fault blocks, bounded by E-W trending, north dipping normal faults, are accompanied by several morphological features and anomalies, noticed in both the terrestrial and the marine environment.

The main aim of this study has been to examine how the tectonic evolution, in combination with the attendant fierce erosional and sedimentary processes, has affected the morphology through geodynamic processes often expressed as failures in the wider coastal area. High-resolution multibeam bathymetry in combination with the available land surface data have contributed to accurate submarine and subaerial morphological mapping, revealing a wealth of information with regard to the geomorphological and tectonic insight. These have been used as a basis for the detection of the most recent brittle deformation (fault structures) and all those geomorphic features that indicate instabilities probably triggered, directly or indirectly, by the ongoing tectonic activity.

2 Geodynamic Setting
of the Aegean Region

2.1 The connection to the Gulf of Corinth

The present-day physicogeographic character of the Aegean, located at the eastern Mediterranean, is mainly characterized by its geotectonic position and history. Its overall complex structure is a result of the continuous tectonic activity in the framework of the Hellenic orogenic arc evolution (Papanikolaou, 1984; 1993) within the upper plate of a system of convergent plate boundaries (Eurasia and Africa).

The wider Aegean region, until recently, has been a typical example of active back-arc extension related to normal faulting, which is concentrated above the northeast dipping subduction zone of the Hellenic arc (McKenzie, 1972; 1978; Angelier et al., 1982). The tectonic regime of the Aegean domain, from Oligocene to Miocene, was characterized by extension which had been controlled by arc-parallel extensional structures, bounding a number of recent back-arc to fore-arc extensional basins (Mercier et al., 1989; Papanikolaou & Royden, 2007). Compressional events of minor significance have also been detected but their amplitude and duration is not comparable to that period's extensional tectonics (Angelier, 1979).

Last decade geodetic monitoring of the Aegean's tectonic activity (McClusky et al., 2000), which has not changed since McKenzie's first studies (1972; 1978), has contributed to the conclusion that the Aegean's arc regional extension has been transformed. Active deformation still exists but it is accommodated by a transtensional, right-slip shear zone which extents from the North Anatolian Fault in the east to the northern end of the Hellenic Trench in the west and corresponds to the "Central Hellenic Shear Zone" (McClusky et al., 2000, Goldsworthy & Jackson, 2002; Papanikolaou & Royden, 2007). The Central Hellenic Shear Zone (Fig. 2.1, 2.2), which continues westwards in the offshore region of the Ionian Sea to Kefalonia Transform, is associated with the most of the modern seismicity, especially in the central Greece where the Gulf of Corinth is located (Ambraseys & Jackson, 1990; Roberts & Jackson, 1991).
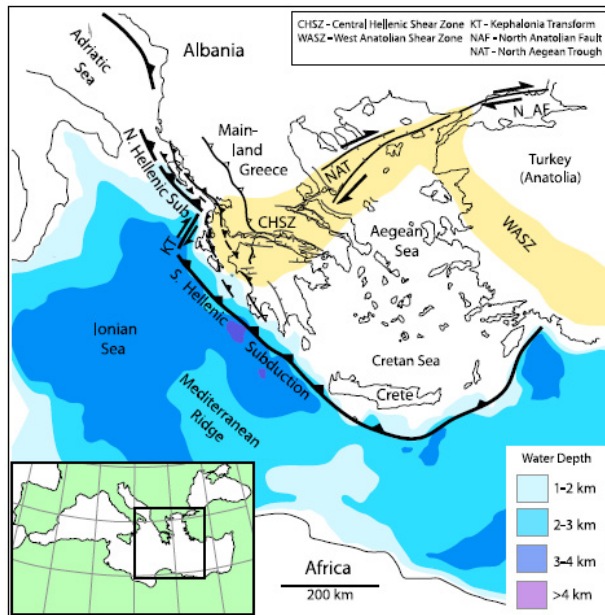
Figure 2.1 A simplified map of the tectonic setting of the Hellenic Orogenetic System, indicating the modern position of the active Hellenic trench, the main Miocene thrust faults and the band of active oblique extension (orange areas), which bound the Aegean domain (after Royden & Papanikolaou, 2011).
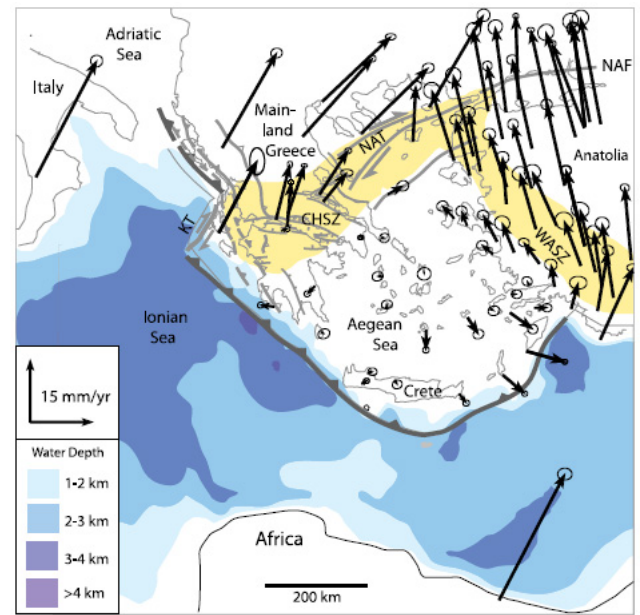
Figure 2.2 Selected GPS velocities by McClusky et al. (2000) in a reference frame that minimizes the average velocities in the Aegean region. The orange shaded areas indicate the areas of active oblique extension (after Royden & Papanikolaou, 2011).

Some of the extensional deformation of this band, first established in Pliocene times, is localized in large E-W trending active normal faults, which bound the Corinth rift and crosscut the older tectonic structures of the NW trending orogenic system of Hellenides (Mariolakos & Papanikolaou, 1981). These young and seismically active faults are related to north-northeast extension of the Corinth Rift, which is expressed either by the recent distinct fault planes or by the inactive uplifted structures (Armijo et al., 1996; Papanikolaou et al., 1997a). This extensional tectonic regime has contributed to the deepening of the central part (Brooks & Ferentinos, 1984) and the uplift of the south side of the Gulf of Corinth at elevations of over 1200m, a fact which can be easily verified by the uplifted marine terraces noticed in the coastal zone of the north Peloponnesus (Keraudren & Sorel, 1987; Armijo et al., 1996). It is important to be mentioned that these young E – W trending fault structures are not only important for the inception and growth of the Corinth Rift but also for reflecting the change of the tectonic setting near Pliocene, indicating the transition from the arc-parallel structures of Oligocene – Miocene to Plio-Quaternary arc-crossing fault systems (Papanikaou & Royden, 2007 – Fig. 2.3 & 2.4).
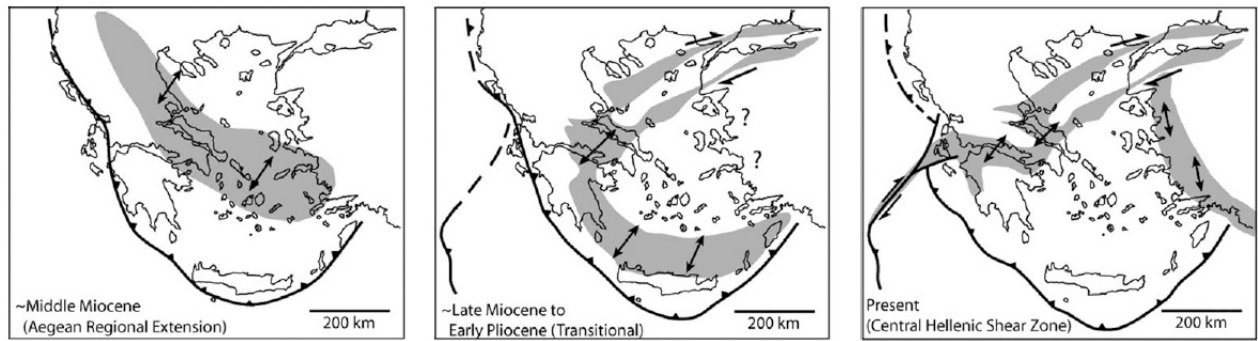
Figure 2.3 Progression of the upper plate deformation within the Aegean region from approx. middle Miocene until present. The shaded areas indicate the approximate locations of extensional and / or strike-slip activity (after Papanikolaou & Royden, 2007).
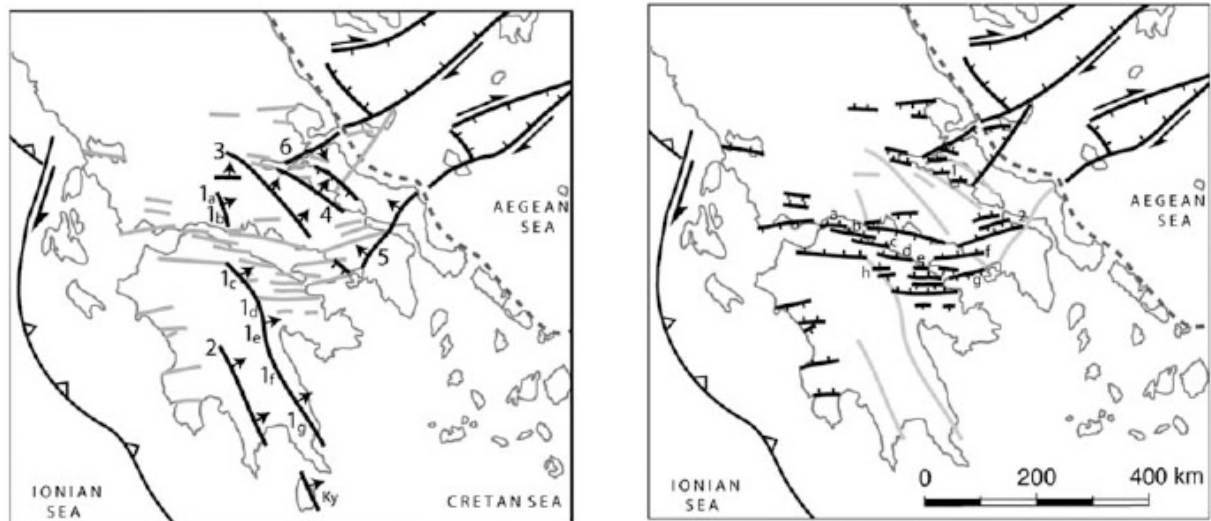
(a) Late Miocene to Early Pliocene

(b) Late Pliocene to Quaternary

Figure 2.4 The extensional tectonic structures as they appear from (a) Late Miocene to Early Pliocene to (b) Plio-Quaternary times (after Papanikolaou & Royden, 2007).

11

3 The Corinth Rift; Geological Setting

3.1   The Corinth Rift – General Information

The Gulf of Corinth, the currently active part of the Corinth rift, is a ~N100°E oriented elongated half-graben located in central Greece that separates the Peloponnese from the western mainland Greece. Geographically, it is bounded by the Isthmus of Corinth in the east, including the Gulf of Alkyonides, and in the west by the Strait of Rion, which separates the Gulf of Corinth from the outer Gulf of Patras and the Ionian Sea.

The active extensional – transtensional deformation field of the Aegean region includes a lot of currently stretching areas. The fact that most them are evolving under the sea level makes the Gulf of Corinth the most prominent rift structure, a natural laboratory accessible to detailed observation (Armijo et al, 1996).

3.2   Active Tectonics

Since Late Cenozoic, active tectonic deformation in Greece, expressed by widespread normal faulting related to back-arc extension behind the Hellenic subduction zone (Doutsos & Piper, 1990), is mainly concentrated in a broad shear zone of active oblique extension (Central Hellenic Shear Zone – Papanikolaou & Royden, 2007; Royden & Papanikolaou, 2011).

According to several geological, geomorphic, geodetic and seismotectonic studies of the past years, the Gulf of Corinth constitutes a high-strain ~100x30km band that can be characterized as one of the largest zones of active normal faulting. The extensional field related to the Corinth rift inception and evolution develops in a N – S direction and has a history of about 2÷5 Ma. The rift probably started being formed in early Pliocene times and comprises an onshore

inactive, early rift structure uplifted and preserved in the northern Peloponnese towards south and, to the north, the currently active Gulf of Corinth (Ford et al., 2012).

In a simplified approach, according to geomorphological indices and seismic profile analysis in the Gulf of Corinth, its overall structure has been characterized as a complex asymmetrical half-graben, with definite evidence of isostatic footwall uplift on the southern margin and significant hanging-wall subsidence and sedimentation towards north (Brooks & Ferentinos, 1984; Armijo et al, 1996; Westaway, 2002; McNeill et al., 2005a).

From a geotectonic point of view, the Gulf of Corinth corresponds to a post-alpine sedimentary basin, bounded by very young and active, rift-controlling faults, which crosscut the alpine (pre-rift) basement of Pindos mountain chain. The major of these en-echelon E-W trending normal faults lie along the southern margin of the Gulf and dip towards north, creating the sharp and linear coastline, the steep morphology and the high uplifted flanks of the northern Peloponnese. Conversely, the northern margin of the basin is characterized by a more sinuous coastline and a gentler topographic relief, fault-controlled as well, but by smaller-scale antithetic E-W trending normal faults dipping southwards.

High resolution seismic reflections and multibeam bathymetric surveys, which have been carried out and analysed during the past years in the Gulf of Corinth region (Heezen et al., 1966; Stefatos et al., 2002; Moretti et al., 2003; McNeill et al., 2005a; Lykousis et al., 2007), have also led to the construction of a detailed stratigraphic and tectonic insight as far as the offshore area is concerned. The results of these studies show the identification of major offshore fault structures, E-W trending as well, which may accommodate significant extension and potentially have a large component in controlling the rift structure.

Taking into consideration that the southern margin's fault activity has contributed more in the Corinth Rift's evolution, the corresponding tectonic structures are being further discussed below.

Onshore faults of the south margin

Armijo et al. (1996), who first attempted to present the evolution of the Corinth Rift during Quaternary, suggested the existence of three main en-echelon normal fault segments bounding the steep southern margin of the Gulf of Corinth (Fig. 3.1). From west to east, the Psathopyrgos, the Eliki and the Xylokastro faults, correspond to major, almost E - W trending, active features (average strike of N90° to N105° E), dipping ~50° towards north and ranging from 15 to 25km in length. Progressive eastward width and depth increase in the Gulf, as resulted from bathymetric studies, as well as an increase in the sediment infill of the basin

(Heezen et al., 1966; Brooks & Ferentinos, 1984; Armijo et al., 1996) had been further correlated to the amount and the distribution of extension that is accommodated by these three major faults.
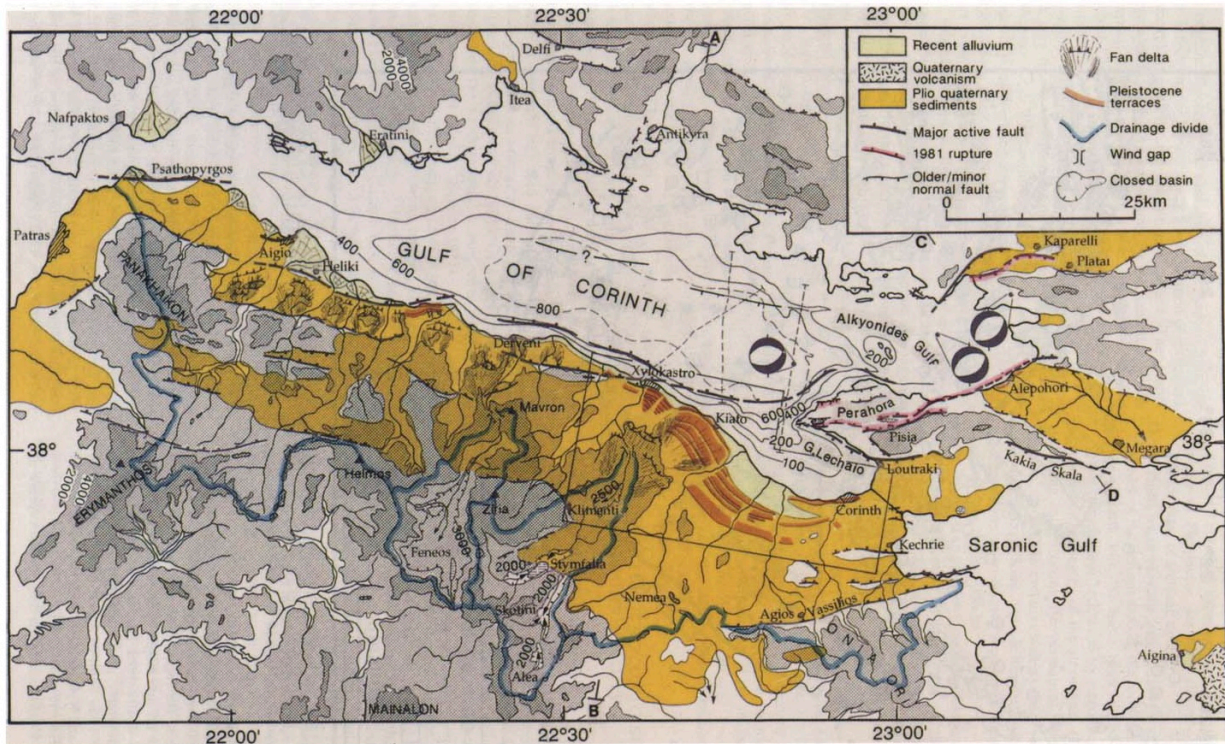

Figure 3.1 Active tectonics in the Gulf of Corinth as presented by Armijo et al. (1996).

The general geometry of faulting in the Gulf of Corinth, which shows that the rifting processes have changed since the initiation of the Corinth Rift in Plio-Pleistocene, indicates the fast slip rates of the currently active features and the transition from subsidence and sedimentation to uplift. This transition, in combination with the extensive post-alpine sedimentation towards south (with regard to the Gulf of Corinth), represents the past-activity of other en-echelon tectonic structures, similar in characteristics and attitude to the currently active, which seem to have been the south boundaries of the basin during the Plio-Pleistocene evolution. These faults, including the Mamoussia-Pirgaki, Doumena, Kerpeni, Kalavryta and Helmos faults can be observed at the outcrops of the alpine basement in e.g. Zyria, Erymanthos, Helmos mountains and cannot be connected to Holocene activity despite the fact that they provide evidence of syn-sedimentary and Pleistocene displacement (Doutsos & Piper, 1990; Armijo et al., 1996; Bell, 2008).
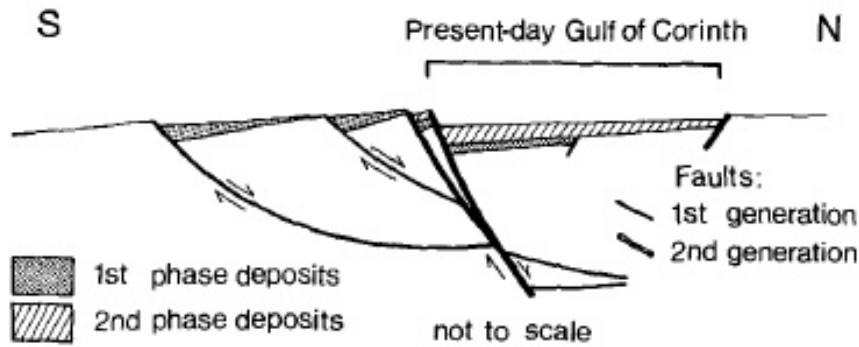
Figure 3.2 N-S trending idealized section across the Gulf of Corinth showing the two generations of faulting and the two phases of depositional processes, related to the tectonic activity (Ori, 1989).

Consequently, it should be mentioned that these older and less active and/or probably inactive structures related to the first stage of the rift development during the Plio-Pleistocene times (Proto-Gulf of Corinth, as named by Ori, 1989), with the contribution of the erosional and sedimentary data, suggest the northward propagation of the fault activity (Fig. 3.2). The overall migration of the active rift edge has been calculated equal to ~5-10km at the western part and ~25-30km at the central and the eastern part (Armijo et al., 1996).
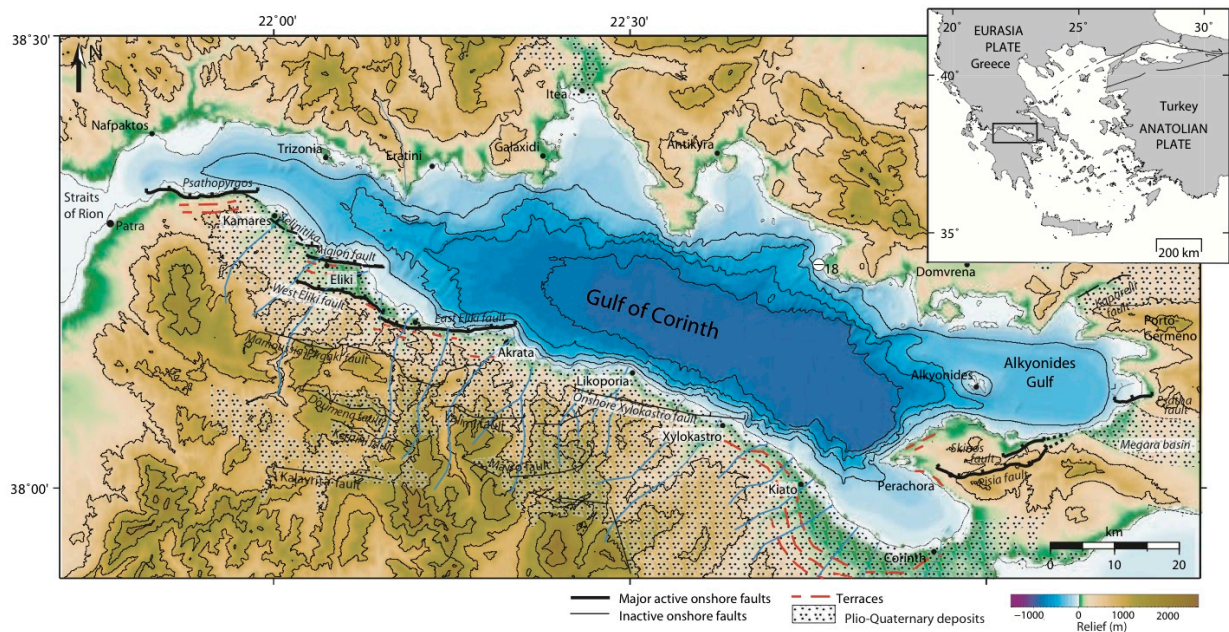
Figure 3.3 Tectonic framework of the onshore Corinth rift after Bell (2008). The locations of major onshore fault locations after Armijo et al. (1996), Stefatos et al. (2002), Leeder et al. (2005), McNeill et al. (2005b), Palyvos et al. (2005), Rohais et al. (2007). Topography is from the Shuttle Radar Topography Mission (http://srtm.usgs.gov), bathymetry is derived from the swath bathymetry M.V. Vasilios 2003 cruise (McNeill et al. 2005a) and R/V Maurice Ewing 2001 (Zelt et al. 2004). South coast drainage from Zelilidis (2000). Areas of Plio–Quaternary sediment deposition from Armijo et al. (1996), Stefatos et al. (2002). Un-ornamented areas are basement rock.

Further studies that have been carried out recently relative to the onshore fault activity in the Gulf of Corinth region (after Armijo et al., 1996), show that the southern shoreline of the Corinth rift is bordered by a greater number of E - W trending, en-echelon fault segments, of approximately 15 – 20km in length, including from west to east: the Psathopyrgos, Selianitika, Aigion, East Eliki, West Eliki, Xylokastro, Pisia, Skinos and Psatha normal faults (Bell, 2008, Fig. 3.3). These fault features, which strike 90° – 105° and dip ~40° – 60° towards north, are subsiding the rift basin in their hanging wall and uplifting the Plio-Pleistocene Gilbert-type fan deltas in their footwall.

Offshore faults

Except for the onshore tectonic features, E-W to ESE-WNW trending faults located in the offshore region accommodate a large component of the extension in the Gulf of Corinth. These structures have been characterized as potentially important in controlling the active rift structure (Sakellariou et al., 2001; Stefatos et al., 2002; Moretti et al. 2003; McNeill et al. 2005a; Bell, 2008) and have been identified by high resolution multichannel seismic (MCS) reflection profiles and multibeam swath bathymetric surveys.

Figure 3.4 Neotectonic framework of the Corinth basin. 1: Major active faults, 2: Secondary active faults, 3: Continental platform boundary, 4: Active submarine landslides areas, 5: Isobaths (offshore) 6: Contour lines (onshore) – after Papanikolaou et al, 1997.

Figure 3.5 Structural map of the Gulf of Corinth area after Moretti et al. (2003) modified from Armijo et al. (1996), Sakellariou et al. (2001a) and Stefatos et al. (2002). The onshore structural pattern in the area of Aigion is modified from the map of Ghisetti et al. (2001).
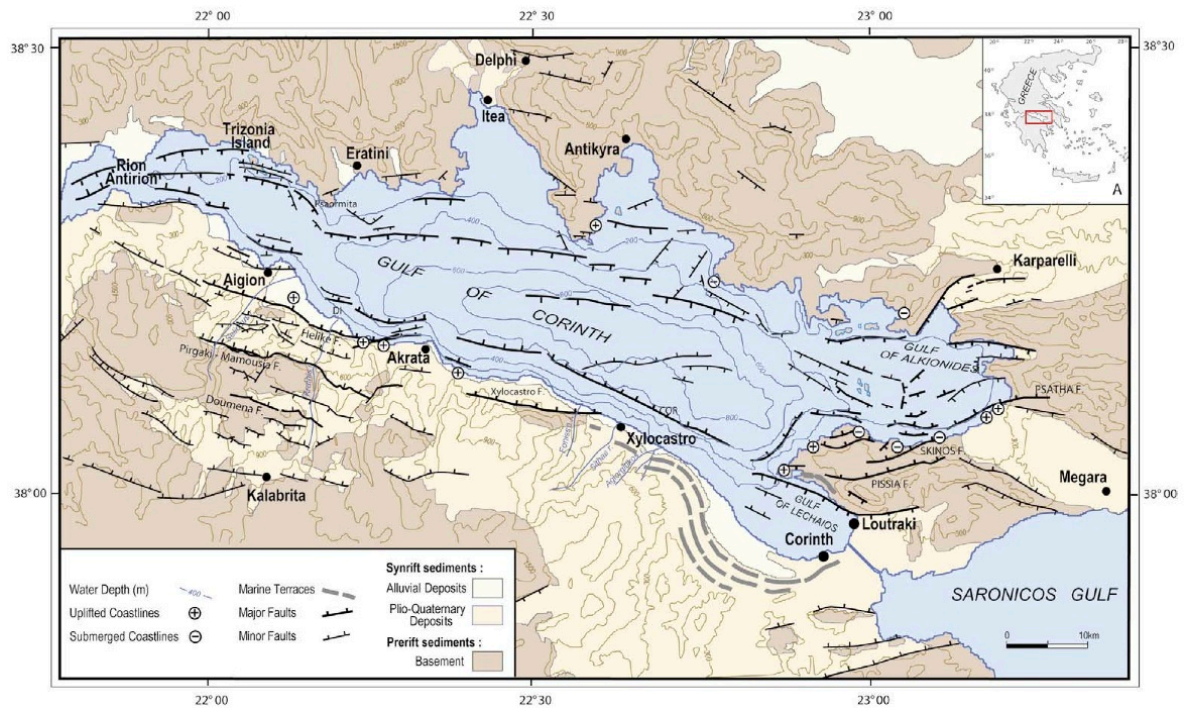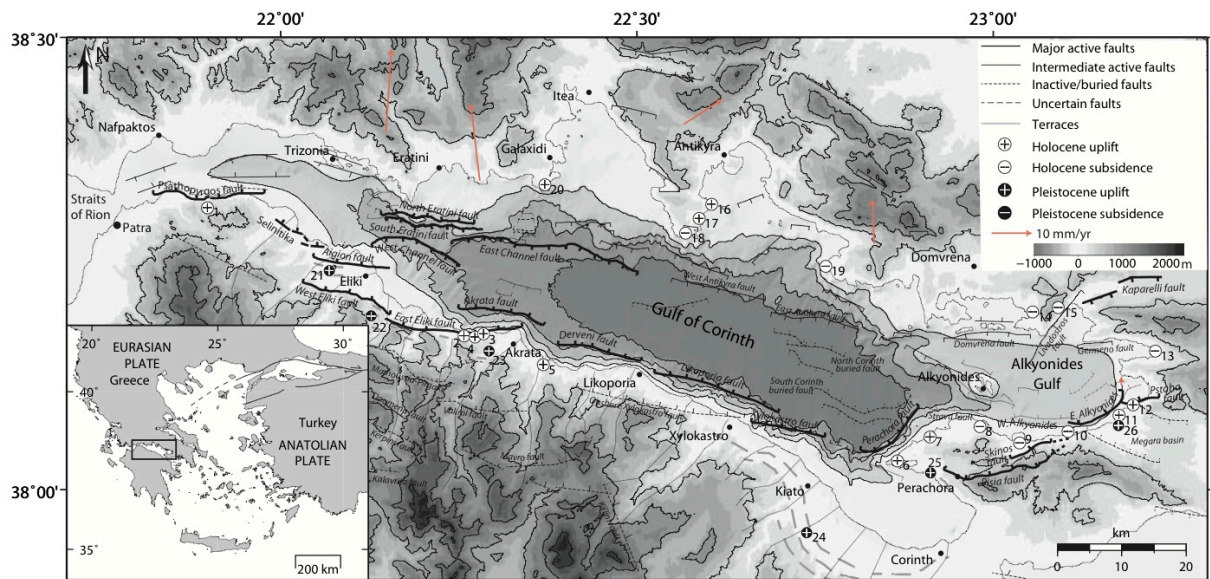

Figure 3.6 Tectonic framework of the Corinth rift after Bell (2008). The locations of major offshore faults have been interpreted by Bell (2008) based on the fault maps developed by Armijo et al. (1996), Stefatos et al. (2002), Leeder et al. (2005), McNeill et al. (2005b), Palyvos et al. (2005), Rohais et al. (2007). Topography is from the Shuttle Radar Topography Mission (http://srtm.usgs.gov), bathymetry is derived from the swath bathymetry M.V. Vasilios 2003 cruise (McNeill et al. 2005a) and R/V Maurice Ewing 2001 (Zelt et al. 2004). South coast drainage from Zelilidis (2000). Uplift and subsidence measurements at the coastline are explained in Tables 6.1 and 6.2. Arrows are north coast GPS velocity vectors from Clarke et al. (1998).

17

Previous studies of Papanikolaou et al. (1997), Stefatos et al. (2002), Sachpazi et al. (2003), McNeill et al. (2005a) and Lykousis et al. (2007) have been further supplemented by Bell's work (2008) aiming to interpret the geometry of the major rift-controlling offshore faults in the western part of the Gulf of Corinth, and contribute to the overall understanding of the Corinth rift structure. The dominant resulting active features, the South Eratini, North Eratini, East Channel, West Channel and Akrata faults, dissect the basin's basement and show a throw of more than 450m. In combination with the East and West Eliki, Aigion and Derveni faults of the southern coastline, they can be responsible for the current geometry of the basin. The geometry and the characteristics of the major interpreted offshore faults are further discussed below.

The North Eratini fault, dipping ~60° towards north and the South Eratini fault, dipping ~50° - 60° towards south, have a similar length of approximately 15km and correspond to two of the major features of the basin exposing steep basement fault scarps that are visible in the bathymetric data. The tectonic horst structure, which is produced by these two faults, is well depicted in Fig. 3.7.

Figure 3.7 Structural interpretation of the sub–bottom structure towards the western part of the Gulf of Corinth. NEF: North Eratini Fault, SEF: South Eratini Fault, WCF: West Channel Fault. The position of the seismic profiles is marked on the picture on the bottom right corner (after Bell, 2008).

The West Channel fault (Fig. 3.7) is a major structure of the basin as well, responsible for the position of the central axial channel for at least 15km. It dips ~45° – 60° towards south, overlaps the North and South Eratini faults and lies ~3 km south of the South Eratini fault.

18

To the east, the East Channel fault (Fig 3.8) develops in shallow sediments dipping ~60° – 70° towards south decreasing to ~45° – 55° in basement. The East Channel fault occurs an overlapping of the eastern tip of the South Eratini fault for approx. 5 km.

The Akrata fault (Fig 3.8) dips N at ~60° and lies ~4 km north of, and can be related to an offshore extension of the major East Eliki fault. The Akrata fault is responsible for the production of steep sediment slopes along the southern margin of the Gulf and causes significant basement offset for a distance of approx. 15 km.

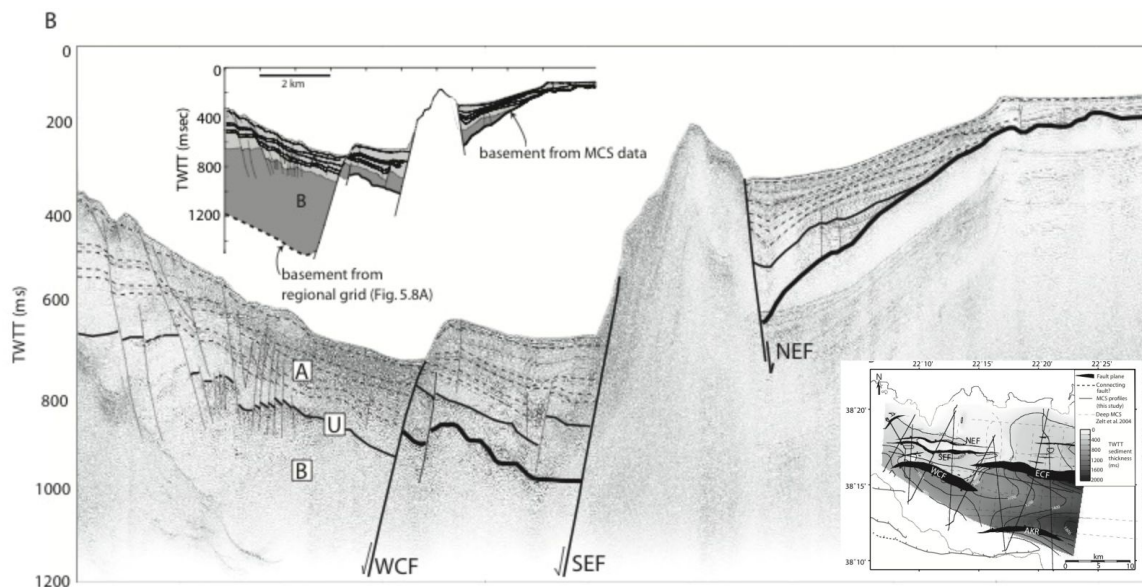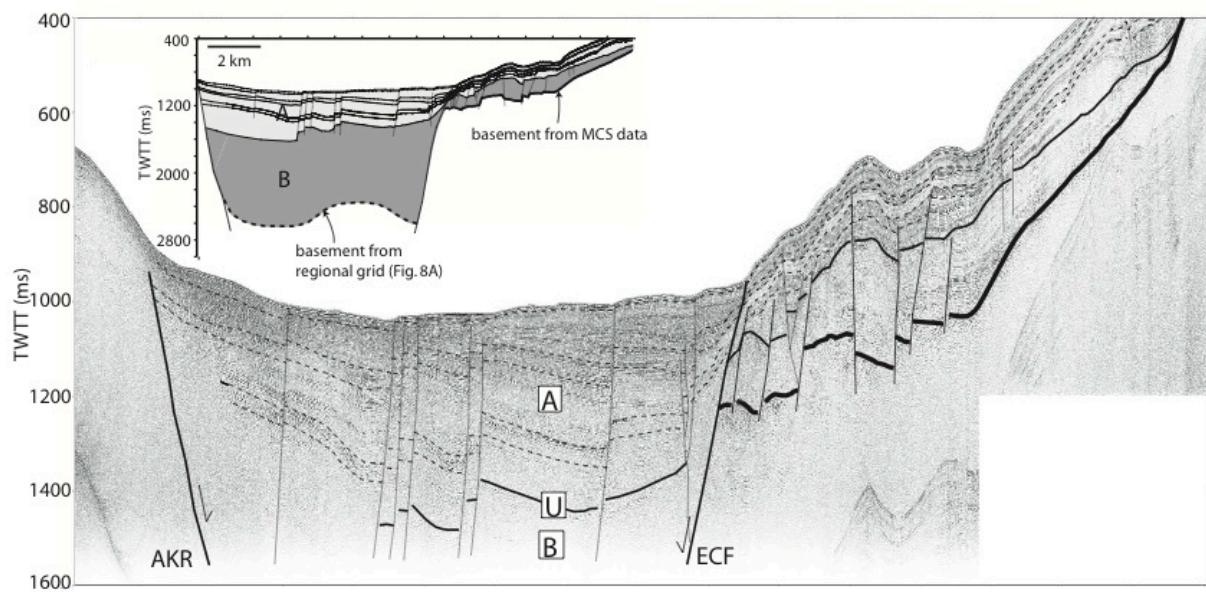**Figure 3.8** Structural interpretation of the sub–bottom structure towards the western part of the Gulf of Corinth. AKR: Akrata Fault, ECF: East Channel Fault (after Bell, 2008). The position of the seismic profiles is marked on the picture on the bottom right corner of Fig.3.7 of this study.

It should be mentioned that smaller scale faults also exist in the offshore region but they are of minor importance, as they appear less than 5km in length. These faults do not affect the basin's basement and they have limited or no surface expression.

3.3 Stratigraphy in the Southern Margin of the Gulf of Corinth

General

The sedimentary sequences in the Gulf of Corinth reflect the impacts of the active extensional tectonics. Calculations on the vertical offsets between specific layers of the existing prodelta sequences in the submarine region by Lykousis et al. (2007), have denoted continuous subsidence rates in the order of 0.7 – 1.0 kyr^{-1} during the late 250 ka, with a maximum value observed for the depocenter of the basin, equal to 3.6 kyr^{-1}. The fact that this maximum

subsidence rate (3.6 kyr^{-1}) is twice as the maximum calculated sedimentation rate (1.8 kyr^{-1}) implies that both the 870 m maximum depth of the basin, as well as the 2.2 km maximum sediment thickness, have been formed during the last 1Ma following uniform sedimentation processes throughout the basin's evolution. Fault slip rates up to 5.8 kyr^{-1} have been also calculated between the northern and the southern basin's bounding faults, suggesting a total minimum N - S extension of 5.8 km over the last 1Ma.

Consequently, the intense neotectonic activity, in combination with the eustatic sea level changes, seems to have affected both the geographical and the sedimentary evolution of the Gulf of Corinth region. Late Quaternary sedimentation has been controlled not only by the sediment input and deposition from the rivers but by the position of the sea level relative to the Rion Strait as well.

Perissoratis et al. (2000), Collier et al. (2000), Lykousis et al. (2007) and Roberts et al. (2009) have presented evidence concerning the Gulf transformation into a lake when sea level fell below the level of the Rion Strait sill (currently existing at ∼ -66 ÷ -67 m according to new data from HCMR) and into an open marine environment by the time the sea level has been above the Rion Strait sill (Fig. 3.10).
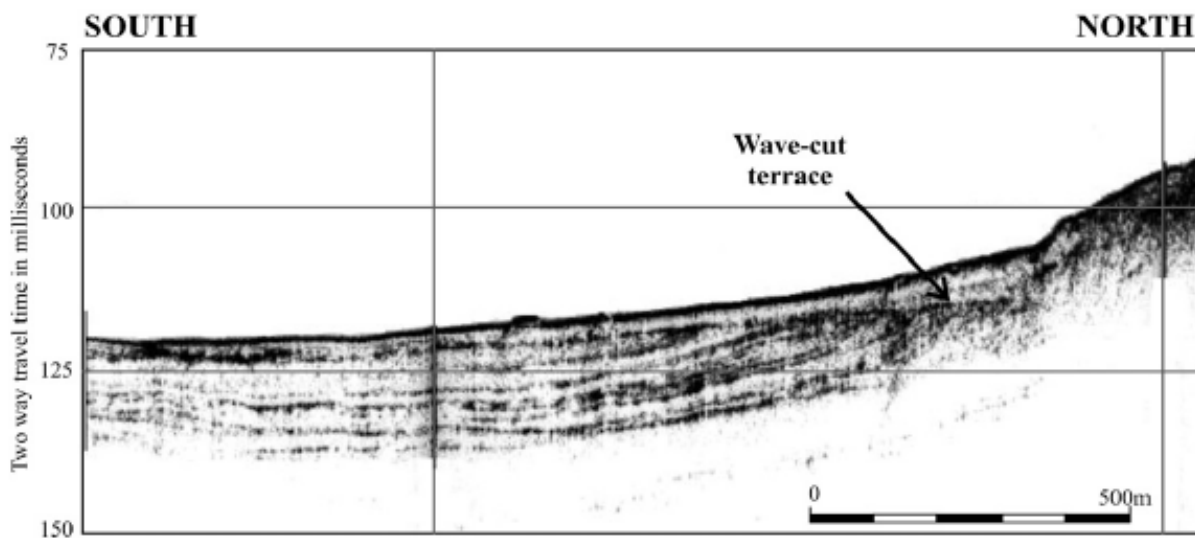
Figure 3.9 High-resolution sub-bottom profile (3.5 kHz) indicating the late glacial wave-cut terrace in the shelf break of Eratini bay at 110 ms (77–78 m) depth (Lykousis et al., 2007).

The lacustrine conditions have been extensively studied with the contribution of detailed seismic profiling and piston coring in the deepest part of the Gulf suggesting that the Lake of Corinth had remained isolated from the open marine environment of Mediterranean from about up to 13 ka. Identified wave-cut, late glacial terrace located towards Eratini bay (Fig. 3.9) has been for the first time correlated to the late glacial lake level which has been calculated equal to 77 ÷

78 mbmsl (meters below mean sea level), depth comparable approx. up to 10m deeper than the Rion – Antirion sill (Lykousis et al., 2007).
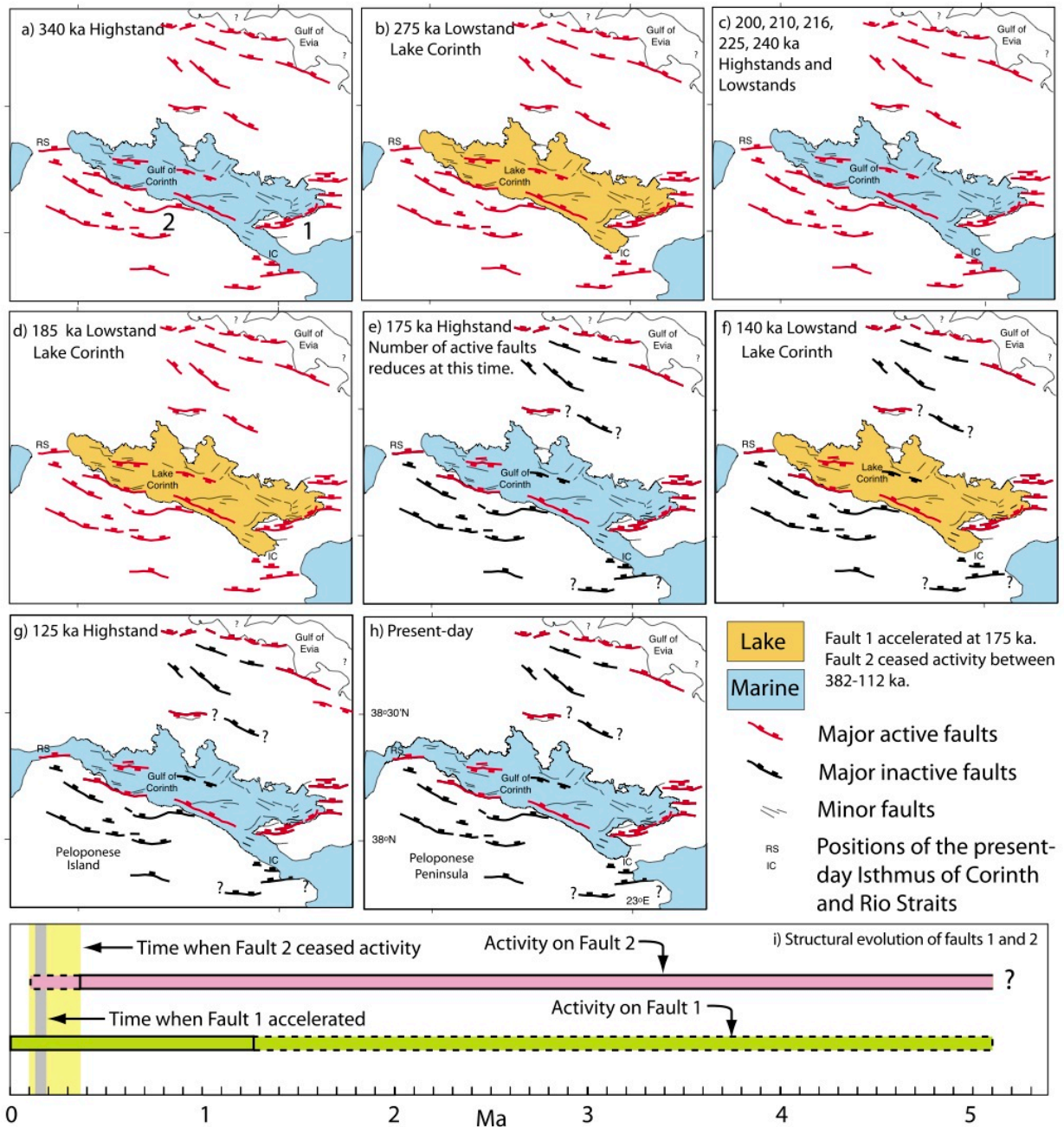
Figure 3.10 Speculative paleogeographic and structural evolution of the Gulf of Corinth and locations of active faults, (a–h) after Roberts et al. (2009). Changes in fault length are not shown because of a lack of data. Shoreline geometries are shown schematically to illustrate opening and closure of the eastern and western ends of the Gulf to the Mediterranean Sea. The locations of active faults are speculative, but on the basis of the scenario explained in the text where regional strain rates are maintained as some faults accelerate by cessation of activity on other faults. Activity on faults 1 and 2 shown in the bottom diagram, with dashed lines indicating uncertainty in timing. It can be observed that faults were active synchronously, but fault 1 accelerated when fault 2 ceased activity.

Post-Alpine Sediments; onshore and offshore region

Plio-Pleistocene

Considering that the Gulf of Corinth corresponds to one of the recent typical examples of currently active extensional tectonics, it is expected that the effects of the neotectonic movements, which have controlled the formation and growth of the basin, and the eustatic sea level movements as well, could be clearly observed in the sedimentary and structural setting of the study area. The lithostratigraphy and the sedimentary facies of the southern part of the Gulf of Corinth are definitely related to its tectonic evolution (Ori, 1989).

The southern margin of the Gulf of Corinth is characterized by extensive occurrence of Post-alpine deposits (Fig. 3.11), which are located up to hundreds of meters above sea level, in a distance less than 3 kilometres from the coast, indicating the high uplift rates of the south flanks of the Gulf. The supply of the sediments in the south margin, where our study area is located, reflects the intense neotectonic activity that takes place in this region, in contrast to the northern side of the Gulf, where the tectonic activity also acts but in a lower rate.

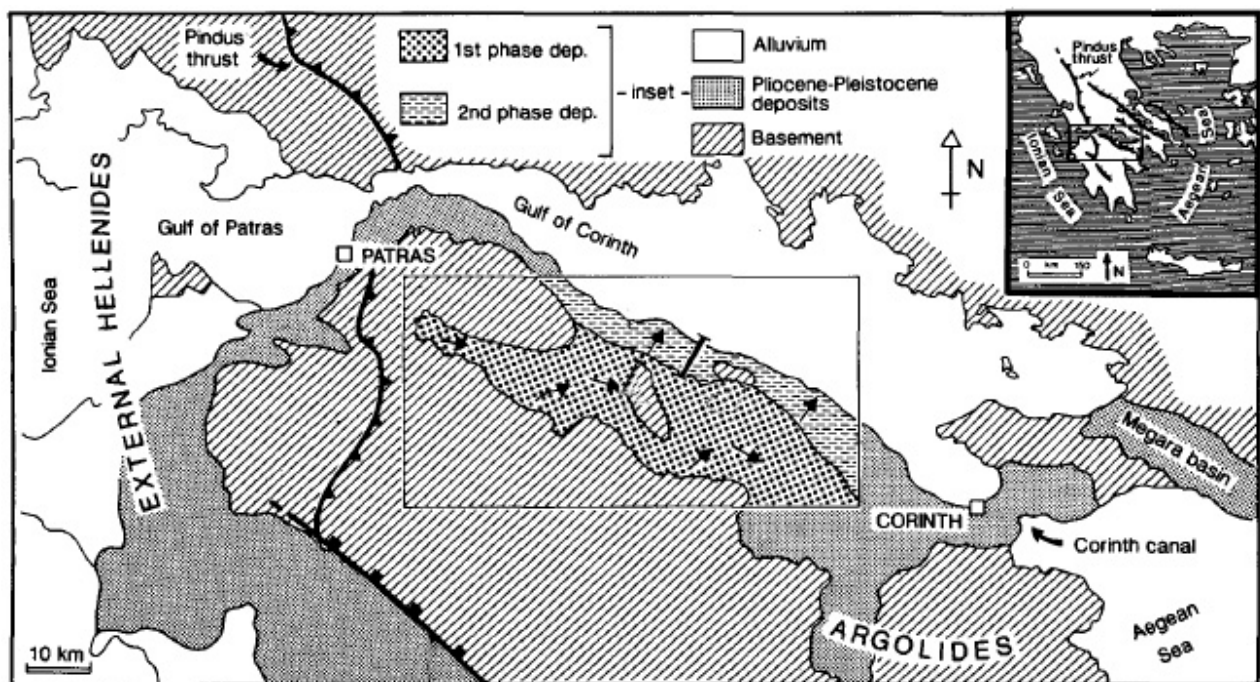**Figure 3.11** Simplified geologic map of the Gulf of Corinth by Ori (1989). The area marked by a rectangle shows the region where Ori further set the paleocurrent directions and discriminated the subdivisions of the Plio-Pleistocene lithostratigraphy.

The main sedimentary processes in the Gulf of Corinth have been analysed in detail by Ori (1989), who has mentioned that its south part has been formed by the products of two

sedimentary cycles, separated by an angular unconformity, which have resulted from two different phases of the basin evolution.

The deposits of the first stage, which crop out extensively far from the coastal zone towards south, vary in thickness from 1000m to 3000m and correspond to various sedimentary facies, indicating from alluvial fans to shallow water lacustrine environments. These first-cycle deposits represent the first stage of the basin development, which is known as Proto-Gulf of Corinth, as it differs in characteristics (sediment fill and shape) from the present-day geological setting of the basin. The Proto-Gulf indicates a continental to shallow water paleoenvironment, where the subsidence rate has never exceeded the sedimentation rate.

A further discrimination in the first-cycle deposits can be done due to characteristic alternations of transgressive and regressive events (Fig. 3.12). The lower sedimentary sequence of the transgressive event consists of alluvial fan conglomerates, which develop in sediments representative of alluvial plain and near-shore facies (mainly conglomerates with enclosed organic mudstones, indicative of the seasonally flooded forests in a tempered climate which existed at that time) and, finally, pass into lacustrine marls. The alluvial plain deposits are covered by transgressive beach deposits characterized by tabular bodies with cross-stratification, interbedded with fine-grained sediments (marly formations) and lignites. By that time, the paleoenvironment had been fresh / brackish shallow water to fresh-water lacustrine. It is remarkable that the knowledge of the paleoenvironments, which result from the evaluation of the Plio-Pleistocene stratigraphy, suggests that the basinal part of the Corinth Rift had been very shallow with no contact to seawater and the nearby marine environment.
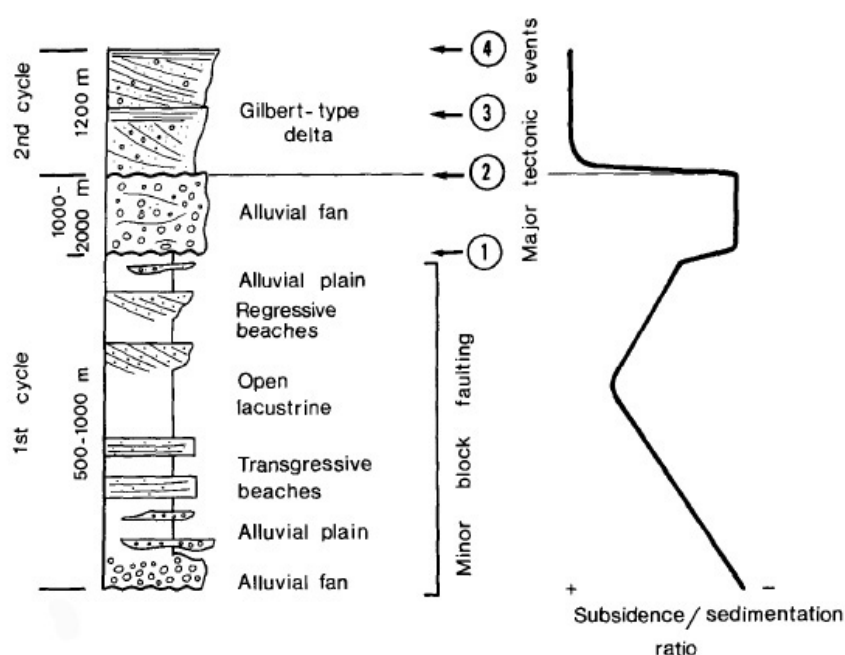

Figure 3.12 Vertical section showing the typical sedimentary sequence in the south part of the Gulf of Corinth in correlation to the tectonic activity and sedimentation processes (Ori, 1989).
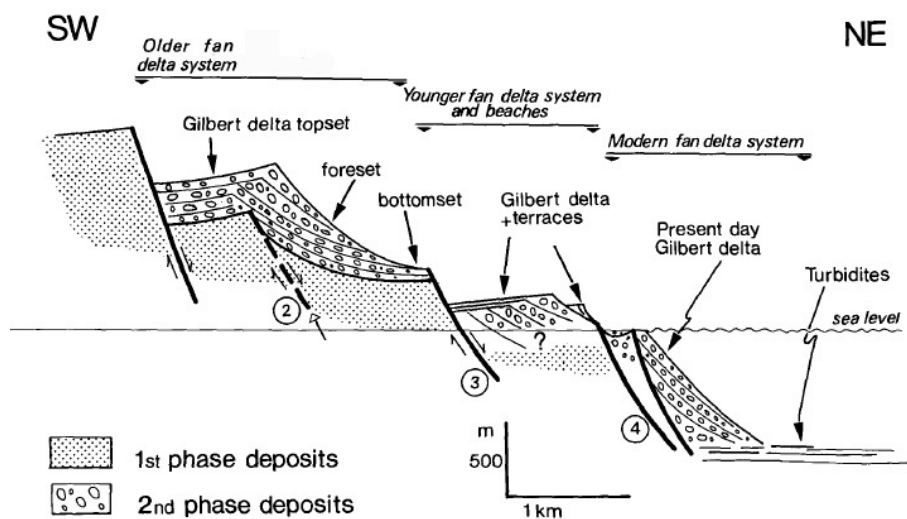
Figure 3.13 Simplified geological section presenting the typical fault blocks structure and the stratigraphy in the south part of the Gulf of Corinth (after Ori, 1989). The numbers 1÷4 are related to the major tectonic events shown in the previous figure (Fig. 3.11).

The regressive event lies above the transgressive sequence. It consists of beach deposits, different from the beach deposits of the transgressive event, as they comprise of more coarse sediments which pass into foresets of ~1000m-thick fan conglomerates. This large-scale body of the fan conglomerates terminates the first stage of the evolution of the Gulf of Corinth by marking a significant change in the basin development related to high levels of fault activity and subsidence.

The second phase of the basin evolution is represented by the following sedimentary cycle indicative of the presence of very steep and deep basin margins due to intense fault activity. Gilbert-type fan deltas and deep-sea deposits can be observed, unconformably deposited over the first-stage sedimentary sequence (Fig. 3.13). The actively forming Gilbert-type fan delta deposits, which develop along the basin's margins, are controlled by fault structures perpendicular to the main extensional regime and consist of inclined sequences of high thickness. These deltaic sediments are very extensive in the wider south coastal zone of the Gulf of Corinth and have been studied by a lot of scientists in detail during the last decades. It is important to be mentioned that this second phase of sedimentation, in contrast to the first phase, highlights increased subsidence rates (with fault displacement up to 650m), which are not balanced by the sedimentation.

Multi-channel seismic profiles indicate that the present-day Gulf of Corinth contains a maximum of 2.2 km thick Plio-Pleistocene syn-rift sediments (Myrianthis, 1984; Clément, 2000; Lykousis et al. 2007). According to Makris et al. (2003), along a profile located on the southern margin of the main depocenter of the basin, the syn-rift deposits show a maximum thickness of 1.5 km.

24

The lowermost marginal slopes and the basin, as interpreted by piston core sampling investigations (Heezen et al., 1966; Brooks & Ferentinos, 1984;Lykousis et al., 2007; Lykousis et al., 2009), are mainly filled by prodelta sediments and a thick sequence of gravity deposits corresponding to successions of sand, silt and/or mud turbidites, slumps, translational slides, mudflows and debris flow materials. Fan delta progradation combined with extensive slumping during Pleistocene sea level changes, occur as the predominant sedimentary processes on the steep flanks of the Gulf, mostly related to seismically induced mass gravity movements initiated in the coastal zone and/or the uppermost slope (Perissoratis et al., 1984; Ferentinos et al., 1988; Lykousis, 1990; Lykousis et al., 2007).
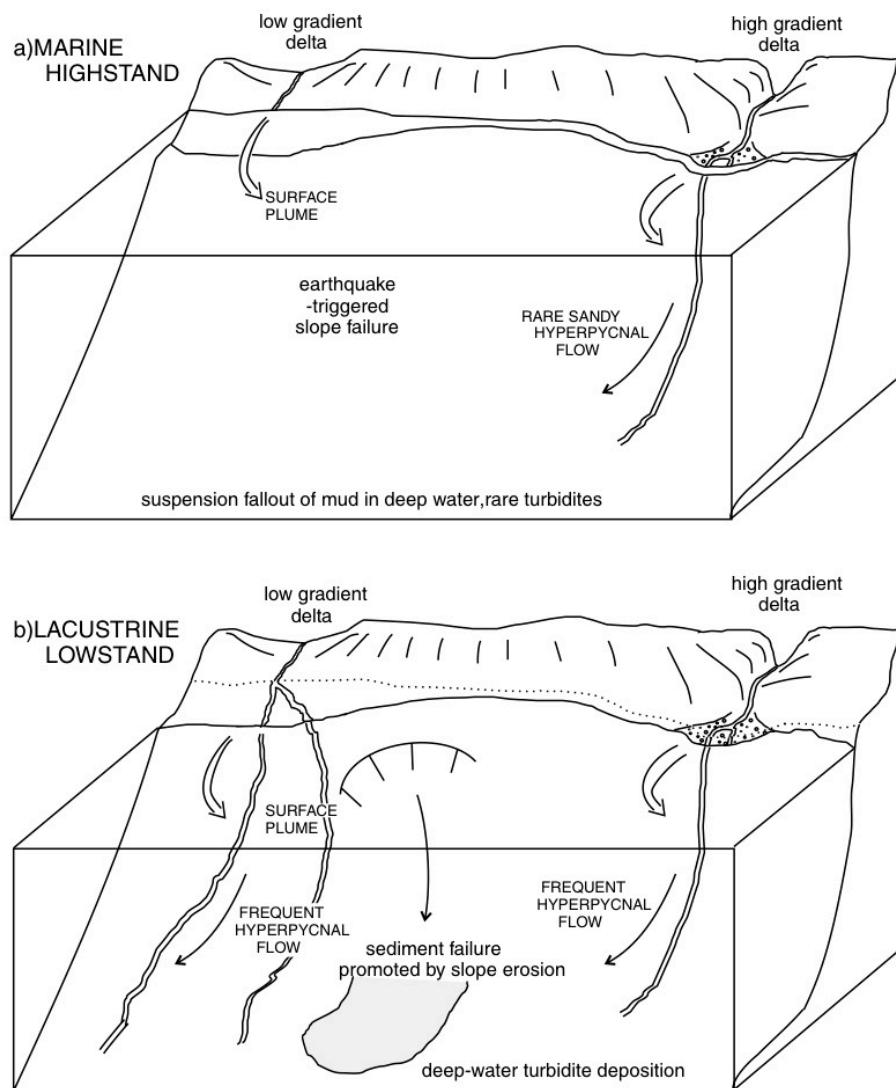
Figure 3.14 3D models after seismic profile analysis by Perissoratis et al. (2000) showing contrasts in sedimentation processes within the basin resulting from the two different types of paleogeographic conditions. The Gulf of Corinth has been repeatedly transformed between a lake and marine basin during the Late Pleistocene due to the fluctuation of global sea level and the shallow depth of Rion Strait.

Different gradients of the deltas show different type of sediment supply between the marine and lacustrine phases.

(a) High-stand fully marine conditions and (b) Low-stand lacustrine or brackish conditions.

Consequently, with the remarkable contribution of many scientists, including Heezen et al. (1966), Brooks & Ferentinos (1984), Ori (1989), Perissoratis et al. (2000) and Lykousis et al. (2007; 2009), the history of the Gulf of Corinth could be approached, with regard to the stratigraphic architecture and the sedimentary evolution. The two depositional phases mentioned above, indicate at least two generations of fault structures (low-angle and high-angle normal faults), which have uplifted the Plio-Pleistocene deposits of the Gulf of Corinth in different high levels (up to 1200m). The present-day Gilbert-type fan deltas can be observed at high altitudes above sea level while the new deltaic systems are currently being formed below sea level in the south coastal zone of the Gulf of Corinth, probably suggesting a third phase in the evolution of the Corinth Rift (Moretti et al., 2003; Lykousis et al., 2007).

Alpine Formations; Pre-rift basement

Lower Cretaceous-Eocene

The pre-rift basement, which outcrops on the footwall of the major faults in the Gulf of Corinth Region, consists of alpine formations that belong to the Pindos mountain chain that is cut across by the rift structure. The basement rocks are Mesozoic cherts and radiolites of Jurassic – Lower Cretaceous and limestones of Upper Cretaceous overlain by Transition beds of Maestrichtion – Palaeocene and flysch formation of Palaeocene – Eocene.

More specifically the characteristics of these alpine formations are mentioned below:

- Paleocene – Eocene Flysch, consisting of medium to thick-bedded sandstones with intercalations of clayey - marly beds.
- Transition beds of Maestrichtion – Paleocene. This formation corresponds to alternations of limestones, sandstones and shales, which mark the transition of Upper Cretaceous limestones to the flysch.
- Upper Cretaceous Limestones, which are characterized by alternations of thin-bedded, clastic, crystalline limestone with nodules and chert layers.
- Jurassic – Lower Cretaceous Cherts. This formation corresponds to alternations of cherts, radiolarites and shales with intercalations of bedded, reddish to grey-white coloured limestone.

3.4 Seismicity

The high extension rates in the Gulf of Corinth are accompanied by a high level of microseismic activity, especially at its western part, which is characterized by frequent earthquake swarms and also by the occurrence of large earthquakes across the whole section of the Gulf (Bourouis

& Cornet 2009). Although the Gulf of Corinth is geographically limited, numerous onshore and offshore earthquakes, with magnitudes up to 7, have been instrumentally recorded or historically reported (Papadopoulos et al. 2000). Some of the large and destructive earthquakes that occurred during the last three decades are the Alkionides seismic sequence in 1981 (Jackson et al. 1982), the Galaxidi earthquake in 1992 (Hatzfeld et al. 1996), the Patras earthquake in 1993 (Tselentis et al. 1994; Karakostas et al. 1994) and the Aigion earthquake in 1995 (Bernard et al. 1997). The seismicity in the Gulf of Corinth is summarized in the following figures (Fig. 3.15, 3.16, 3.17).
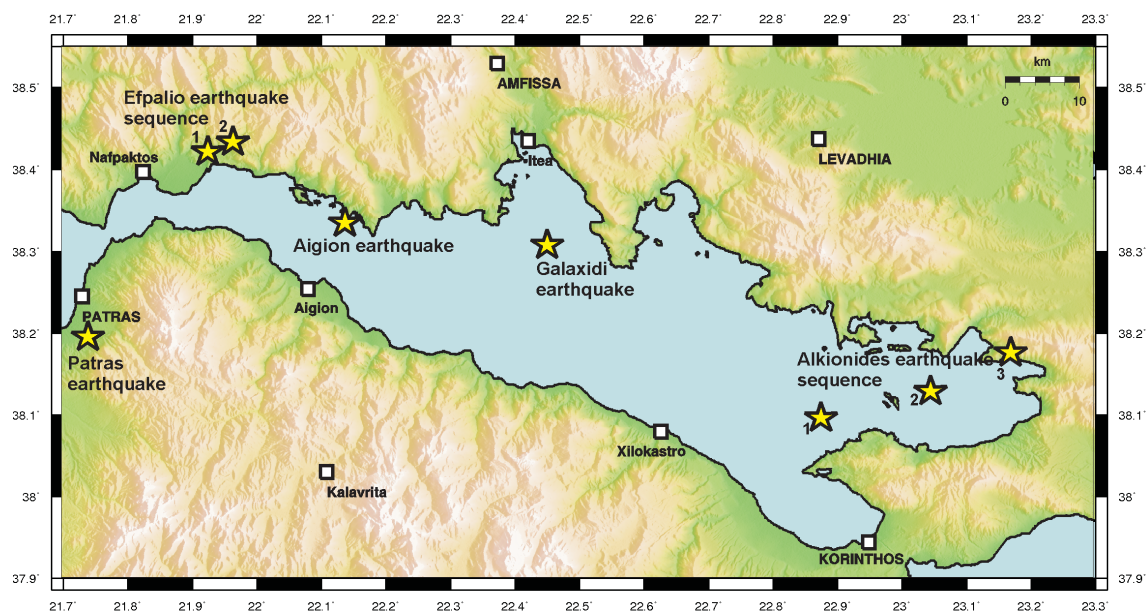

Figure 3.15 A Gulf of Corinth map presenting the most important seismic events of the last 30 years (kindly provided by D. Giannopoulos – University of Patras).

Table 3.1 The major seismic events in the Gulf of Corinth region within the last 30 years (kindly provided by D. Giannopoulos – University of Patras).

Earthquake Event	Date	Magnitude	References
Alkyonides Seismic Sequence	24 February 1981	6.7 M_s	Jackson et al., 1982
	25 February 1981	6.4 M_s	
	4 March 1981	6.4 M_s	
Galaxidi	18 November 1992	5.9 M_s	Hatzfeld et al., 1996
Patras	14 July 1993	5.4 M_s	Tselentis et al., 1994 & Karakostas et al., 1994
Aigion	15 June 1995	6.2 M_s	Bernard et al., 1997
Efpalion Seismic Sequence	18 January 2010	5.3 M_w	Sokos et al., 2012 & Ganas et al., 2013
	22 January 2010	5.2 M_w	

Figure 3.16 Seismicity map presenting the seismic events instrumented in the wider Gulf of Corinth region during the last 10 years (2003 – 2013). The red circles correspond to the epicenters of the seismic events and the white squares to the major cities. Data obtained from the "Hellenic Unified Seismological Network-HUSN" / Institute of Geodynamic / National Observatory of Athens (kindly provided by D. Giannopoulos – University of Patras).
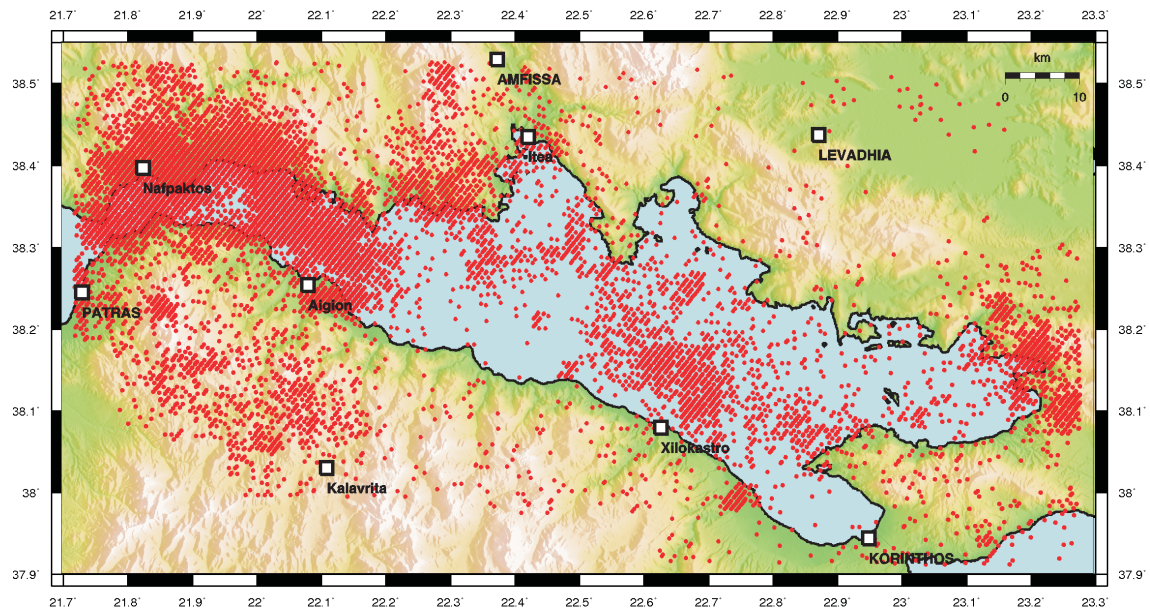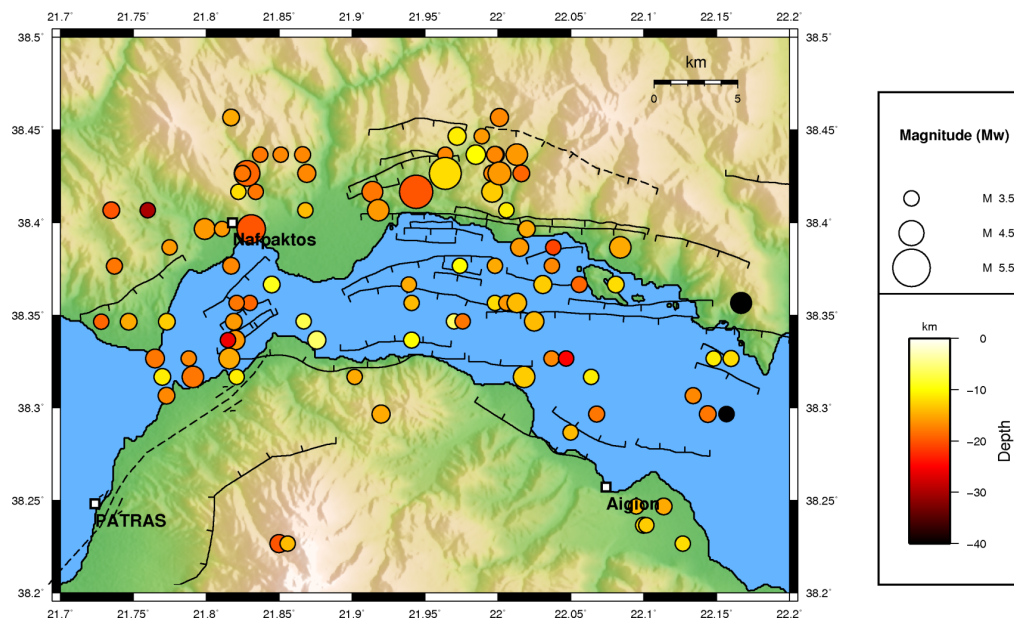

Figure 3.17 Seismicity map presenting the seismic events instrumented in the wider Gulf of Corinth region during the last 10 years (2003 – 2013) with magnitude Mw ≥3.5. Data obtained from the "Hellenic Unified Seismological Network-HUSN" / Institute of Geodynamic / National Observatory of Athens. The main fault traces have been marked according to Doutsos and Poulimenos (1992), Flotté et al. (2005), Papanikolaou et al. (1997) and Valkaniotis (2009) (kindly provided by D. Giannopoulos – University of Patras).

4 Southwestern Gulf of Corinth

4.1 General

The extremely high rates of concentrated seismicity (Fig. 3.15, 3.16), the continuous neotectonic activity deforming the coastal region of the NW Peloponnese, the exposal of the well preserved sedimentary sequences and the evidence of the intense geomorphological processes indicate the consequences of the active deformation in the Gulf of Corinth. This active deformation, resulting from the high extensional rates (reaching approx. 14±2mm/yr) renders the western part of the Gulf as the most active of the Corinth Rift, arising special interest for a detailed morphotectonic approach.
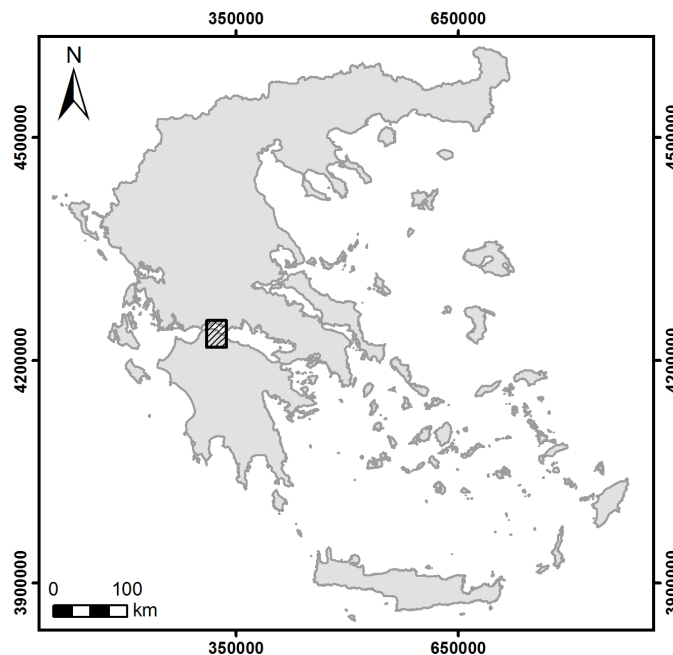

Figure 4.1 The location of the study area, indicated by the hatched rectangle.

The narrow study area of the current work (Fig. 4.1) has been selected with regard to the Psathopyrgos - Lakka fault block, which is bounded by two major E - W trending normal faults: the Psathopyrgos fault to the north and Lakka fault to the south. Laterally, it is bounded by the drainage divides of Foinikas river to the east and Volinaios river to the west.
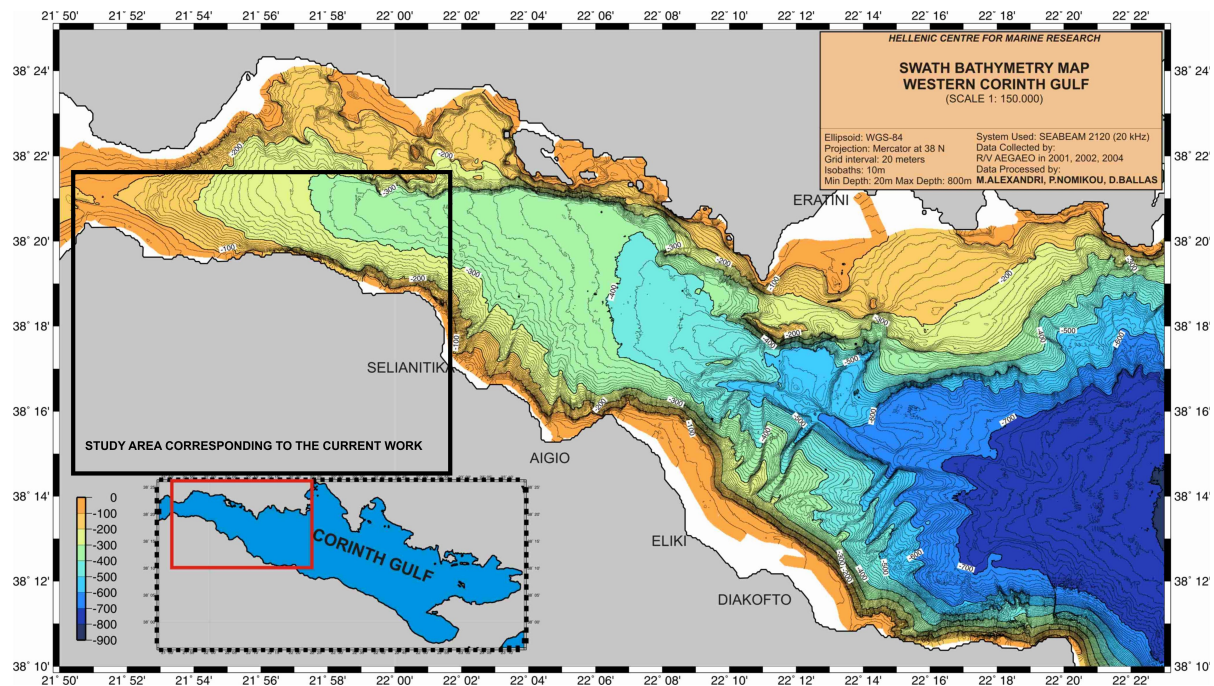

Figure 4.2 Detailed swath bathymetry map of the Western Corinth Gulf using 10m isobaths (Nomikou et al., 2011). The black rectangle corresponds to the current study area.

4.2 Materials and Methods

The dominant fault blocks, which form the southwestern part of the Gulf of Corinth and are defined by E –W trending, north dipping normal faults, are accompanied by several morphological impacts, noticed in both the terrestrial and the marine environment. Since the main aim of the current study has been to examine how the tectonic evolution, in combination with the attendant fierce erosional and sedimentary processes, has affected the general morphology, an interpretation of submarine and subaerial morphological mapping has been of utmost importance.

The construction of a Digital Elevation Model (DEM) corresponds to the basis of the morphotectonic analysis as it provides a representation of the terrain's surface from which various quantitative values may be extracted. These values may allow the evaluation of specific morphostructural elements and characterise various processes that affect the landscape.

High-resolution multibeam bathymetry combined with the available land surface data have been primarily used for the construction of a DEM, which is subject to further detection of all those geomorphic features and anomalies that indicate the on-going active tectonic deformation. It

30

should be highlighted that the whole morphotectonic approach of this study has been based on the combined onshore and offshore datasets. Both the datasets and methodologies that were used for the processing of this work are analysed briefly below.

The whole study has been performed by the ArcGIS software (ESRI, ArcMap V.10) with the additional use of other terrain mapping tools such as Global Mapper V.13 (BLUE MARBLE GEOGRAPHICS) and Surfer V. 10 (GOLDEN SOFTWARE).

Offshore Survey and System Deployment

All the methods used for the exploration of the geological features existing in the marine environment vary from those used for the onland geological surveys due to the water presence, which makes the exploration harder for the researchers. As a result, exploration ships with expensive technical equipment (e.g. multibeam sonars) are often needed to compensate the barrier of water and make scientific observations on a hard to reach environment. Bathymetric data can be collected by multibeam echosounders (MBES), which use hundreds of very narrow adjacent beams arranged in a fan-like swath (typically 90° to 170° across), providing in that way very high angular resolution and accuracy.

The dataset of the offshore region of the current study has resulted from high-resolution multibeam bathymetric surveys which were carried out by the R/V AEGAEO (Fig. 4.3) of the Hellenic Centre for Marine Research (HCMR), using the multibeam sonar SEABEAM 2120 swath system during the 2001-2004 cruises within the frame of various EU and National projects like ASSEM (Lykousis et al., 2006, Nomikou et al., 2011). Four successive missions covered the whole offshore area in the Gulf of Corinth: March 2001, February 2002, July 2002 and October 2002 (Fig. 4.5).

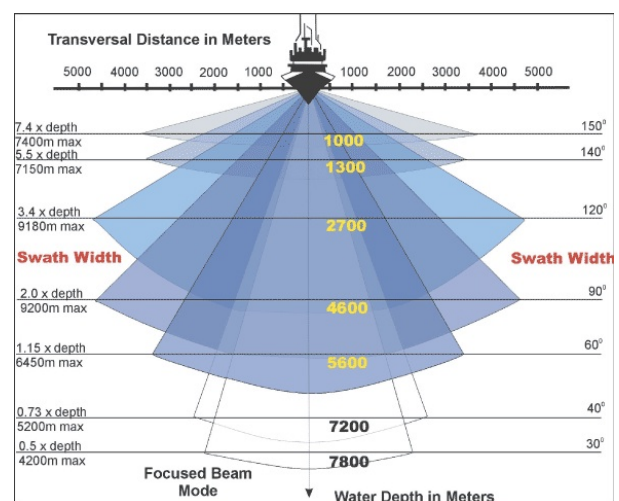**Figure 4.3** Research Vessel AEGAEO (HCMR), 62.00m in length, may reach 12.50 knots maximum speed.

Figure 4.4 Expected performance of the of the SEABEAM 2120 system (image source: GEOWARN).
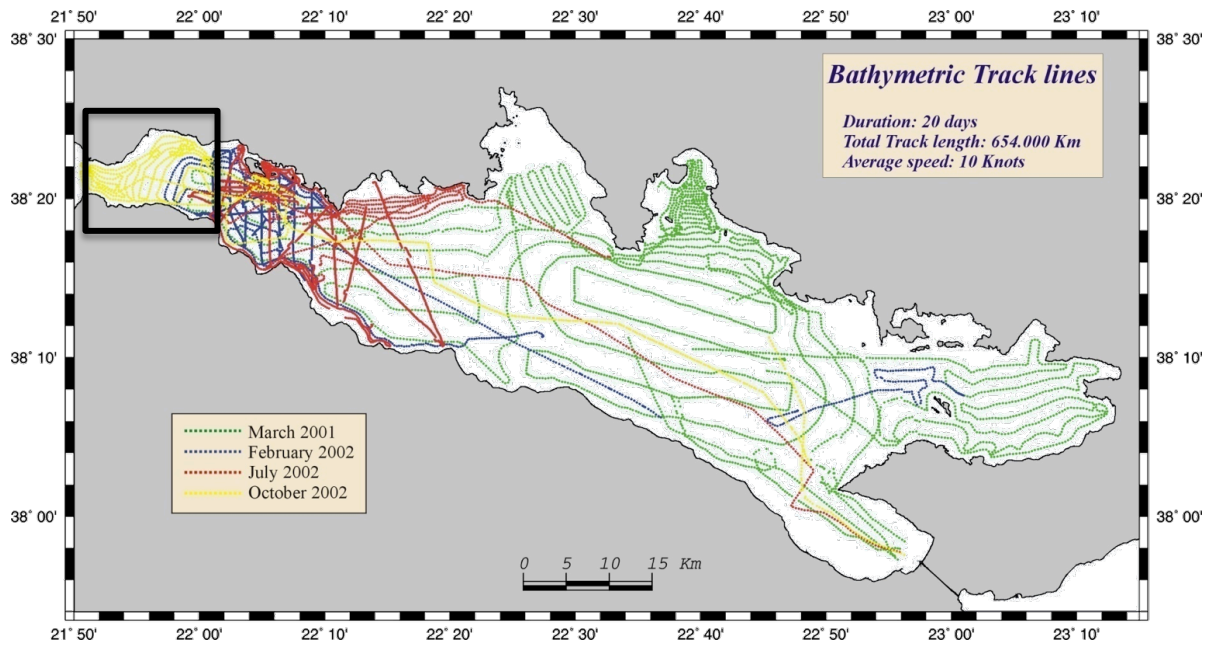
Figure 4.5 Bathymetric Track lines during 2001-2004 oceanographic cruises with R/V AEGAEO (Nomikou et al., 2011). The polygon includes the track lines (yellow lines) related to the dataset used for the offshore DEM of the current study.

The SEABEAM 2120 (Fig. 4.4) corresponds to a hull-mounted swath system operating at 20 kHz in water depths not exceeding 6000 m. It has an angular coverage sector of 150° with 149 beams, covering a swath width from 7.5 to 11.5 times the water depth for depths from 20 m to 5 km. The maximum swath coverage can reach 9 km at maximum depth and gives satisfactory data quality at speeds up to 11 knots. GPS navigation (Trimble 4000) provided the average position of the ship to within ±10 m (Nomikou et al., 2011).

The multibeam data have been extensively processed by means of data editing, cleaning of erroneous beams, filtering of noise, processing of navigation data and interpolation of missing beams. Multibeam bathymetry always includes some erroneous soundings, and consequently, editing or filtering of some sort is required to remove these artefacts (Caress et al. 2008). MB-System provides several tools (MBedit and MBeditviz) for processing bathymetric raw data in order to clean random extreme values.

After the correction procedure, the processed swath bathymetry data are translated into a uniformly spaced terrain model, commonly into a grid file, using a MB-System program called MBgrid. The preferred MBgrid algorithm uses the sonar geometry, altitude, and the angular beam widths to calculate the location and size of the seafloor footprint associated with each sounding. A weighting value is calculated for each grid cell that fully or partially lies within the beam footprint, these weighting values represent the fraction of the beam contained within the cell. This approach allows one to sensibly grid data using a resolution greater than that of the

raw data. The resolution achieved has been a 50m-grid cell, which is a satisfactory resolution for merging with the available land surface data.

Onshore data utilization

The land surface dataset (Fig. 4.6A), combined with the bathymetric grid (Fig. 4.6B) has led to the generation of a complete coverage, high resolution DEM file (Fig. 4.6C). The DEM accuracy has a great influence on the interpretation results obtained by terrain analysis. During the processing of the DEM file, further vector data have been used for the onshore region (coastline and drainage pattern) in order to achieve more detailed processing and, consequently, more valid results. The final merged DEM (Format: Grid / Cell Size x, y: 5, 5), constructed for the purposes of the current study, is referenced to the projected coordinate system GGRS87 (Datum: Greek Geodetic Reference System 1987 or Greek Grid, Method: Transverse Mercator).
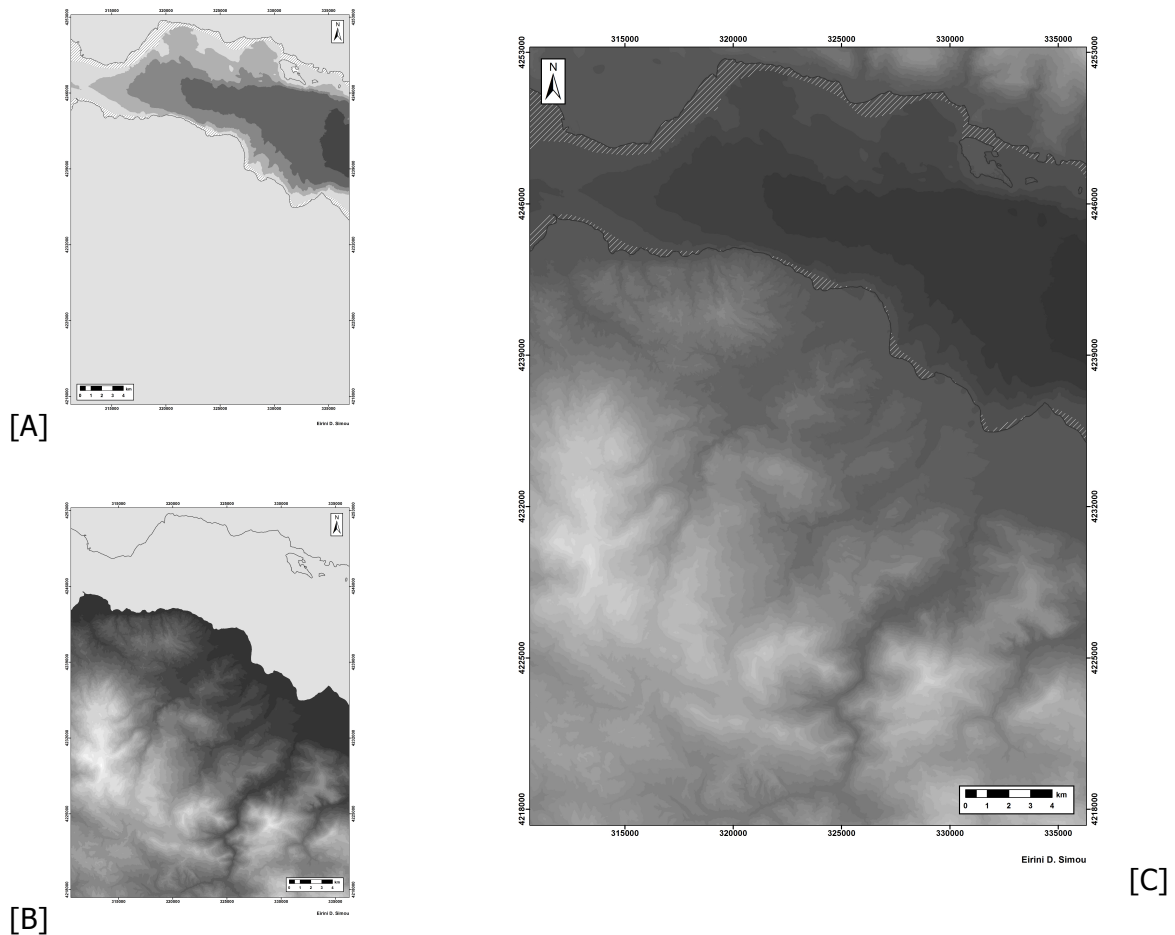

Figure 4.6 Generated DEM files for the wider study area. Darker colours indicate lower topographic values. **[A]** DEM 5m-resolution of the offshore region. **[B]** DEM 5m-resolution for the onshore region. **[C]** Merged DEM 5m-resolution (Synthesis of [A] and [B]). The stripped area corresponds to no data zone where values have resulted from interpolation during the DEM generation.

A series of attribute maps, further created from the merged onshore and offshore DEM, has enabled accurate submarine and subaerial morphological mapping in the southwestern part of the Gulf of Corinth. The conjunction of the individual DEM files provides the possibility of mapping the offshore continuation of the most distinct geomorphic features. The mapping of the extent of the geomorphological elements reveals a wealth of interesting structures, providing an insight into the erosional, sedimentary and tectonic evolution. Most of the attribute maps have been used in combination with a hillshade map (Fig. 4.7) aiming to approach a more realistic final model of the study area.
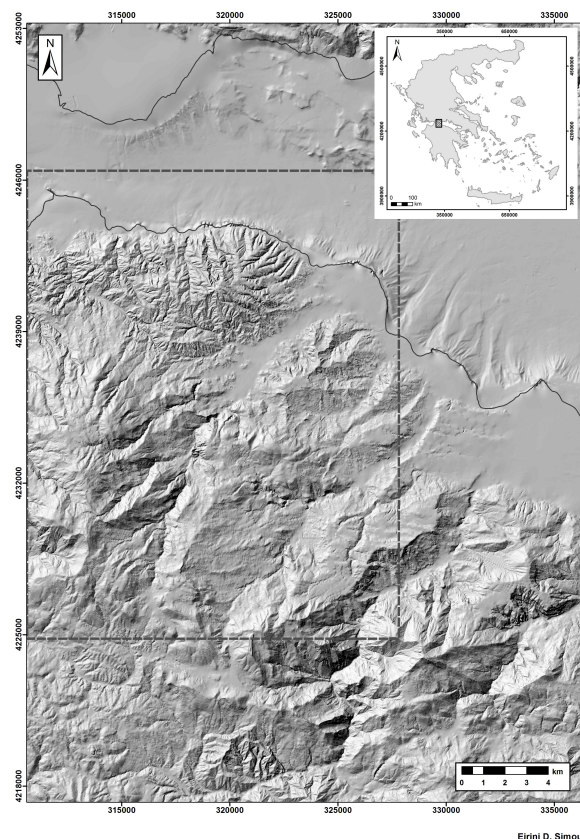
Figure 4.7 Hillshade map generated by using the merged DEM of Fig. 4.6C .The hillshade attribute map has been further combined with the other maps of this study aiming to present a more realistic model. The area marked by the dashed line corresponds to the selected study area.

The attribute maps that have been generated for the morphotectonic analysis are the following:

- Synthetic Topographic Map.

   The topographic map is characterized by large-scale detail and quantitative representation of the relief for both the terrestrial and the marine environment, using contour lines (isohypses for the land surface data and isobaths for the bathymetric data). The selected contour interval is 20m; however the isobath interval is set to be 4m, aiming to display more clearly

the gentle topographic relief of the basinal area. The minimum elevation value in the wider study area is ~ -420m towards the northeastern part and the maximum ~+1924m towards the southern part. The onland topography is based on the maps of the Hellenic Military Geographical Service (Sheets: Aigion, Amygdalea, Chalandritsa, Evinochorion, Nafpaktos and Patra, Scale: 1:50000).

- Slope Distribution Map.

  Slope maps are drawn based on elevation raster datasets to show the areal distribution of the degree of slopes. During the generation of a slope map, the ArcMap algorithm calculates for each cell of the raster the maximum rate of change in slope value from that cell to its neighbour's. The output slope raster, created by the merged DEM, has been calculated in degrees and is classified afterwards in a way that all the significal geomorphological structures are well displayed. The extracted slope values concerning the current study range between 0° and ~66°. The geomorphological signatures, identified from the slope distribution map, have affected topography allowing the configuration of the active faulting in the study area. The slope distribution map processing has contributed to the distinction of the major tectonic structures. The classification and the analysis of the Slope Map are presented in a following paragraph.

- Aspect Map.

  Aspect maps result from raster surfaces and identify the downslope direction of the maximoum rate of change in orientation values from each cell to its neighbour's. The values of the output raster are measured clockwise in degrees from 0° (North) to 360°, presenting a full circle, representing the direction of each slope face. The Aspect Map and the relevant analysis are presented in paragraph 6.1.

- Geomorphological Bathymetric Map

  This map presents the bathymetry in the study area with a distinction of three morphological areas according to the slope distribution in the marine envvironment: the continental slope, the continenat shelf and the basinal area.

- Simplified Geological Map.

  The Simplified Geological Map presents the development of the Pleio-Quaternary sediments and the outcrops of alpine pre-rift basement in the onshore study area. The digitization of the geological formations was accomplished with the contribution of the Geological Maps of Greece (Institute of Geology and Mineral Exploration), sheets: Aigion, Amygdalea, Chalandritsa, Evinochorion, Nafpaktos and Patra, Scale: 1:50000).

- Drainage Pattern Maps.

  Drainage analysis is extremely useful in structural interpretation as long as the drainage disorders reveal tectonic structures that have significant influence on the current topographic relief. The characteristics of the drainage pattern, the drainage texture, individual stream patterns and drainage anomalies can be observed on the drainage maps which have been created in the framework of the current study. The generated maps, including a Classified Drainage Map, a Synthetic Drainage Map and a Synthetic Onshore and Offshore Drainage Map, are presented and analysed in a following chapter. It should be mentioned that in the Synthetic Onshore and Offshore Drainage Map the submarine drainage pattern has resulted from flow accumulation based on the merged DEM of the study area.

More maps, showing the planation surfaces distribution and the deep incision zones that have resulted from the intense erosional processes in combination with the fault activity, have been also generated and interpreted, aiming to build the geological and geomorphological model of the study area.

It should be mentioned that despite the fact that this study's aim has been the morphotectonic analysis between Selianitika (Foinikas river, eastern boundary) and Psathopyrgos (Volinaios river, western boundary), during the processing of the maps a wider area has been taken into consideration (from Eliki to the west and the whole Corinth basin to the north). This was achieved in order to give a better perspective of the general geological and geomorphological model.

The morphotectonic interpretation, finally accomplished by the compilation of the previously presented maps in conjunction with the regional geological, tectonic and geomorphological setting, has led to the construction of the Morphotectonic Map, which illustrates the major morphotectonic features of the project area (Paragraph 6.4).

Field Work

Field work has been carried out during January ÷ May 2013 aiming to collect data from the study area which would be subsequently useful for the verification of the results of the morphotectonic interpretation. The collected field data include sedimentary and, mainly, structural information (dip and dip direction of significant stratigraphic or fault planes), sketches and photographic material. Most of these data have been taken into account during the processing of this study and are presented either on the constructed maps or in the following chapters.

5 Geological Remarks

5.1 Geological Formations in the Study Area

Before continuing to the morphotectonic interpretation, which has been the main aim of this work, the geological setting of the southwestern part of the Gulf of Corinth should be discussed in more detail for the study area. This is of great importance, as all the morphotectonic features are meaningless without being correlated to the lithology on which they develop.

As it has already been mentioned, the NW Peloponnese is mainly characterized by extensive occurrence of post-alpine deposits of Plio-Quaternary (Ori, 1989) and alpine formations of Pindos nappe (Fig. 5.4). The first formations correspond to Gilbert-type fan delta deposits (older or currently evolving) and indicate the high uplift rates of the south flanks of the Gulf of Corinth while alpine formations compose the pre-rift basement.

In detail, the geological formations that can be observed at the onshore part of the study area, within the fault block defined by the Lakka and Psathopyrgos faults (Lakka fault block), are the following:

I. **Holocene deposits**, which correspond to alluvial and river deposits (currently forming alluvial delta fans which are further discussed in the paragraph 6.3), scree material, old and recent landslide material and marine terraces deposits. Alluvial deposits (Fig. 5.1) are mainly silts and sands with scattered limestone gravels of various sizes, and originated from the Pindos alpine basement. River deposits also correspond to loose rounded pebbles and cobbles, originated from the alpine formations (limestone and chert origin), transferred by the active streams, flowing to the Gulf of Corinth. Scree materials (Fig. 5.2) are loose angular limestone and chert fragments with significant proportion of fine-grained sediments (mainly clays). The landslide materials (Fig. 5.3) are products of the successive landslides that have occurred within the Plio-Pleistocene formations or the basement outcrops and they can be classified as: (a) slumped pebbles and cobbles derived from the Holocene river deposits, (b) fine-grained material within

the cohesionless alluvial deposits, (c) fine-grained sediments and gravels that have been washed downslope due to intense erosional processes, (d) fine-grained materials resulted from the slided cherts disintegration and, (e) fine-grained materials with angular pebbles resulted from the slided limestone decomposition. The old slided masses, as well as the scree materials, constitute two the most significant formations in the study area since they are mostly related to the active erosional processes. The thickness of these formations is about 2-10m near the higher topographic areas and exceeds the 30m near the lower topographic areas and the coastline (Sakellariou et al., 2001b).

Figure 5.1 Alluvial deposits consisting of clays with angular fragments of Pindos limestones.

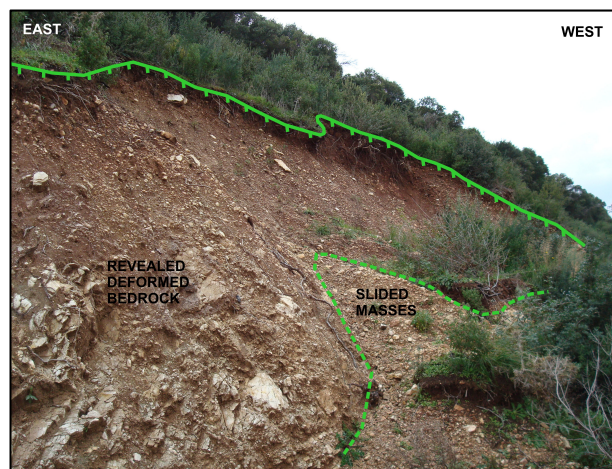**Figure 5.2** Scree material originated from limestone formations.

Figure 5.3 Active sliding masses (fine-grained material with angular limestone fragments) towards the Psathopyrgos fault plane.
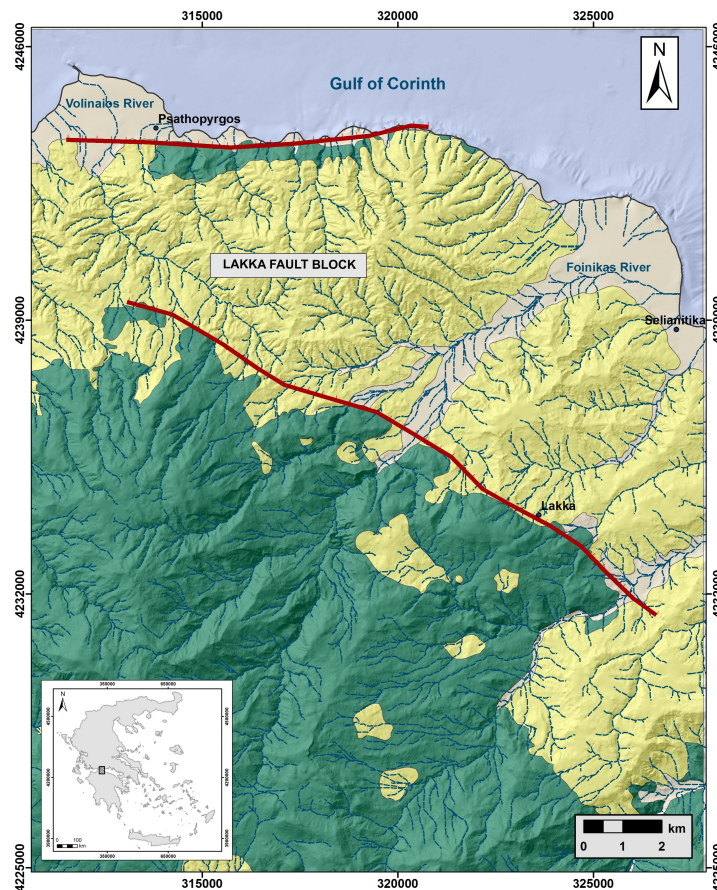
Figure 5.4 Simplified Geological Map of the study area, presenting the development of the Holocene (mainly river) deposits (beige colour), the Plio-Pleistocene formations (yellow colour) and the alpine basement of Pindos Geotectonic Unit (green colour). The red lines represent the Psathopyrgos and Lakka fault traces, which bound the onshore study area (Lakka fault block).

II. **Plio-Pleistocene sediments**. A detailed description of the Plio-Pleistocene deposits is given in Paragragh 3.3 of the current study, based on Ori's (1989) previous work. In the Lakka fault block, these sediments correspond to braided river deposits, which are coarse alluvial conglomerates with fine-grained sediments (mainly sands) of Plio – Pleistocene age (older Gilbert fan deltas), unconformably lying over the alpine basement and tilted 20° - 40° southwards (Papanikolaou et al., 2005).

The stratigraphic sequences of the study area (Fig. 5.7 – 5.9) have been analysed by Palyvos et al. (2010). According to their studies, the Plio-Pleistocene formations of the Lakka fault block are composed by Early – Middle Pleistocene alluvial fan deposits (pebbles and gravels turning out to silts) and, locally, Early – Middle Pleistocene fluvial to fluvio-lacustrine and younger marine deposits (fine-grained materials and gravels), overlain by Middle Pleistocene lacustrine and brackish or marine sediments (Fig. 5.5, 5.6).
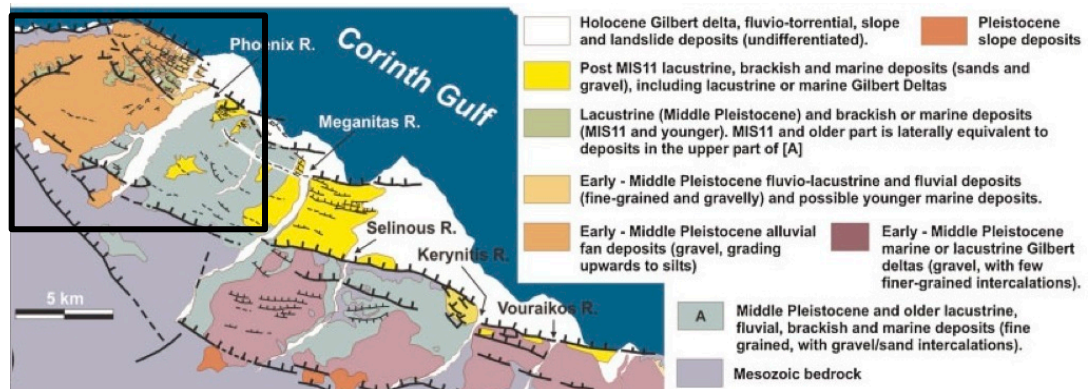
Figure 5.5 Geological sketch map of the onshore part of the western Gulf of Corinth (Palyvos et al., 2010), showing the distribution of the post-alpine sediments and the identified fault structures. The rectangle on the map represents the current study area.

More specifically, recent studies of Palyvos et al. (2013) further defined two syn-rift groups recognized in the uplifted Lakka fault block; the Profitis Elias group and the Galada group. The lithostratigraphic units are being presented on the following table (Tab. 5.1).
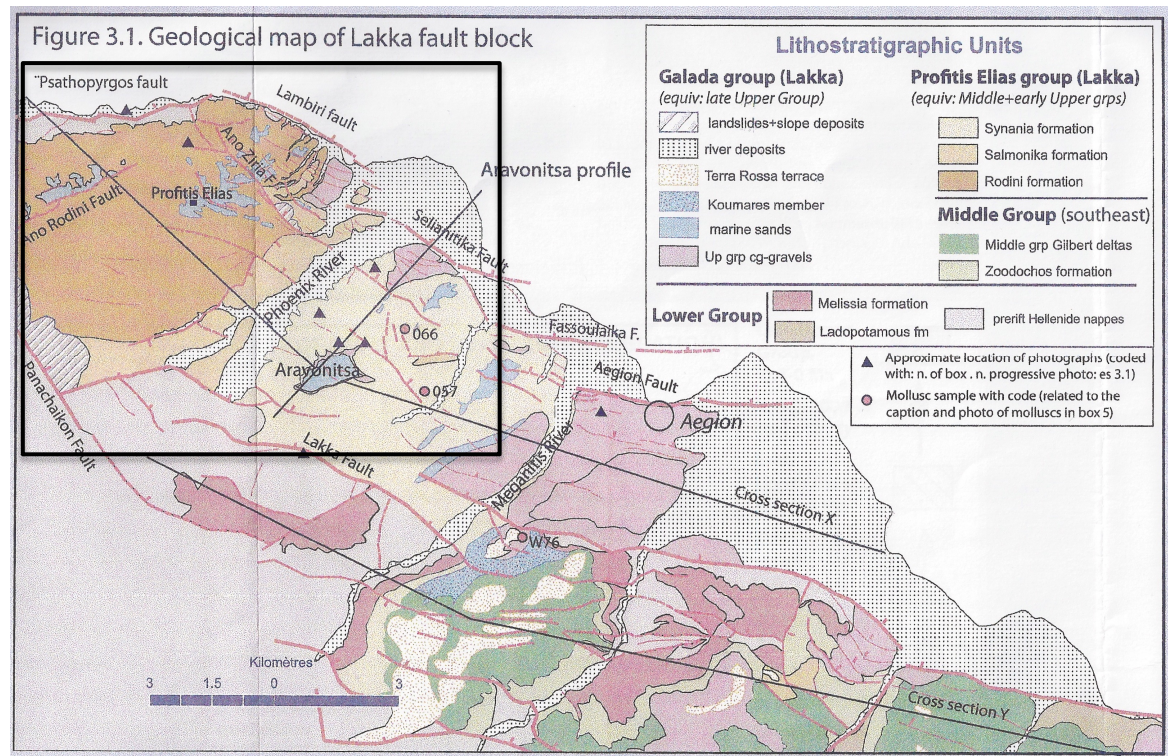

Figure 5.6 Geological map of the Plio-Pleistocene formations of the Lakka fault block by Palyvos et al. (2013). The description of the formations displayed on the map is given in detail in the text. The black rectangle indicates the onland area of the current study.

Table 5.1 Syn-rift lithostratigraphic groups in the area of interest by Palyvos et al. (2010; 2013)

GALADA GROUP (Middle Pleistocene – Holocene)		It comprises marine deposits and terraces that mainly document the footwall uplift due to the activity of the Psathopyrgos fault zone. This formation is characterized by: - Fine sands with marine influence. - Pebbly Gilbert-type fan deltas. - Coastal gravels.
PROFITIS ILIAS GROUP (Lower-Middle Pleistocene)	Synania Formation	Deltaic and shallow water sandstones in alternations with lacustrine marls, silts, siltstones and fine sandstones, with rare layers of conglomerates and lignites. Freshwater to brackish conditions with occasional marine levels are also indicated supporting an Early to Middle Pleistocene age.
	Salmonika Formation	Fluvial sandstones, siltstones and conglomerates towards the eastern and southeastern part of the study area.
	Rodini Formation	Most extensive formations in the Lakka fault block. Coarse alluvial conglomerates with sands, located in the immediate footwall of the Psathopyrgos fault.

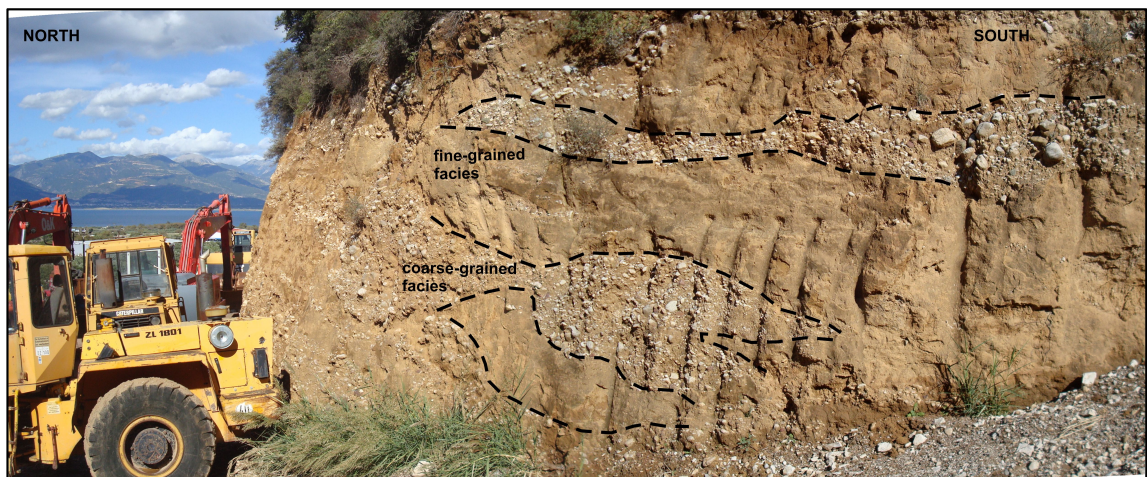**Figure 5.7** Different facies of the Plio-Pleistocene formations.

Figure 5.8 Profile of alluvial fan deposits (alternations of pebbles and gravels turning out to silts) near Psathopyrgos.

Figure 5.9 Panoramic view of the Plio-Pleistocene deposits in Lakka fault block, dipping ~30° towards south (Rodini formation).

III.   **Alpine formations**. They conform the geological basement of the wider area which is the Pindos Geotectonic Unit (Fig. 5.10). The alpine formations in the study area correspond to Upper Cretaceous Limestones, characterized by aternations of thin-bedded, folded, clastic, crystalline limestone with nodules and chert layers and Jurassic – Lower Cretaceous Cherts. This latter formation corresponds to alternations of cherts,

radiolarites and shales with intercalations of platy, reddish to grey-white coloured limestone.

Towards the Psathopyrgos fault plane, remnants of the hanging wall formations can be observed (Papanikolaou et al., 2005), presenting a specific bedding (pseudo-bedding) which is not representative of the undeformed bedrock.

Figure 5.10 Outcrops of the thin-bedded, folded Upper Cretaceous limestones of the Pindos Geotectonic Unit towards Panagopoula.

As far as the offshore area is concerned, the geological conditions are, briefly, the following:

I. Tourbidites at the upper parts of the slope, with a thickness of about 100-150m near the centre of the basin. These deposits are sandy silts in intercalations with sandy gravels and silty clay (Papanikolaou et al.1997; Upper lithoseismic group - Sakellariou et al. 2001b).

II. Debris avalanche deposits (Fig. 5.11), completely chaotic and deformed, which have resulted from older landslide movements (Middle lithoseismic group - Sakellariou et al. 2001b). This formation is relevant to the onshore scree material.
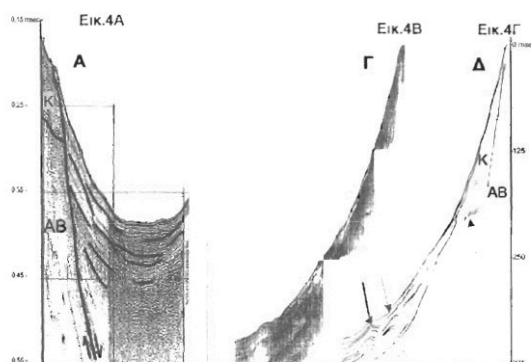

Figure 5.11 Seismic profiles near Panagopoula area and interpretation by Sakellariou et al. (2001). Arrows indicate landslides. AB: Alpine basement. K: Debris avalanche deposits.

I. Alpine basement that consists of Upper Cretaceous limestones of Pindos Geotectonic Unit (Lower lithoseismic group - Sakellariou et al. 2001b).

5.2 Major Tectonic Structures

The three main distinct fault structures, already known for their morphological implications on the land surface and the marine environment, which are structurally related to the study area, are the Lakka, the Psathopyrgos and West Eliki fault.

The Lakka fault

The Lakka (or Lakka – Sella) fault (Fig. 5.12, 5.13) represents a westward prolongation of the West Eliki fault (Stemberk & Košťák, 2007). The fault structure bounds the study area to the south, presenting the alpine basement of the footwall, south of the Lakka village (Fig. 5.4). The fault plane is oriented in a SE – NW direction (~110° to 130°), dipping 45° to 55° towards north. The fault plane is formed on Pindos limestones and debris materials (Fig. 5.17) have covered the fault slope toe. Well-preserved striations (Fig. 5.16), inclined towards northwest (~35°/345°) are distinct on fault plane.
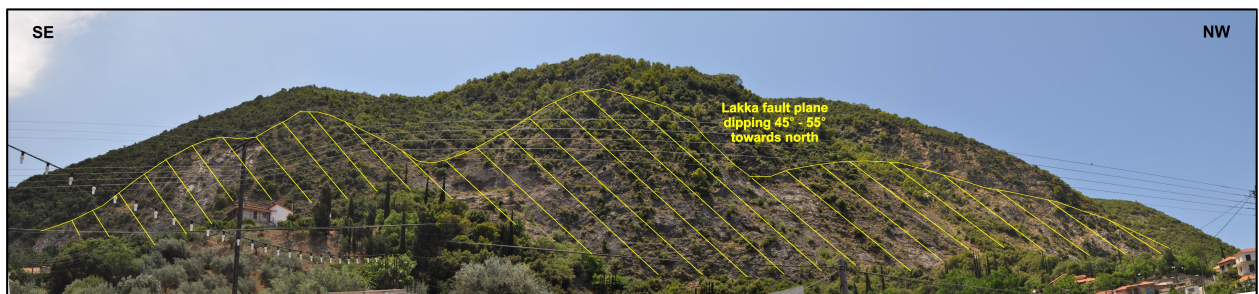

Figure 5.12 The E –W trending, north dipping, normal Lakka fault, as it can be observed south of the Lakka village, Achaea (view from the N).
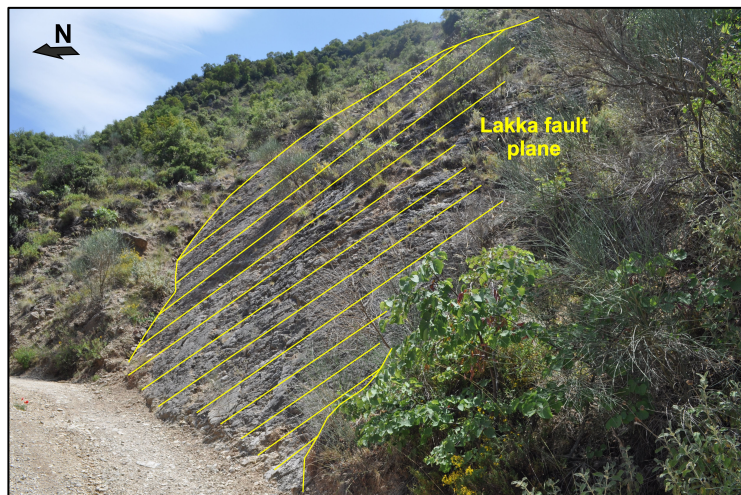

Figure 5.13 View of the Lakka fault plane, developed in limestones of Pindos Geotectonic unit.

44

Figure 5.14 Part of the Lakka fault plane with the preserved 35°/345° striations.

Figure 5.15 Debris and scree material on the toe of the fault plane.

The Psathopyrgos fault

The E - W trending, north dipping Psathopyrgos fault (Fig. 5.4) is considered to be the presently active structure bordering the westernmost part of the Gulf of Corinth to the south (Doutsos et al., 1988; Doutsos & Poulimenos, 1992; Palyvos et al. 2007). The steep coastal escarpment of the fault plane exposed at the coastal zone (Fig. 5.18, 5.19), related to the high topographic relief and the outcrops of the alpine pre-rift basement, indicates the high rates of the tectonic activity, which is demonstrated by rapid uplift (in the order of ~0.7-0.8 mm/year) of the footwall (Houghton et al., 2003).
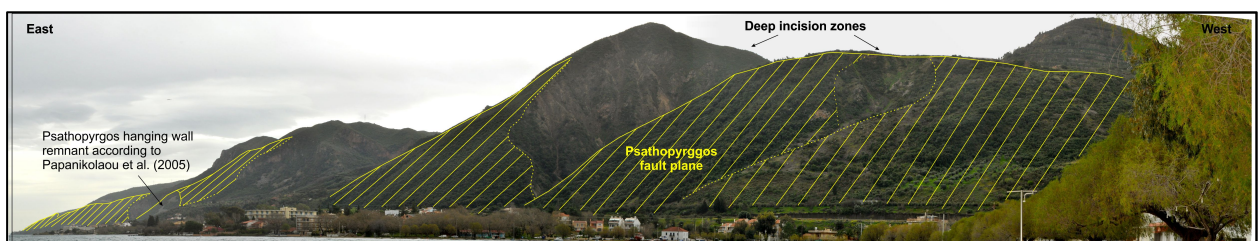

Figure 5.16 Panoramic view of the Psathopyrgos fault plane (picture taken from the Psathopyrgos village, view from NW).
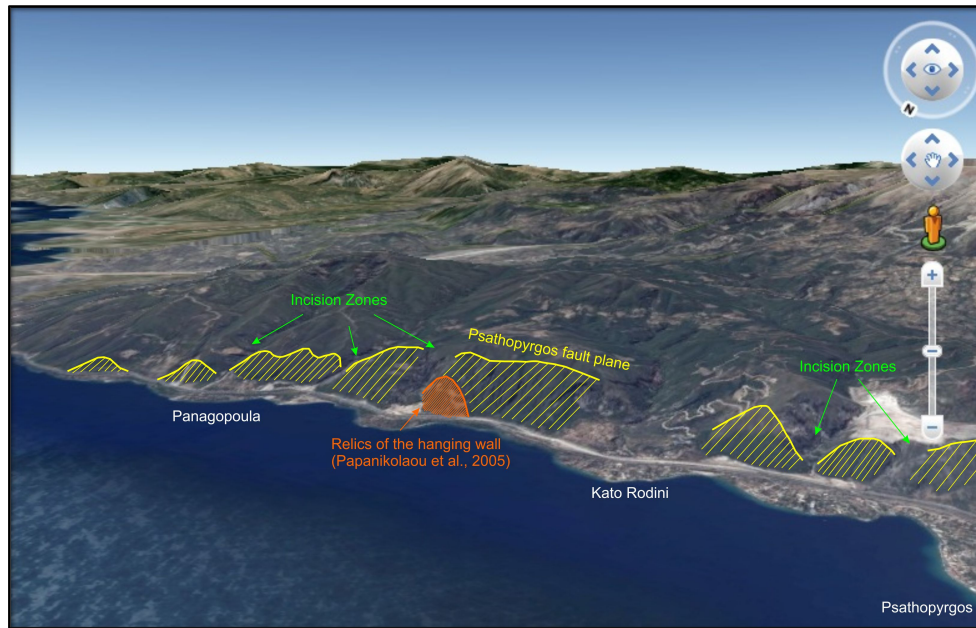
Figure 5.17 The Psathopyrgos fault (Google Earth photo, view from northwest).

The Psathopyrgos fault, mainly developing in the Upper Cretaceous limestones of the Pindos geotectonic unit (Fig. 5.20), corresponds to the most dominant structure of this study as its onshore geomorphic expression exceeds 15km in length. The dip of the fault plane has been locally measured approx. 40° - 65° while the fault throw has been determined more than 400m since Lower – Middle Pleistocene, as it can be calculated by the subsidence of the Pleistocene deposits which unconformably overlie the Pindos alpine basement (Papanikolaou et al., 2005). In several localities, the fault plane is characterized by superimposed remnants of the hanging wall formations, presenting distinct pseudo-bedding (Fig. 5.21), which seems to be continuous along the entire length of the fault structure and is representative of the deformed bedrock.

Figure 5.18 Different views of the Psathopyrgos fault plane towards Panagopoula and Rodini respectively. In the second photo, the deformation zone in front of the fault plane can be observed.

Figure 5.19 Part of the Psathopyrgos fault plane (~60°/350°) south of Rodini village. In front of the fault plane, pseudo-bedding (~55°/075°) has been developed within the thin-bedded limestones, as a result of the tectonic deformation.

The West Eliki fault

The Eliki fault zone is formed by a system of major normal fault segments that border part of the western Gulf of Corinth towards south (Stewart, 1996; Stewart & Vita-Finzi, 1996; Stemberk & Košťák, 2007). The total length of the Eliki fault system can be divided into two main fault segments of approx. 15 – 20km in total length, which are generally referred as eastern and western Eliki faults. The fault surface of the western Eliki fault (Fig. 5.12, 5.13) trends from 82° to 125°, dipping 55° – 70° towards the north. On the fault surface remarkable vertical striations can be observed, in correspondence with the dip of the fault plane. Ghisetti et al. (2001) have estimated a maximum vertical offset of approximately 700 – 800 m while many scientists have attempted slip rates calculations during the past decades. More specifically Pantosti et al. (2002) have assumed a minimum slip rate of 2 mm/year and estimated the age of about 300 – 325 kyr, Armijo et al. (1996) and De Martini et al. (2002) obtained a slip rate of 5 mm/year for an age of about 120 – 130 kyr.

The West Eliki fault characterizes the western segment of the Eliki fault and is evaluated in this study only in the framework of instabilities distribution (Chapter 7). It is considered as a currently inactive structure with regard to the Corinth rift evolution and its relative impact on the morphology of the surrounding area (including the coastal zone) will be a matter of

discussion in comparison to the currently active Psathopyrgos fault as far as coastal zone mass failures are concerned.

Figure 5.20 Part of the West Eliki fault segment as it can be observed from the New Corinth – Patras Highway (view from the N).

All the above-mentioned major tectonic features, the West Eliki, the Lakka and the Psathopyrgos faults, have been identified during the fieldwork, which was carried for the aims of this study but they have been recognized by their morphological impact as well. Further details are presented in the following Morphotectonic interpretation.
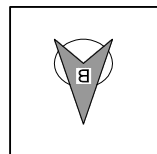
Figure 1 :
Revield part of the Psathopyrgos fault plane towards Panagopoula.
Dip & dip direction of the fault plane:
41° / 348° & 41° / 355°.

Figure 2 :
Part of the Psathopyrgos fault plane. Dip and dip direction range between 48° / 354° & 60° / 350°. The fault plane observed southwards corresponds to the Psilos Vrachos fault (Papanikolaou et al., 2005).
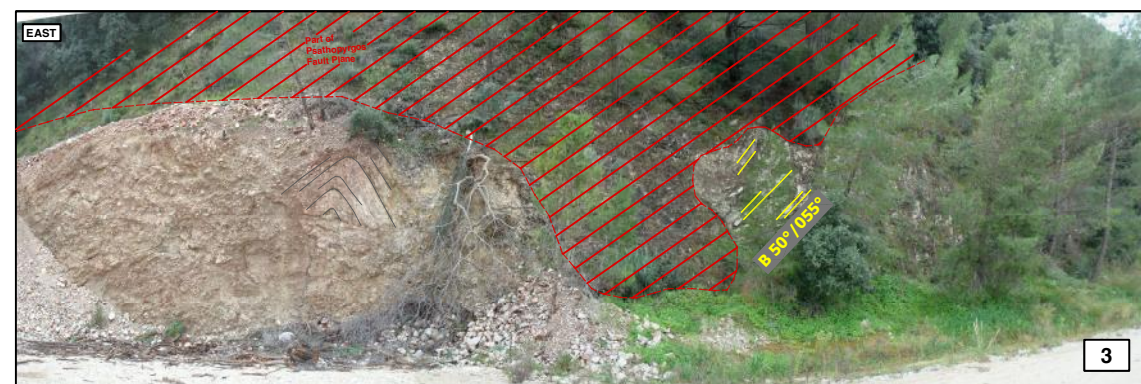

Figure 3 :
The Psathopyrgos fault plane (65° / 358°) south of Rodini.
A part of the folded alpine bedrock (limestones) of Pindos geotectonic unit can be observed on the footwall of the fault (in general, the formations of the footwal appear deformed towards the fault zone).
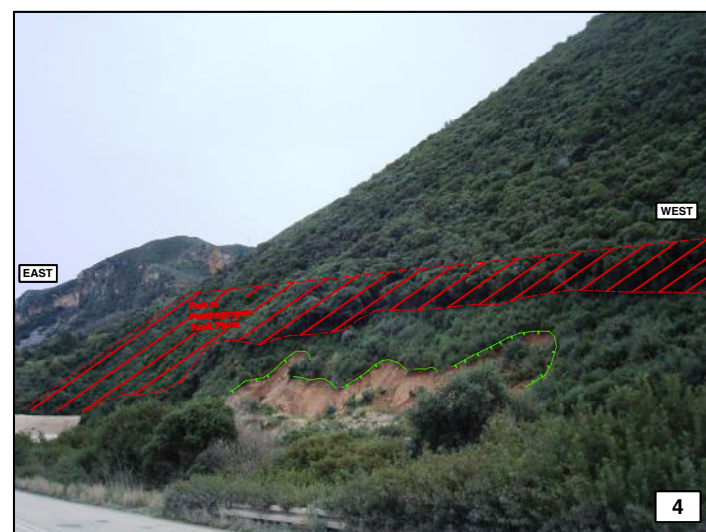

Figure 4 :
Part of the Psathopyrgos east-west trending fault plane south of Rodini, related to local instabilities.

Figure 5 :
Part of the Psathopyrgos fault plane south of Rodini (towards Psathopyrgos village).

Dip and dip direction of the fault plane:
62° / 345° to 66° / 352° .

Pseudo-bedding (~ 55° / 070°) appears in front of the fault plane, indicating the intense tectonic deformation.
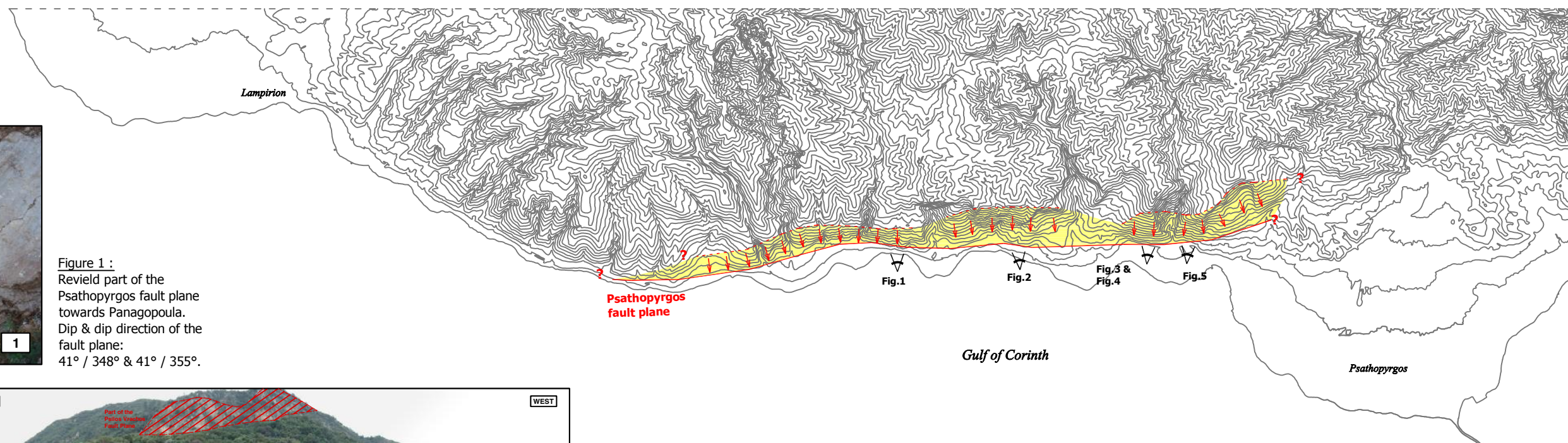
DIFFERENT VIEWS OF THE PSATHOPYRGOS FAULT PLANE

6 Morphotectonic Interpretation

6.1 Slope Distribution and Morphological Slope Analysis

The geomorphological signatures have affected topography allowing the configuration of active faulting in the study area. Synthetic Topographic map and Slope Distribution map processing have contributed to the morphological and morphotectonic analysis of the study area. The topographic map produced by the combined land surface and bathymetric data, offers an initial quantitative representation of the relief for both the terrestrial and the marine environment.
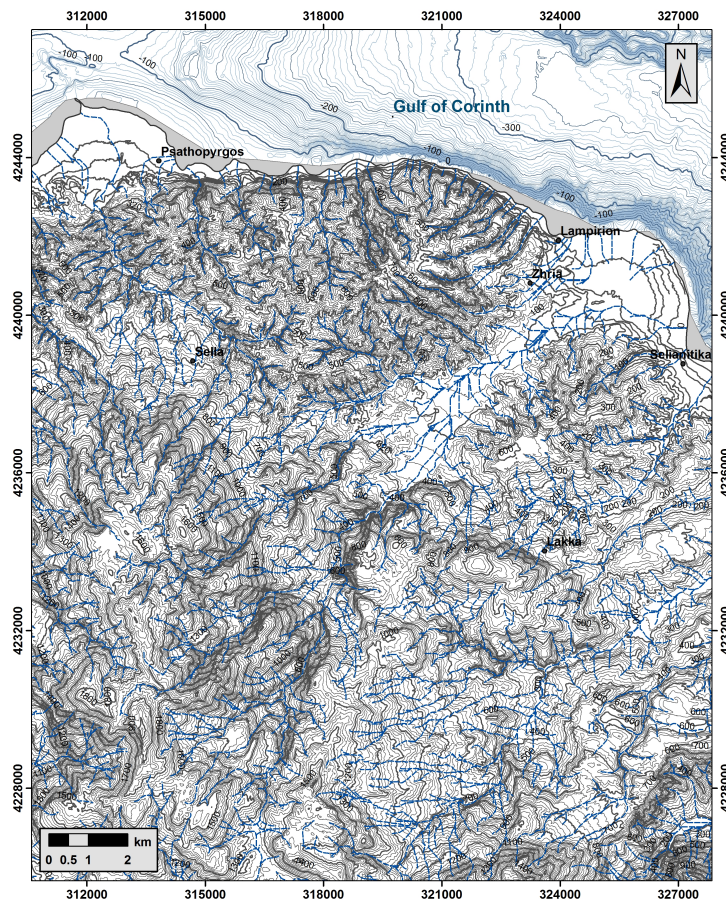

Figure 6.1 Synthetic Topographic Map. The illustrated contour interval is 20m; the isobath interval is set to be 4m, aiming to display more clearly the gentle topographic relief of the basinal area. The minimum elevation value in the study area is ~ -420m towards the northeastern part of the Corinth basin while the maximum is ~+1920m towards the middle/southernwestern part. The onland topography is based on the primary topographic maps of the Hellenic Military Geographical Service (Sheets: Aigion, Amygdalea, Chalandritsa, Evinochorion, Nafpaktos and Patra, Scale: 1:50000). The map is also presented in Appendix I.

The morphological analysis of the study area was processed from the perspective of slope value distribution (Papanikolaou et al., 2002; Nomikou et al., 2011) and the results are presented on the Slope Distribution map (Fig. 6.2). On this map, which has been composed by the combined onshore and offshore datasets, the slope values have been subdivided into seven classes:

a) flat areas of 0°-2°, which can only be observed in the marine environment and correspond to the basinal area of the Gulf of Corinth,

b) areas of mean morphological slope values in the order of 2°-5°,

c) areas of 5°-10°,

d) areas of 10°-15°,

e) areas of 15°-25°,

f) areas of 25°-45°,

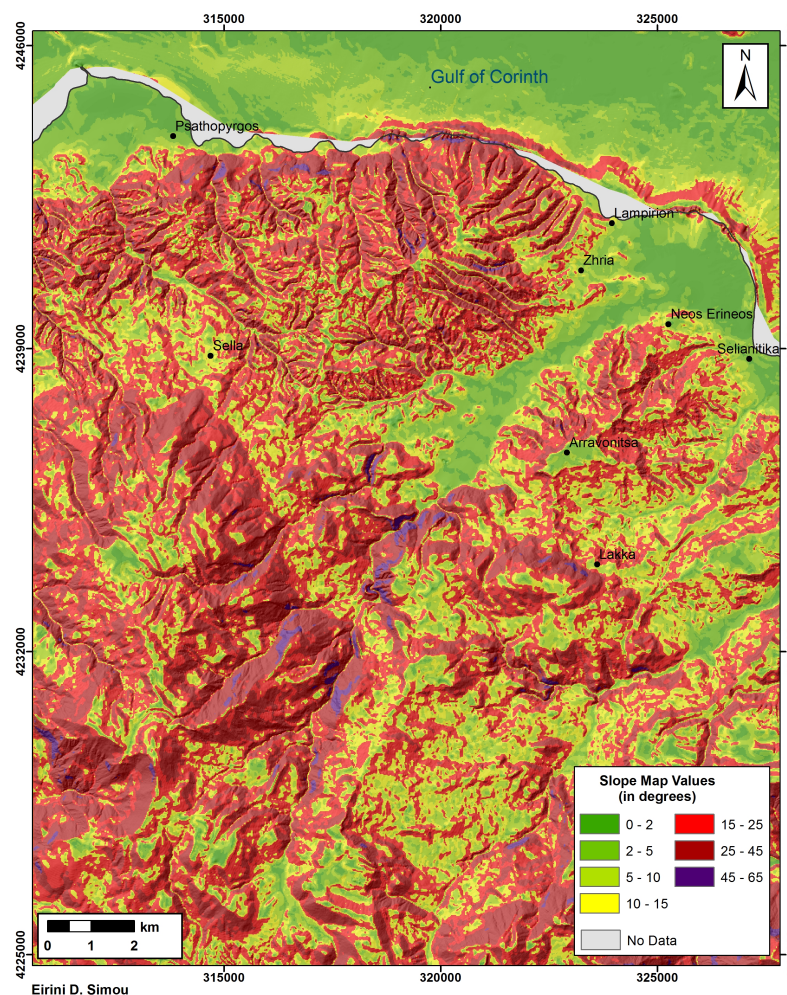g) areas steeper than 45° (maximum slope values are in the order of 65°).

Figure 6.2 Slope Distribution Map of the study area (in GGRS87). The slope values (in degrees) are subdivided into 7 classes as shown in the legend on the map. The grey area corresponds to a no data zone. The map is also presented in Appendix I.

The above classification aims to indicate all those areas, both in the marine and the terrestrial environment, which are characterized by abrupt change of slope values, probably reflecting the position of active tectonic structures or deep incision zones, as a result of active extensional tectonics and intense erosional processes respectively, which have affected extensively the topographic relief.

The study area, according to the classification of the slope values, can be divided into the following areas:

i. The basinal area of the Gulf of Corinth as well as the delta plains of Foinikas and Volinaios rivers. These areas correspond to localities characterized by very gentle topographic relief (almost horizontal planes) with slope values ranging between 0° – 1°. They are related to high rates of sedimentation, especially the basinal area, within the framework of active extensional tectonics in the Gulf of Corinth.

ii. The coastal zone, including the continental slope and the continental shelf (nearshore and foreshore zone, Fig. 6.3), as well as a part of the onland coastal area (backshore zones). The coastal zone in this study can be further divided into two subareas with similar morphology.

   – The first subarea corresponds to the area which extents from the Psathopyrgos fault plane to approximately the half of the continental slope (towards north). This part is mainly characterized by steep slopes of more than 25°. Gentler topographic relief, characterized by slope values in the order of 5° – 15°, can be noticed at the mouths of the north – south trending streams of the NW Peloponnese. The continental shelf, which is generally characterized by very smooth topographic relief, is very narrow, hardly seen in this area due to the effects of active faulting.

   – The second subarea, where slope values range between 5° – 15°, corresponds to the other half part of the continental slope and extends to the limits of the basinal area.
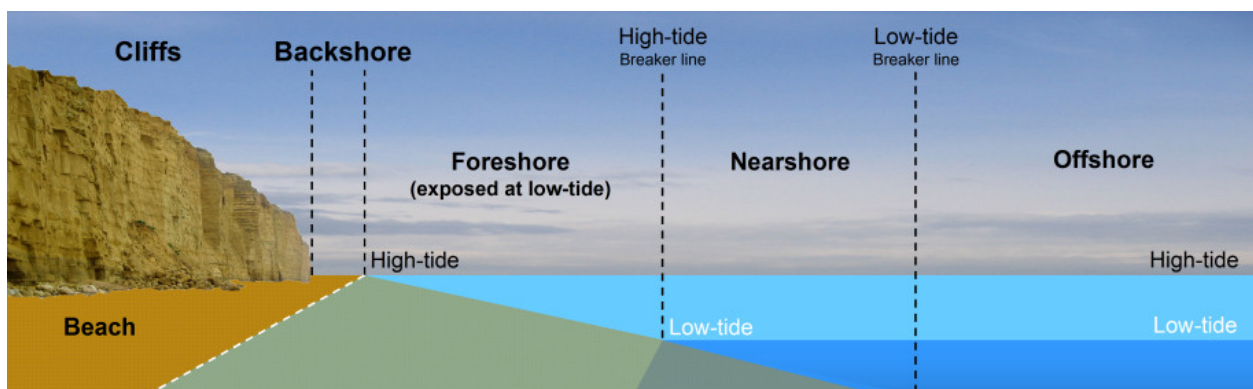

Figure 6.3 Schematic illustration showing the coastal geomorphology.

iii. The hilly – mountainous area (corresponding to the footwall of the Psathopyrgos fault). This area extends to the Lakka fault towards south and is characterized by variable slope values which characterize the maturity stage of the entire onshore area. The intense landform is a result of the interaction of three basic controlling factors: active tectonics, fierce erosional processes and lithology. The steep slopes in the onshore study area clearly reflect existing tectonic structures (such as the Psathopyrgos and Lakka faults) or deep incision zones.

The slope values interpretation of the combined datasets shows that the southwestern margin of the Gulf of Corinth is characterized by very intense coastal relief and a narrow, almost absent, continental shelf, which passes abruptly to the steep submarine slopes. These steep slope values clearly denote the effects of the most recent brittle deformation, which has occurred towards the currently active Psathopyrgos fault zone. The high uplift rates and the rapid sedimentation, indicative of the regional high-energy terrestrial and submarine environment, are subsequently balanced by the transportation of the seafloor currents, especially where slope gradients decrease.
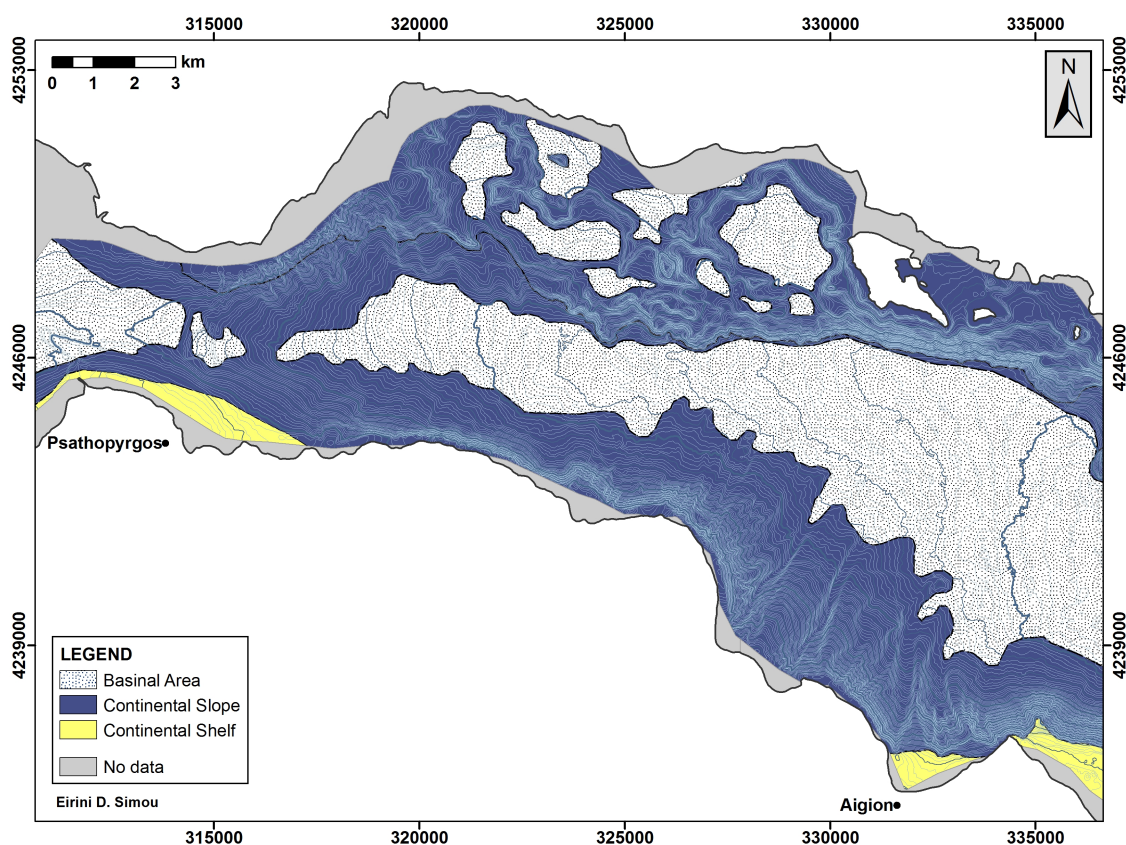

Figure 6.4 Geomorphological Bathymetric Map (in GGRS87), with distinction of the continental shelf, the continental slope and the basinal area in the western part of the currently active Corinth rift. This distinction has been processed with the contribution of the Synthetic Topographic map and the Slope Distribution Map. The map is also presented in Appendix I.

For further analysis, the values of the Slope Distribution Map (Fig. 6.2) were plotted on a histogram chart as shown at Fig. 6.5. The graphical representation of the distribution of data shows that the 49% of the slope values are almost equally distributed into the four first classes (0° - 2°: 10%, 2° - 5°: 11%, 5° - 10°: 13% and 10° - 15°: 15%), which are related to gentle topographic relief. The highest percentage is concentrated between 15° - 25° and 25° - 45° (29% and 20%) respectively, meaning that the majority of the slopes of the study area belong in these classes. Moving on highest degrees, the percentage reduces significantly to 1%.
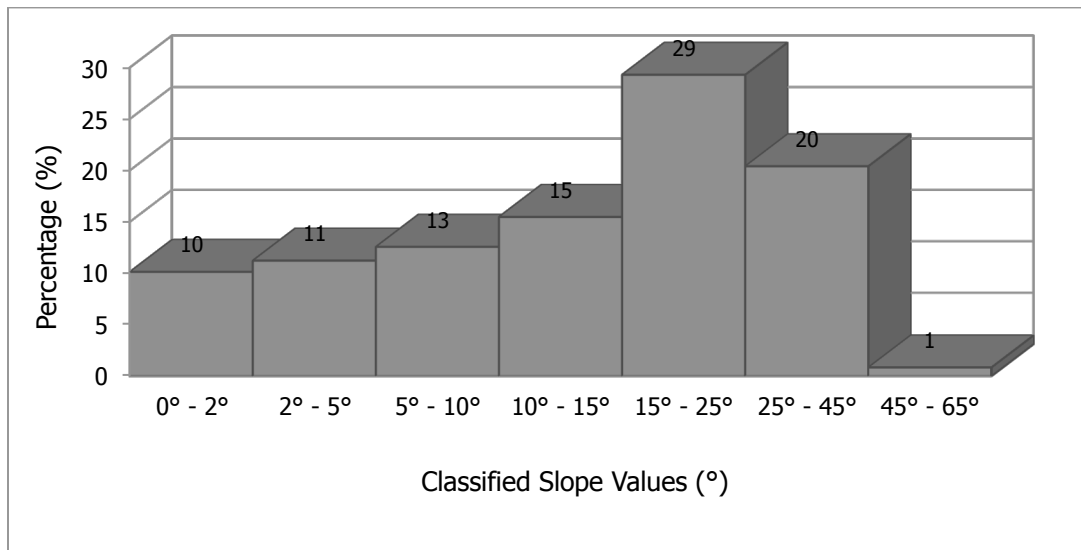

Figure 6.5 Graphical representation of the slope values distribution. The classification of the slope values is in agreement with the Slope Distribution Map.

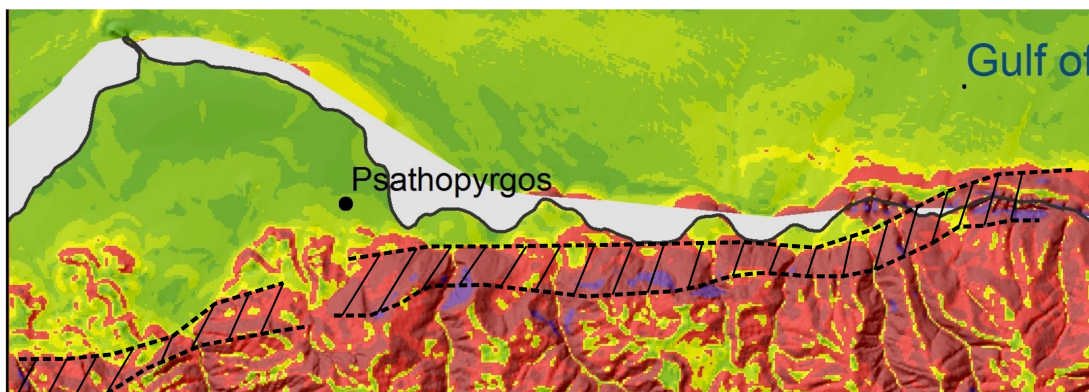**Figure 6.6** Morphotectonic feature (hatched area) extracted from the Slope Distribution Map, in this case corresponding to the Psathopyrgos fault plane.

Consequently, it is of great importance to be mentioned that in the wider study area, the mean slope values rarely develop exceeding 45°, probably as a consequence of the fierce erosional processes acting in the framework of active tectonics (high uplift rates) in correspondence to

the lithological background. On the contrary, the majority of the morphotectonic features, which have resulted from the interpretation of the Slope Distribution map, are expressed through morphological slopes in the order of 25°-45°. This suggests that morphotectonic features may correspond to low angle (normal) faults, which is quite expected as these tectonic elements are usually related to crustal extension and rift structures. In localities where a fault plane is well preserved and revealed on the alpine basement, slope values may increase but this is not representative of the existing structure and its entire geometry.

All the morphotectonic features that have resulted from the distribution of the slope values are given in a following paragraph (6.4) and are presented on the Morphotectonic Map (Fig. 6.31) after the co-evaluation of the orientation of the slopes and the drainage asymmetries.

Slope Azimuth Orientations

Focusing on the azimuth orientations of the land surface and seafloor fabric an Aspect Map (Fig. 6.8) has been generated. Aspect maps result from the slope surfaces and identify the downslope direction of the maximum rate of change in orientation values. The values of the output map are measured clockwise in degrees from 0° (North) to 360°, presenting a full circle and represent the direction of each slope face (dip direction).
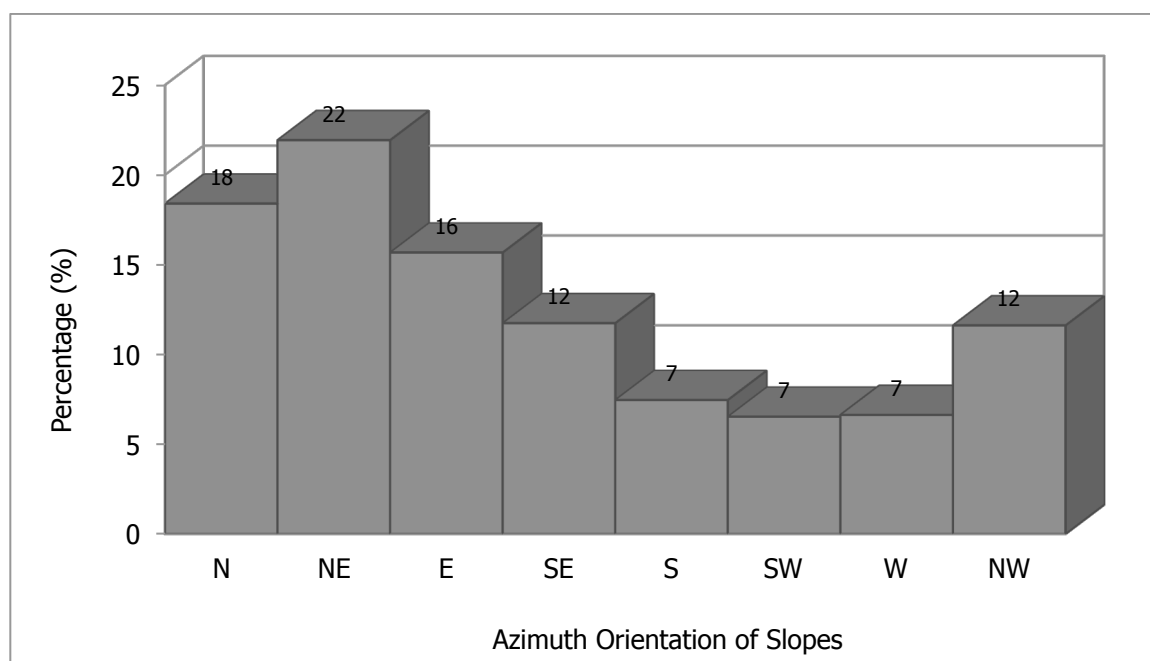

Figure 6.7 Graphical representation of the azimuth orientation of slopes in the onshore and offshore area. The majority of the slope faces (22%) dip towards NE, which means that the most of the slopes in the study area are of NW – SE direction.
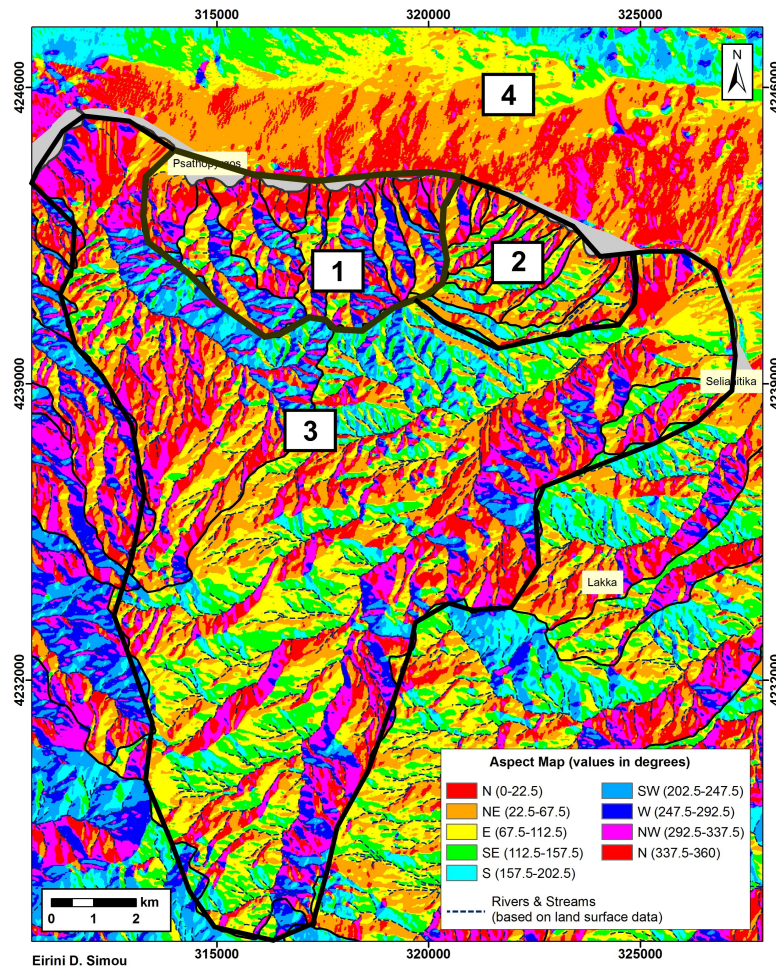
Figure 6.8 Aspect Map (in GGRS87), indicating the downslope direction of the slopes in the study area. The azimuth orientations are presented on the legend of the picture. Rivers and drainage divides for the onshore area are marked on the map aiming to give a better perspective. Numbers are explained in text. The map is also presented in Appendix I.

With the contribution of the Aspect Map, the entire study area has been subdivided into four smaller areas of almost similar slope face orientation. This procedure was accomplished through detailed evaluation of the orientation data distribution and offers valuable information concerning the probable tectonic structures or geomorphological features (such as streams or canyons) that have affected the total morphology of the onshore and offshore area.

The largest and most representative part of Area No1 (Fig. 6.8) is characterized by elongated slopes of E - NE and W - SW direction on either side of the approx. N – S trending streams. A local disruption towards the northern part of this area, characterized by N to NW dipping slopes can be related to the existence of a significant, large-scale tectonic structure, more specifically the Psathopyrgos fault, which has morphologically affected the entire coastal zone of the south margin of the Gulf of Corinth.

Area No2 (Fig. 6.8) is mainly characterized by NE – SW trending slopes, dipping N – NW and S – SE on either side of the NE – SW oriented streams. Despite the fact that this area is in close proximity to the Area No1 it is obvious that it is being affected by a different tectonic structure that has locally changed the strain pattern.

 Area No3 (Fig. 6.8) corresponds to the major drainage divides of the two main rivers in the study area, which are correlated to older tectonic structures that have acted during Plio-Pleistocene. They extend many kilometers towards south, far away from the currently active structure of Psathopyrgos fault. The largest part of Area No3 seems to be characterized by NE – SW trending slopes, dipping N – NW and E –SE.

Finally, Area No4 (Fig. 6.8) corresponds to the Gulf of Corinth region. The south margin is characterized by E – W trending slopes dipping towards N – NE while the north margin is composed by E – W trending slopes as well, dipping towards E – SE. This simple geometry of the Gulf clearly indicates the E – W trending axial channel of the western part of the basin, which evolves with the same direction until it disappears towards the central part of the Gulf (Fig. 6.9). Localized alternations in the orientations of the slopes within each margin of the basin show incision by transverse to the main channel submarine canyons.

The information given by the Aspect Map, in combination with the slope values distribution and the drainage pattern analysis have contributed to the morphotectonic interpretation and permitted the compilation of the Morphotectonic Map, which is presented in a following paragraph.
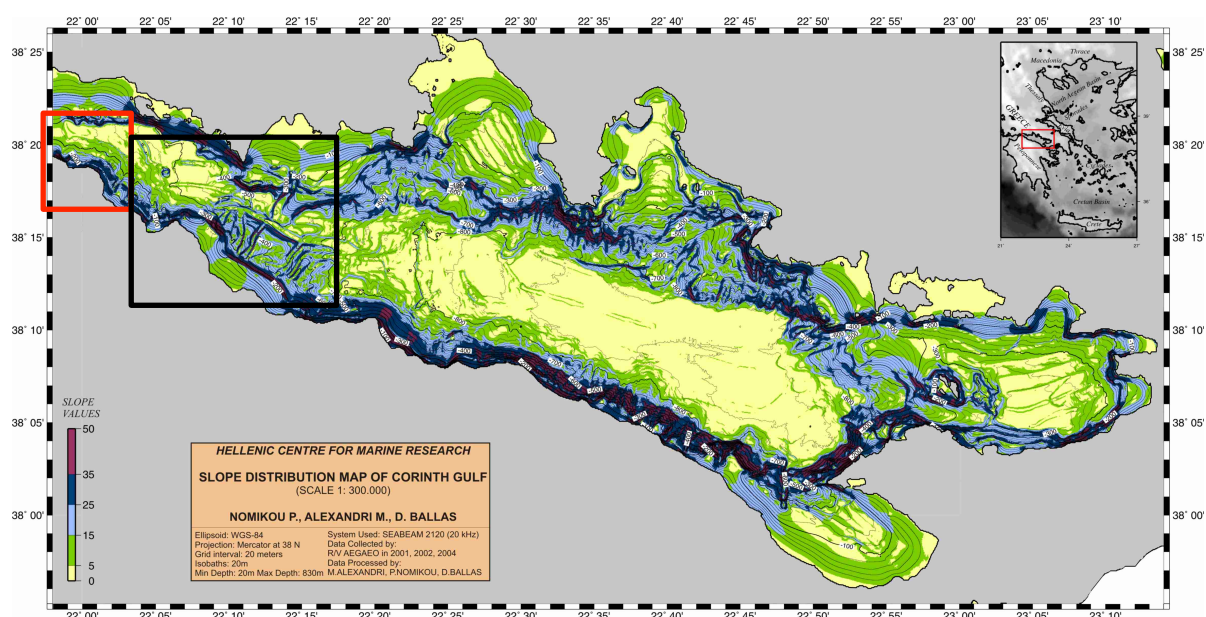

Figure 6.9 Slope Distribution Map of the entire Corinth Gulf (Nomikou et al., 2011). The area marked by the black rectangle shows the evolution of the main axial channel of the submarine drainage pattern towards the central part of the basin. The current study area is marked by the red rectangle.

6.2 Drainage Pattern Analysis

Actively deforming landforms that evolve over thousands to millions of years are produced from a long-term interplay between structural and erosional processes. Fault activity is related to spatial patterns of tectonic uplift or subsidence that drive the evolving shape of the tectonic landforms whereas the erosional and depositional processes are responsible for their modification over time.

Some landscape responses to active geodynamic processes are best viewed at long time scales. Dynamic topography, for example, motivated by crustal processes and expressed through tilting of fault blocks can only be observed by its geomorphological impact over time. Local asymmetries in drainage patterns or drainage divides' migration are commonly difficult to be discerned at intermediate or shorter time scales.

The interaction of short-term deformation and surface processes is often difficult to be recognized due to their incremental impact on the present-day landform. Stratigraphic data though, combined to the geometry of the topographic relief and the geographic character of streams and rivers may provide valuable information concerning the interpretation of the requested tectonic-geomorphic history. Drainage and geomorphological analysis is difficult to be documented only by field data so the technological advancement (GIS software) and the increasingly available digital datasets have allowed rapid and reliable statistical characterization of landscapes in large scales (Burbank & Anderson, 2012).

Drainage basins play an important role in the erosional process as they transport the sediment flux from the tectonic uplands to the sedimentary basin (Leeder & Jackson, 1993). The drainage pattern in tectonically active regions reveals the background active processes, such as extensional faulting, which are responsible for river incision (related to tectonic uplift in regions such as the Gulf of Corinth), asymmetries of the catchments and river diversions.

Consequently, drainage analysis is a necessary tool for structural evaluation as it may contain information about fault activity and evolution (specific structural features exposed at the surface, structural features currently active or buried structural features). The geometry and the density of a drainage pattern can be related to the permeability and the texture of the basement materials (Howard, 1967) while the drainage disorders may reveal tectonic structures that have significant influence on the current topography, which is dominated by the effects of fault activity.

The current work aims to evaluate the Quaternary tectonic activity in the Lakka fault block by the analysis of the drainage pattern and the interpretation of the resulting geomorphic indices. The geomorphic data obtained suggest that tectonic activity in the study area is concentrated

along the south - western margin of the Gulf of Corinth where the active normal fault scarp of Psathopyrgos fault zone is well developed.

Stream Order Analysis

The first step in drainage basin analysis is the stream order designation following Strahler's classification of streams and rivers (Strahler, 1952; Strahler, 1957), which is one of the earliest methods developed, and the most commonly used method today (Fig. 6.10).

Assuming that the composed drainage pattern map includes all the significant flows located in clearly defined valleys in the study area (here obtained from the maps of the Hellenic Military Geographical Service, Sheets: Aigion, Amygdalea, Chalandritsa, Evinochorion, Nafpaktos and Patra, Scale: 1:50000), the smallest tributaries are classified as first-order (Order 1) streams. Where two first-order channels join, a second-order channel (Order 2) is formed and so forth. The stream segment of the highest order, which is defined after the stream classification, corresponds to the trunk stream of the basin through which all the discharge of water and sediment is being accomplished.

The stream classification, being dimensionless, has the advantage of understanding, exploring and comparing two different drainage basins as far as their geometry and evolution is concerned (Strahler, 1957). Stream order is an important characteristic of stream systems as it can be related to drainage area and stream size.
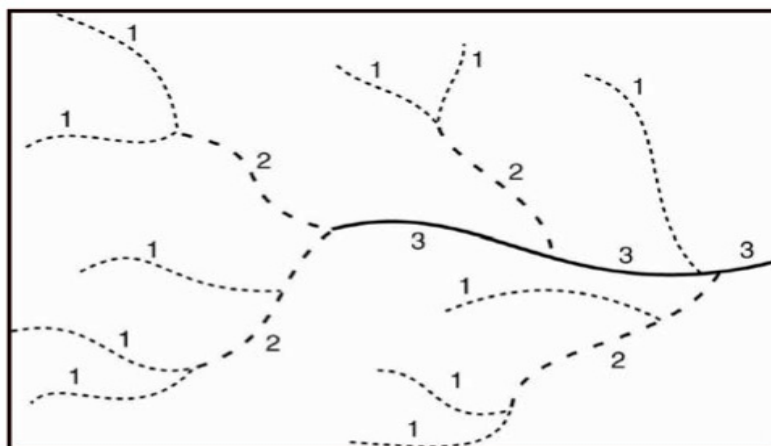

Figure 6.10 Strahler Stream Order Classification Method. In this classification system the smallest tributaries are classified as first-order streams, where two first-order channels join, a second-order channel is formed and so on.

The onshore study area, corresponding to the Lakka fault block as mentioned above, has been divided into 21 individual drainage basins of various size and geometry (Fig. 6.11). This discrimination was accomplished with regard to the Psathopyrgos fault, which is the major active tectonic structure in the area. The 21 drainage basins are characterized by first-order to

fifth-order streams and divides according to Strahler's stream order classification. The flow into these basins is accumulated towards north, in an N – S to NE – SW direction.
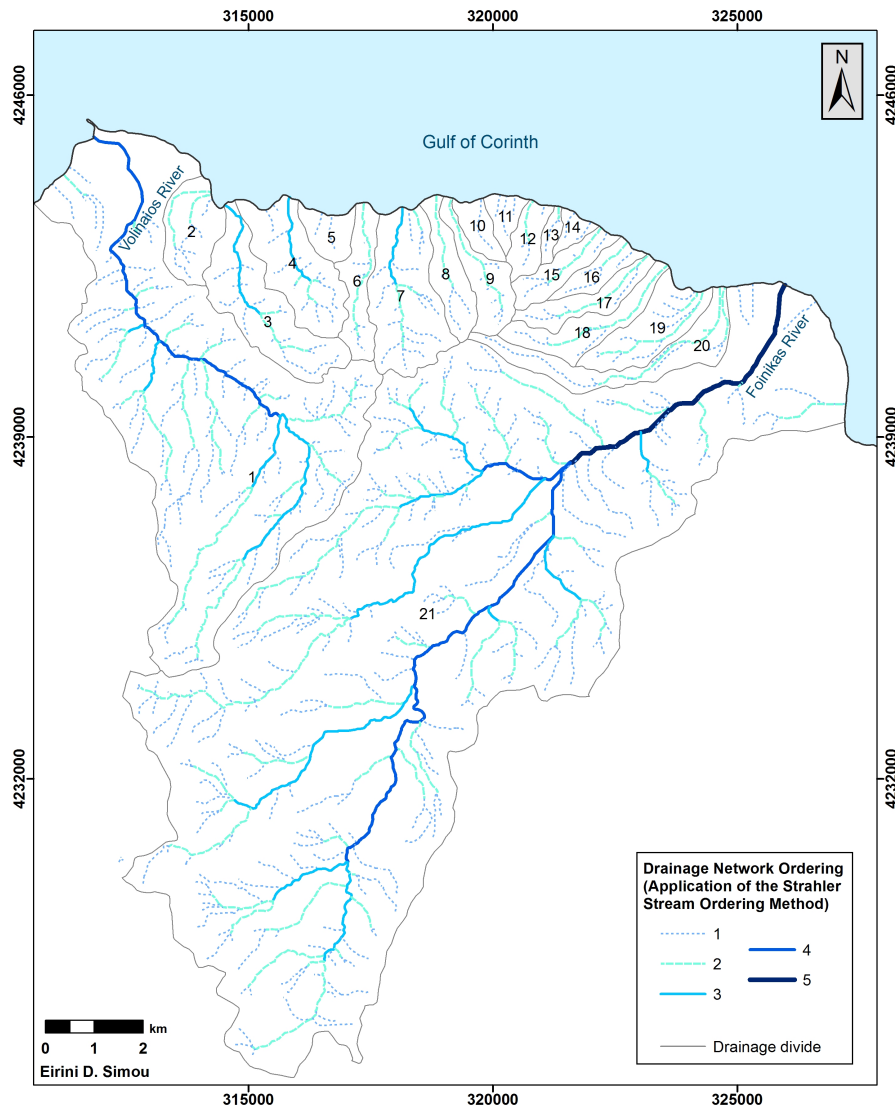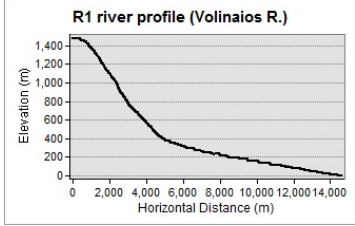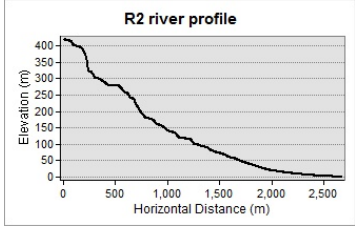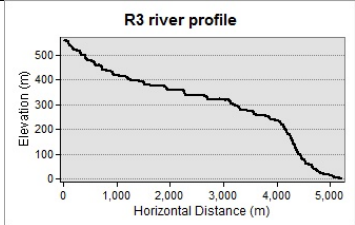

Figure 6.11 Stream Order Classification Map (in GGRS87), generated according to Strahler 's Stream Order Classification Method. The map is also presented in Appendix I.
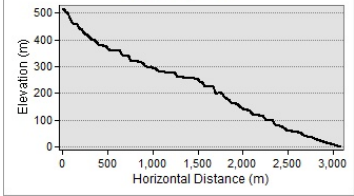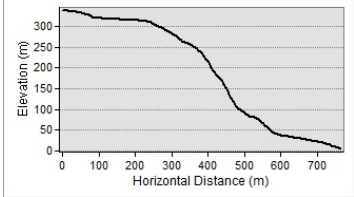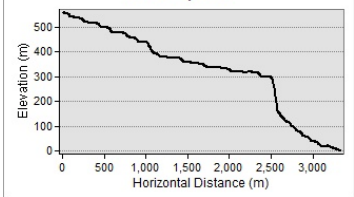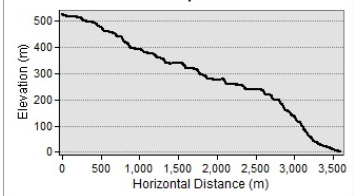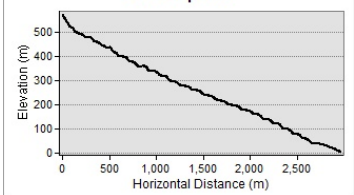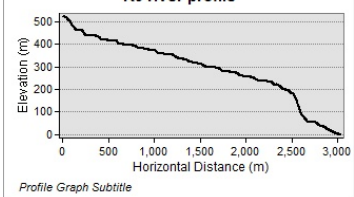
The fifth-order NE-SW trending basin corresponds to Foinikas River (Drainage basin No 21 – Fig. 6.11), which bounds the study area to the west, covers an area of about 95 km^2 and extends approximately 20km towards south. Volinaios River (Drainage basin No 1 – Fig. 6.11), which is the western boundary of the study area, is the second largest basin (approx. 33km^2) and is characterized by a fourth-order truck stream. The rest of the drainage basins, mainly defined by third-order and second-order streams, cover significantly smaller areas, ranging from a few hundreds of m^2 up to 5 km^2. The orientation of each drainage basin, as well as the direction of the trunk streams and the number of the tributaries, varies mainly according to the
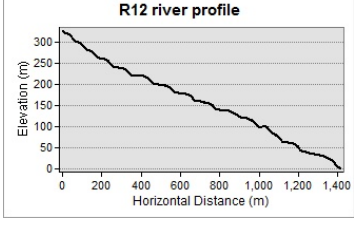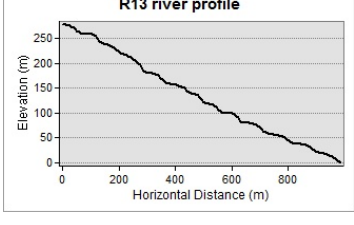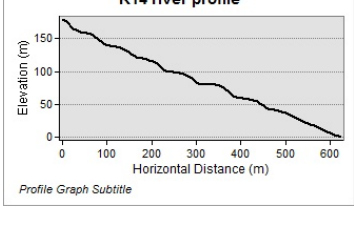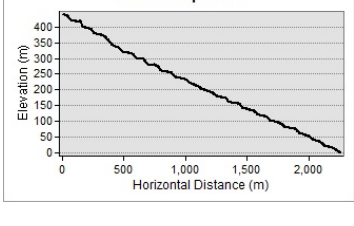
position of the main tectonic structures and the lithological background, factors which both have significant influence on the developing drainage pattern.
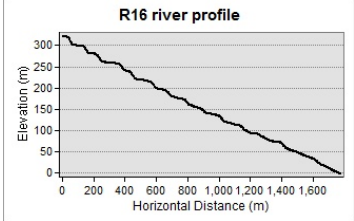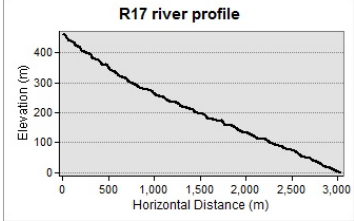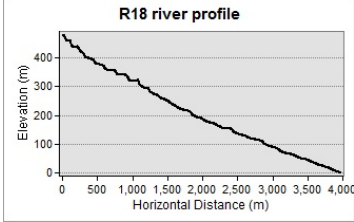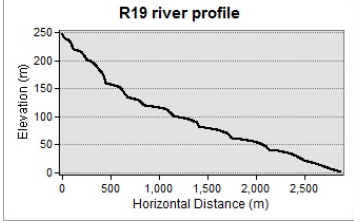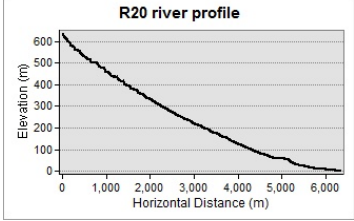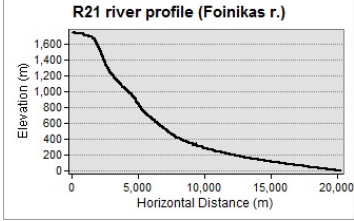
Longitudinal river profiles that have been have been extracted for the main rivers draining the study area show that the mean gradient of the drainage basins are in the order of 15° to 30°. These gradient values indicate the influence of the high uplift rates uplift that characterizes the wider area of the southwestern part of the Corinth rift. The profiles at the ends of the currently active region of Psathopyrgos fault (towards Volinaios and Foinikas rivers) present mainly concave shape while 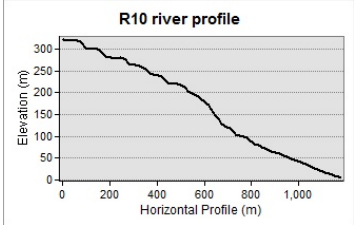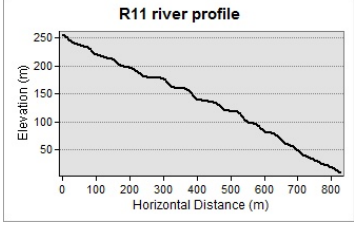at the center of the fault zone, the profiles are convex to linear depending of the degree of impact within the active tectonic processes. The steep slope of Psathopyrgos fault plane is clearly reflected in several profiles, such as R3, R4, R5, R6, R7, R9, R10 (Table 6.1).

Table 6.1 Relationships between stream order, drainage area, maximum stream and mean gradient for each drainage basin. The graphs of the last column correspond to longitudinal profiles of the streams in their maximum length inside each watershed. It is worth mentioning that some of the profiles indicate a steep slope corresponding to the Psathopyrgos fault plane (e.g. R3, R4, R5, R6, R7, R9, R10).

Drainage Basins (Watersheds)				
Number	Strahler Stream Order Classification	E_{tot} (km^2)	L_{max} (km)	Mean Gradient (°)	River Longitudinal Profile
1	4th	32,86	~14,602	19	R1 river profile (Volinaios R.)
2	2nd	2,04	~2,670	18	R2 river profile
3	3rd	4,07	~5,211	24	R3 river profile

Drainage Basins (Watersheds)					
Number	Strahler Stream Order Classification	E_{tot} (km^2)	L_{max} (km)	Mean Gradient (°)	River Longitudinal Profile
4	3rd	3,36	~3,080	25	
5	1st	0,91	~0,764	26	
6	2nd	1,70	~3,332	22	
7	3rd	4,32	~3,593	24	
8	2nd	1,61	~2,961	32	
9	2nd	1,60	~3,028	27	

Drainage Basins (Watersheds)					
Number	Strahler Stream Order Classification	E_{tot} (km^2)	L_{max} (km)	Mean Gradient (°)	River Longitudinal Profile
10	1st	0,75	~1,177	24	
11	1st	0,60	~0,827	25	
12	2nd	0,92	~1,413	27	
13	2nd	0,33	~0,985	28	
14	1st	0,41	~0,474	28	
15	2nd	1,27	~2,258	27	

	Drainage Basins (Watersheds)				
Number	Strahler Stream Order Classification	E_{tot} (km^2)	L_{max} (km)	Mean Gradient (°)	River Longitudinal Profile
16	2nd	0,91	~1,775	24	
17	2nd	1,42	~3,032	24	
18	2nd	1,93	~3,964	23	
19	2nd	2,36	~2,873	12	
20	2nd	2,86	~6,335	15	
21	5th	94,76	~20,266	20	

Submarine Drainage Analysis

The onland drainage network, flowing towards north and northeast, obviously continues towards the basinal area of the Gulf of Corinth. The recent, currently evolving gentle marine environment does not allow the sufficient configuration of the existing submarine flows. Consequently, the drainage network for the offshore region has been extracted from the 5-m resolution merged Digital Elevation Model (DEM) of the study area. The methodology that has been followed takes into account the accumulation of upwards-curved grid cells being adaptive to spatial variability in drainage density (Pérez-Peña et al., 2010). The resulting drainage network (Fig. 6.12) has been cleaned and validated before the evaluation, according to the bathymetric data and the topographic lows, in order to avoid DEM-associated errors.
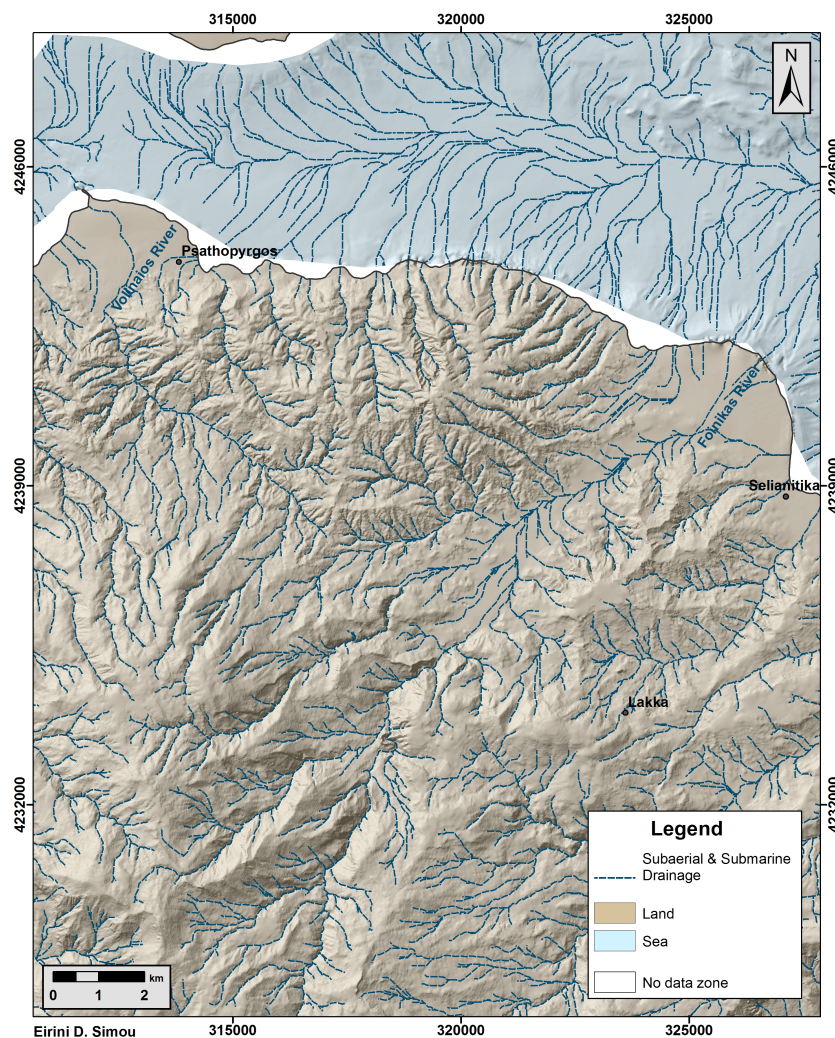

Figure 6.12 Subaerial and Submarine Drainage Map (in GGRS87) presenting the geometry of the drainage pattern in both environments. The drainage network for the offshore region has been extracted from the 5-m resolution merged Digital Elevation Model (DEM) of the study area. The map is also presented in Appendix I.

The evaluation of the Subaerial and Submarine Drainage Map suggests that the marine environment of the study area is characterized by a simple drainage pattern. The central part of the basin is dominated by a central E – W trending drainage runoff axis, exceeding 20km in length, accumulating the flow to the east, towards the deepest parts of the Gulf of Corinth (in this study the maximum depth is -420m while the maximum depth of the entire basin is -800÷ -870m – Nomikou et al., 2011).

Multiple submarine channels cut the continental slope, in which they develop in a N–S direction towards the western and central part of the study area and in a NE – SW direction towards the eastern part (Foinikas river). In these channels (up to 5km in length), the water flows towards north on the south margin and towards south on the north margin of the Gulf of Corinth, until the reach almost transversely the main runoff axis.

The fact that the area is under tectonic control by the Psathopyrgos fault, which is the most active tectonic structure of the currently evolving Corinth rift, suggests that probable impacts of faulting on the drainage pattern can only be observed towards the marginal slopes. In these areas, the developing channels are straight and elongated with a few or no smaller crossing tributaries.

On the contrary, in areas where activity is less or temporarily ceased, submarine gullies develop. The gullies are relatively small valleys, smaller than the submarine canyons, which commonly occur in the continental slopes or within canyon flanks and heads, where they form local tributary networks. Individual gullies and gully networks are considered as initial steps in the development of larger submarine canyons and more mature drainage networks related to less active regions. In the current study, such geomorphological structures can only be observed to the east of Foinikas river.

Drainage Pattern Characteristics and Disorders

The subaerial study area, being in the maturity stage according to Davis' Geomorphic Cycle, is characterized by a landform dissected by streams and the extensive impacts of the erosional processes. Drainage disorders and asymmetries reveal the tectonic structures that have significant influence on the current topographic relief as a result of the interaction between vertical tectonic movements (uplift), tilting and the lithological background.

The study area, according to its drainage pattern characteristics, has been subdivided into three areas (Fig. 6.13), which are actually influenced by the known major tectonic structures, the Psathopyrgos and the Lakka fault zones, bounding the Lakka fault block. Each one of these areas is further evaluated below.
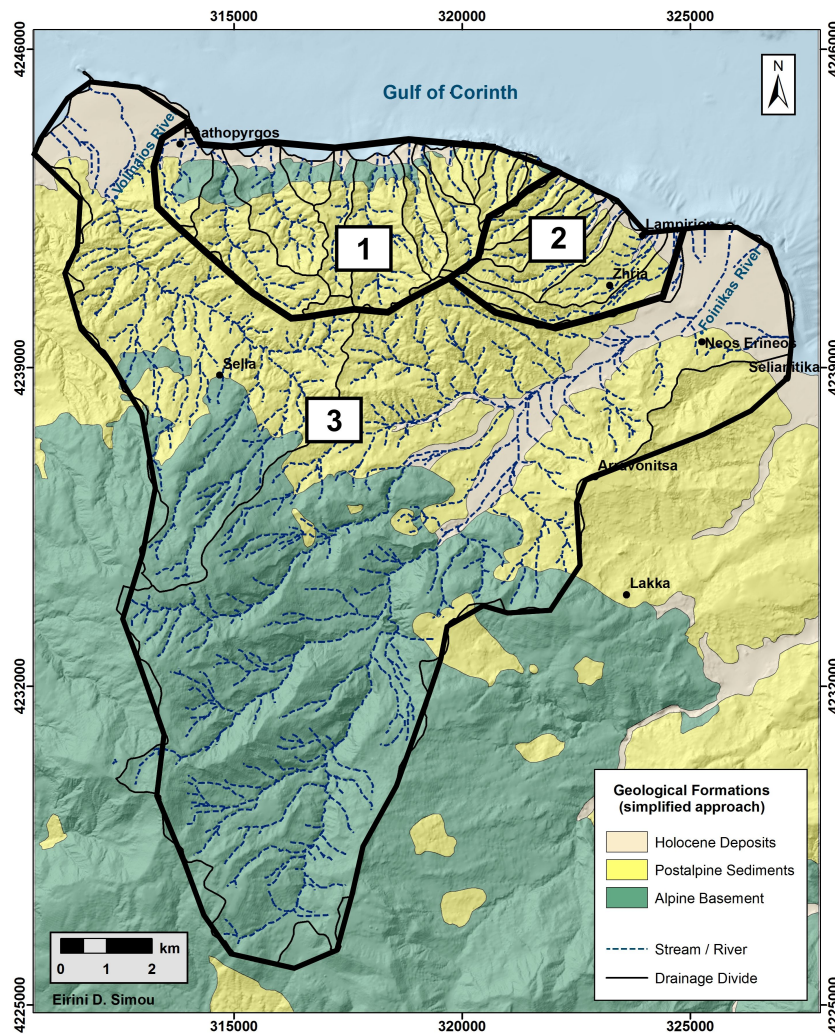
Figure 6.13 Synthetic Drainage Pattern Map (in GGRS87), showing the streams and rivers in the study area, as well as the lithological background, which is a factor having a significant influence on the developing drainage pattern. Drainage disorders presented on this map are further evaluated in the text.

The first area (indicated by No 1 in Fig 6.13) is characterized by a parallel to sub-parallel drainage pattern which develops on moderate to steep slopes. Because of the generally high slope values that define the topographic relief, the main channels are straight and elongated, up to 5 km in length and N – S trending, flowing all in the same direction (towards north). First-order tributaries are very few on the Plio-Pleistocene sediments and almost absent on the outcrops of the alpine bedrock. Deeply incised streams are also indicative of the post-alpine lithologies that extend to the largest part of the study area. The parallel – subparallel drainage pattern is directly related to the Psathopyrgos fault zone, which cuts across the steep landform. The elongated main streams in the drainage basin could be probably explained by the increased uplift combined with tilting of the fault block towards south.
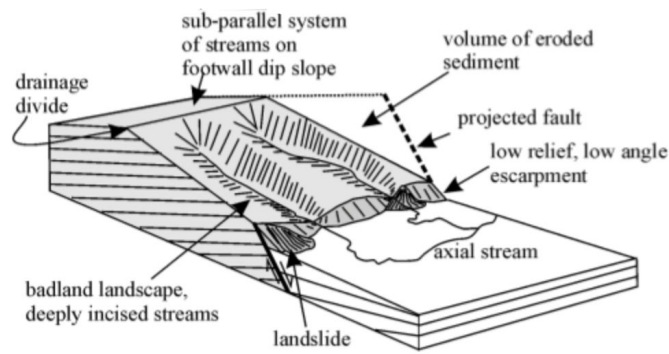
Figure 6.14 Schematic 3D-block summarizing the geomorphological features that are generated by faulting in Neogene / Post-alpine deposits (Goldsworthy & Jackson, 2000). Parallel drainage pattern and deeply incised channels are indicative of such environments.

The second area (No 2 in Fig. 6.13) is similar in characteristics to the first area but flow develops towards NE, by NE – SW trending streams, up to 6 km in length. This change in the direction of the streams shows that this area is probably controlled by another active tectonic structure adjacent to Psathopyrgos fault, which develops in a NW – SE direction. The eastern located drainage basins present a little asymmetry, having their left side (facing downstream) more developed as a response to tilting processes towards ESE - SE.

The area No 3 corresponds to the drainage basins of Volinaios and Foinikas rivers (No 1 and No 21 in Fig. 6.11), which are drainage divides older that are affected by tectonic structures, which are less active now (Lakka fault). They cover significantly larger areas, in the order of 33 km^2 and 95km^2 respectively and they both flow towards north in the Gulf of Corinth. Area 3 (Fig. 6.13) is characterized by sub-dendritic drainage pattern (Howard, 1967), which is different from the typical dendritic type only in the lack of perfection (Fig. 6.15). Deviations are due to secondary regional controls, which in this case are the lithological alternations (alpine and post-alpine formations) and the structural impacts on the topography.
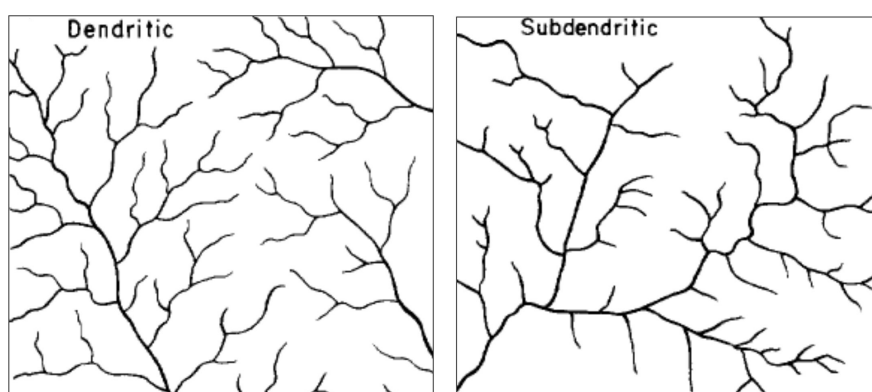
Figure 6.15 Dendritic versus sub-dendritic drainage pattern according to Howard (1967).

Foinikas and Volinaios rivers correspond to antecedent drainage basins (Seger and Alexander, 1993; Zelilidis, 2000) sourced in pre-Neogene basement that have been adjusted to the tectonic movements by elongating and downcutting the new uplifted areas, presenting noticeable incision in the stream valleys. As they have been influenced by local changes in basement

68

lithology, some river catchments have modulated their way through fault offsets, avoiding the more resistant lithologies. The more recent Plio-Pleistocene sediments of the footwall of Psathopyrgos fault have been incised with no change in direction. The deeply incision zones in combination with existing tectonic structures at specific riverbanks have led to steep slope values which are further interpreted as morphotectonic features (Paragraph 6.4). The intense asymmetry in these drainage basins is expressed through the more elongated streams in the left sides (facing downstream) that also show influence by tilting processes (e.g. Fig. 6.16); towards N - NNE in the Volinaios valley and towards E – NE in the Foinikas valley.
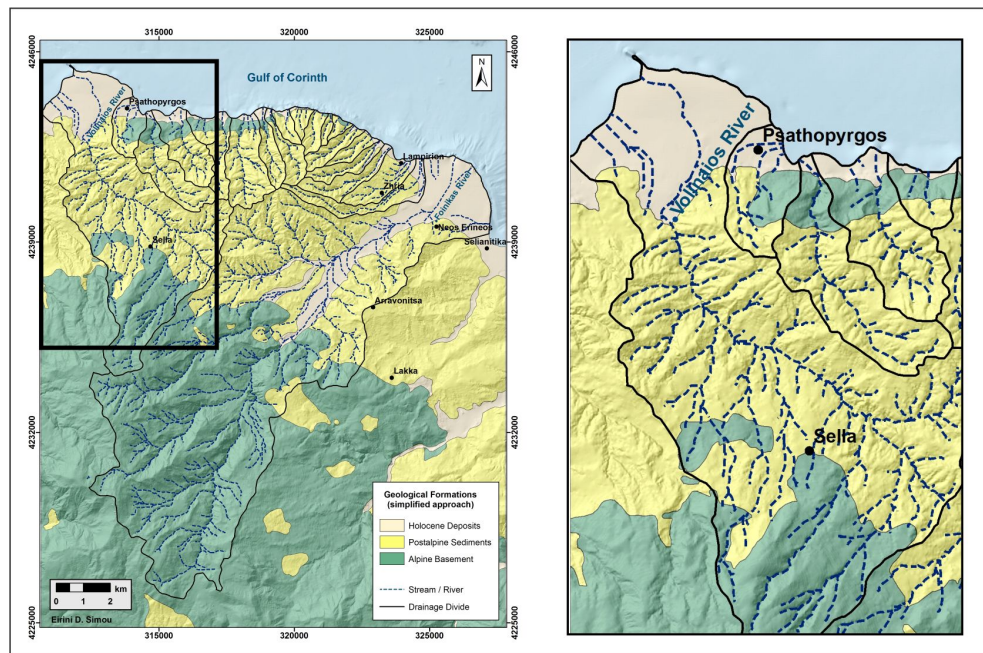
Figure 6.16 Enlarged part of the Synthetic Drainage Pattern Map (Fig. 6.13) showing the longer catchments which develop at the SW part of Volinaios drainage basin indicating regional tilting towards NE.

6.3 Erosion and Sedimentation in the Framework of Active Faulting

Active extensional tectonics can result in new topography produced by high rates of erosion and deposition related to extensive fluvial systems, which have modified the landforms that have been created and deformed by normal faulting. The interplay between the erosional and depositional processes controls not only the deforming landform but also the stratigraphic and structural architecture of an active sedimentary basin such as the Gulf of Corinth.

Erosion

The southwestern part of the Gulf of Corinth is characterized by intense erosional processes interacting with the high uplift rates and the post-alpine lithology on which they develop. High

slope values combined with high hypsometric integral indicate incision while low-slope combined with low to moderate hypsometric integral show steady-state condition.
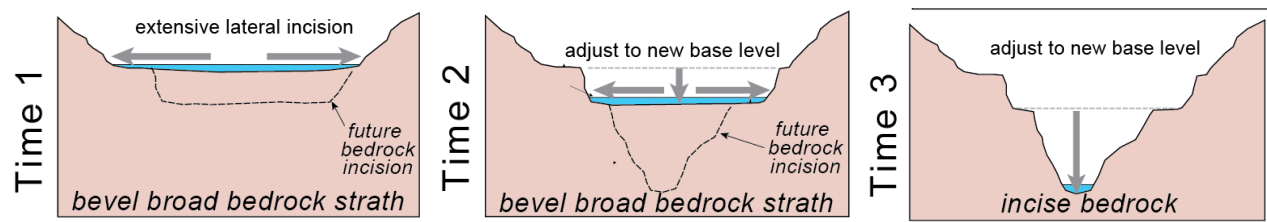
Figure 6.17 The "bedrock incision model" as presented by Burbank & Anderson (2012). According to this model straths are formed at or near the base of the bedrock channel.
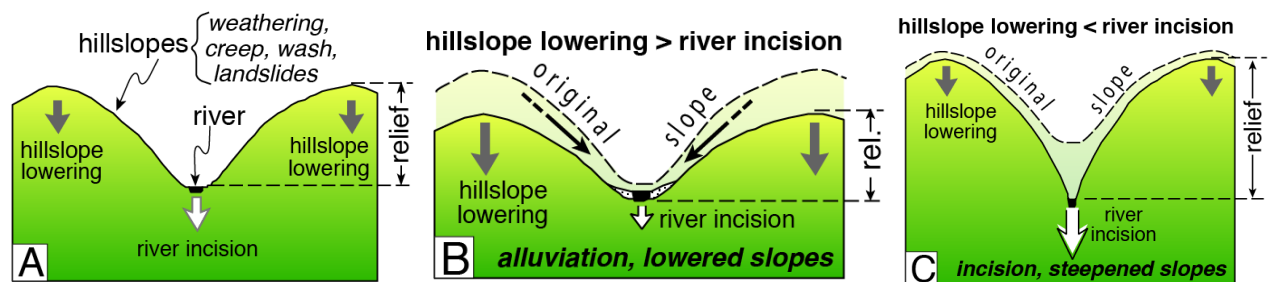
Figure 6.18 Differences in the relative rate of river incision versus hillslope lowering control changes in topographic relief. [A] In a steady-state topography, rates of river incision and of hillslope lowering are balanced. [B] If hillslope lowering exceeds river incision, valleys tend to allouviate and topographic relief decreases. [C] If river incision exceeds hillslope lowering, relief increases and hillslope steepen (Burbank & Anderson, 2012). Case B suites to Volinaios and Foinikas rivers while case C is more relative to the rest drainage basins of the study area.

The use of geomorphic indexes contributes to the quantification and the geomorphic evaluation of a landform influenced by active tectonics. One of the most widely spread geomorphic indices, associated to fluvial systems and erosion and effective for the case study of Psathopyrgos fault is the **Valley floor width-to-height ratio** (V_f index) following Bull & McFadden (1977).

The V_f quantitative index is conceived to discriminate between V-shaped and U-shaped flat-floored valleys and indicates whether streams are actively incising subjected to active uplift, or they are eroding the landform laterally in response to lower rates of uplift and relative tectonic quiescence (Bull & McFadden, 1977; Keller and Pinter, 2002; Pérez-Peña, 2010). This index is defined as:

$$V_f = 2V_{fw} / E_{ld} + E_{rd} - 2E_{sc}$$

where V_{fw} is the width of the valley floor, E_{ld} and E_{rd} are elevations of the left and right valley divides, respectively, and E_{sc} is the elevation of the valley floor.

Transverse valley profiles for determining the V_f index have been generated for all the main channels of the 21 drainage basins of this study, every 500m approx. up to 5km upstream from the mountain front, so the entire length of each drainage valley to be evaluated (Fig. 6.19). The V_f index calculations quantify the impact of the tectonic structures to the drainage basins upwards of the coastal fault systems, especially the Psathopyrgos fault. High values of V_f indicate low tectonic activity valleys while low values of V_f characterize high tectonic activity expressed through high rates of uplift and deep incision zones.
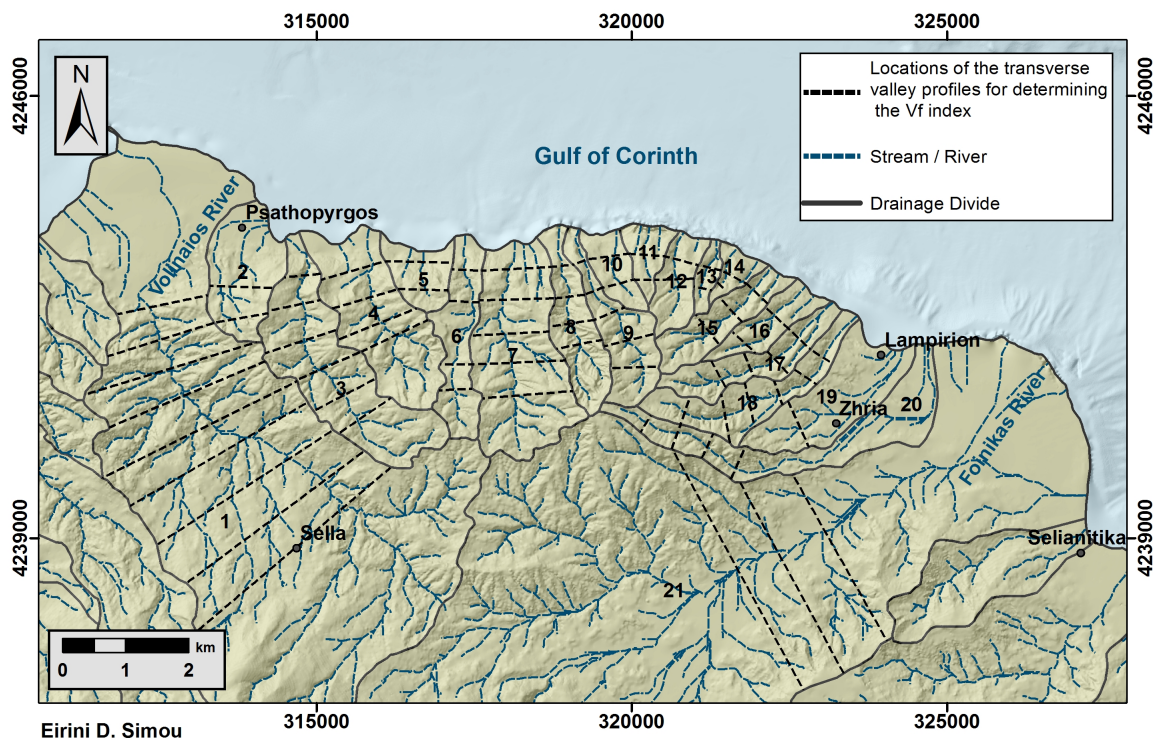
Figure 6.19. Location of the transverse valley profiles for the determination of the V_f index.

The amount of calculated V_f values range from 0.069 to 3.957. For the needs of the current study the mean V_f value for each drainage basin was taken into account, ranging from 0.187 to 2.20. The results are presented on Table 6.2 while all the calculations are presented in Appendix II.

Table 6.2 Mean V_f index results for each drainage basin in the study area. High values of V_f indicate low tectonic activity while low values of V_f characterize high tectonic activity. The calculations are given in detail in Appendix II.

Drainage Basin	Mean V_f Index	Drainage Basin	Mean V_f Index
1 [Volinaios River]	0.315	12	0.278
2	0.321	13	0.273

Drainage Basin	Mean V_f Index	Drainage Basin	Mean V_f Index
3	0.217	14	0.199
4	0.328	15	0.481
5	0.377	16	0.323
6	0.439	17	0.795
7	0.200	18	1.106
8	0.187	19	1.777
9	0.243	20	0.408
10	0.315	21 [Foinikas River]	2.200
11	0.665		

Comparing the results (Fig. 6.20, 6.21) it is noticed that V_f values are lower towards the western part of the study area. These low values indicate high tectonic activity and uplift rates, which are related to the Psathopyrgos active fault zone (Drainage basins 1 to 14, Fig. 6.11). The rest calculated V_f values differentiate significantly towards the eastern part probably indicating another individual nearby tectonic segment (according to several authors, the Lambiri fault) or a step over zone to the West Eliki fault block (defined by Aigion and Eliki faults). In this probably separate structure, the western part seems to interact with the active Psathopyrgos tectonic structure presenting lower V_f values while the eastern part presents higher V_f values as it interacts with the comparably less active Aigion and West Eliki faults.
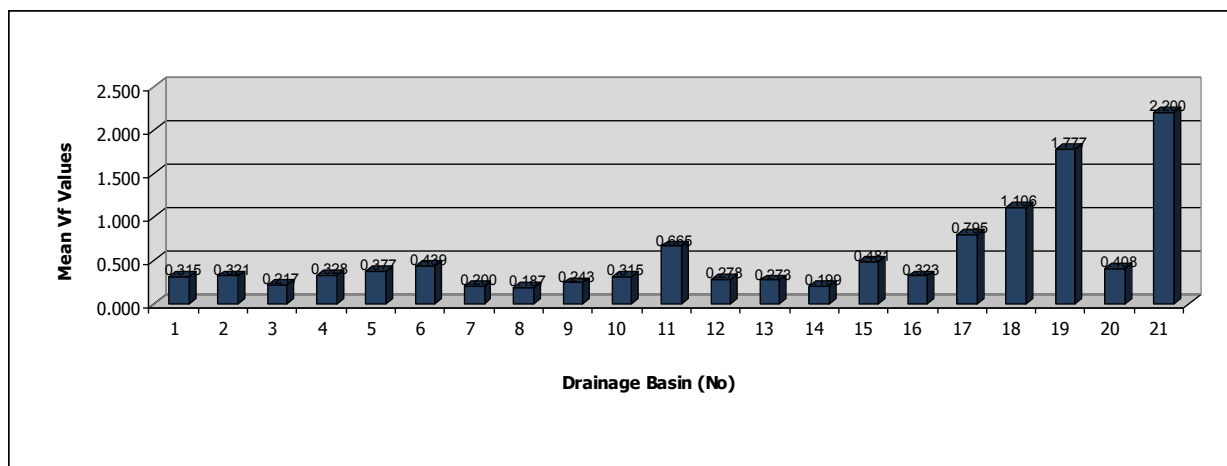
Figure 6.20 Plot of V_f values for the main drainage divides which are related to the study area and the active Psathopyrgos fault. The position of each drainage basin is presented on the Stream Order Classification Map of Fig. 6.11
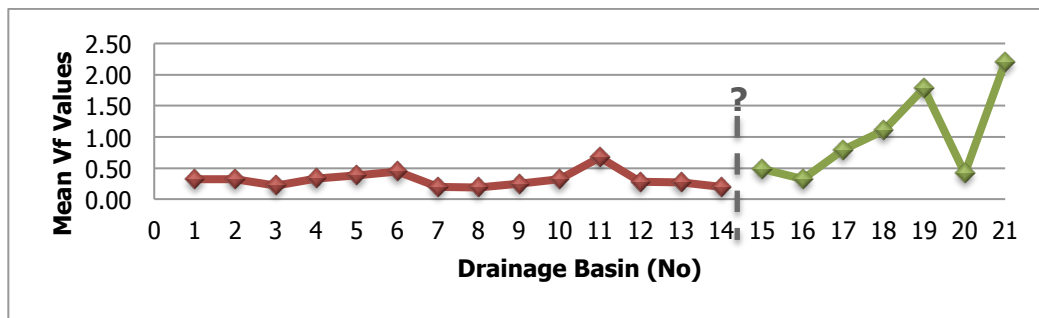
Figure 6.21 Interpretation of calculated V_f values in the study area, indicating the high levels of activity in correspondence to the main tectonic structure of the study area, the Psathopyrgos fault (red data series). Slope values distribution and the geological background have been taken into account. The green data series probably indicates another individual tectonic segment (according to several authors, the Lambiri fault) or a step over zone to the West Eliki fault block (defined by Aigion and Eliki faults) more active towards its western end and less active towards its eastern end.

The approach to the erosional processes through geomorphic markers in correlation to the fault activity and the relative uplift permits a quantification of the interplay of the surface processes that shape landforms (Burbank & Anderson, 2012). As erosion is coupled with hillslope values (Fig. 6.22) the generation of a map has been attempted aiming to present the influences of erosional processes on the topography. The resulting map shows the distribution of the deep incision zones as a response to active extensional tectonics.
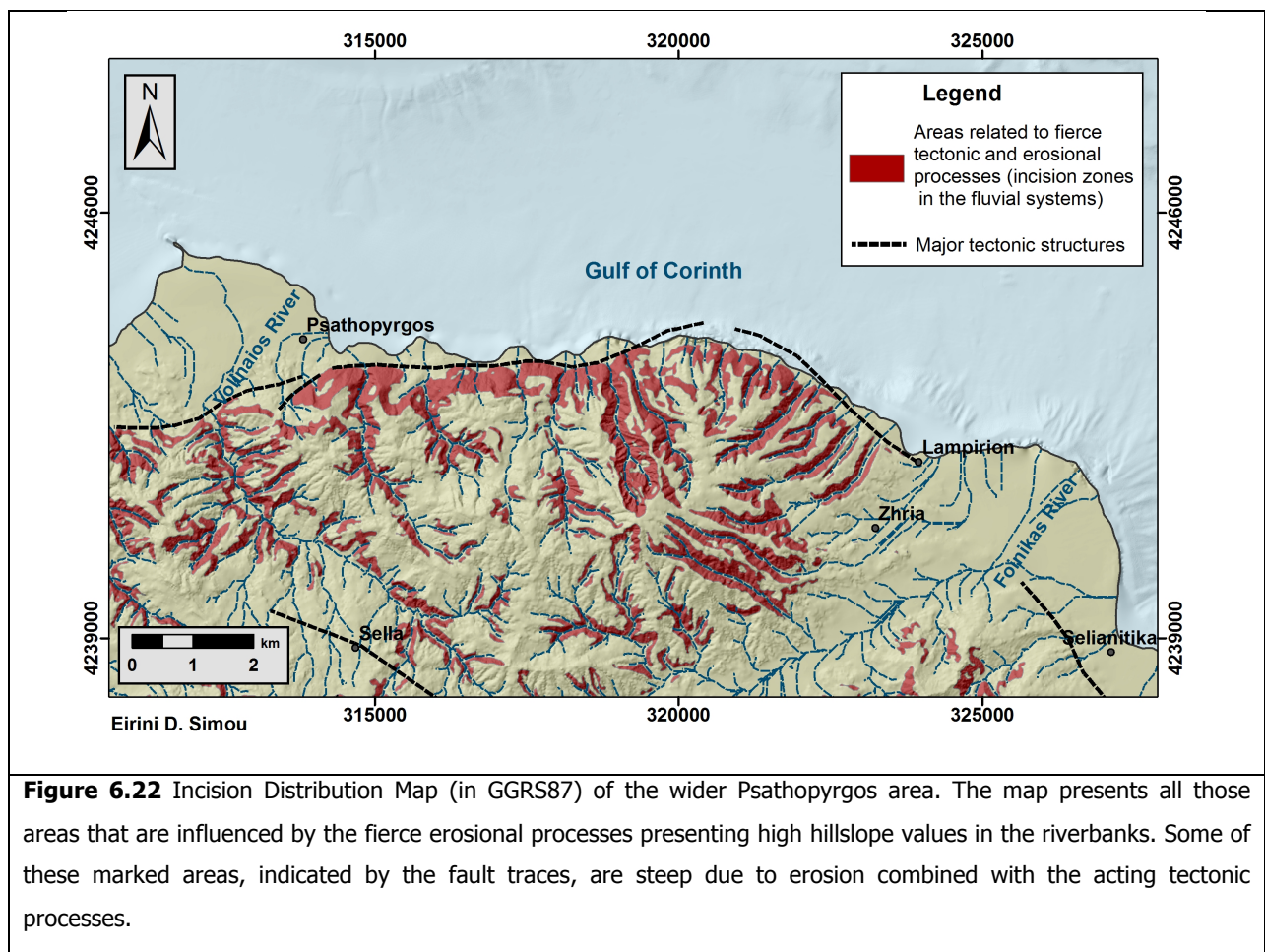
Figure 6.22 Incision Distribution Map (in GGRS87) of the wider Psathopyrgos area. The map presents all those areas that are influenced by the fierce erosional processes presenting high hillslope values in the riverbanks. Some of these marked areas, indicated by the fault traces, are steep due to erosion combined with the acting tectonic processes.

The enduring fault activity combined with the extensive erosion can also be expressed through instabilities and landslide occurrence both in the marine (mainly coastal) and the terrestrial environment, indicating the active geodynamic regime evolving towards the coastal zone of NW Peloponnese. This interaction between landslides and erosional processes is further discussed in Chapter 7.

Sedimentation

The alluvial fans and the fan deltas correspond to fan-shaped accumulations of sediments that are transformed by stream flow (Leeder, 1999). In case of fan deltas, the active front during the deposition is an interface with standing water, marine or lacustrine, into which the fan delta is evolving and prograding and with which it interacts (Nemec & Steel, 1988; Leeder, 1999). The alluvial fans are point-sourced by streams, characterized by perennial or seasonal flow, issuing from drainage catchment and grading gently into the basin floor environment (Fig 6.23). Radial sections along the fan presents straight to concave profiles while, in cross-section the profile is presented as an invariably convex upwards. The control of the runoff and the sediment discharge in a lobe-shaped morphological feature depend on the drainage area, which is the major influence on the structure. In general, the fan size is inversely proportional to the mean fan slope: while the first increases the latter is decreased.

Figure 6.23 Block diagram illustrating stream-flow-dominated alluvial fans adjacent to active normal faults (Leeder, 1999 after Blair & McPherson, 1994).

Active tectonic processes in or adjacent to the drainage catchment have a significant influence on the fan growth and evolution. The majority of the fans are located at basin – margin positions towards to once or still active normal faults. The fault propagation is capable of fan uplift, tilting and deep channel incision (Leeder & Jackson, 1993; Jackson & Leeder, 1994).

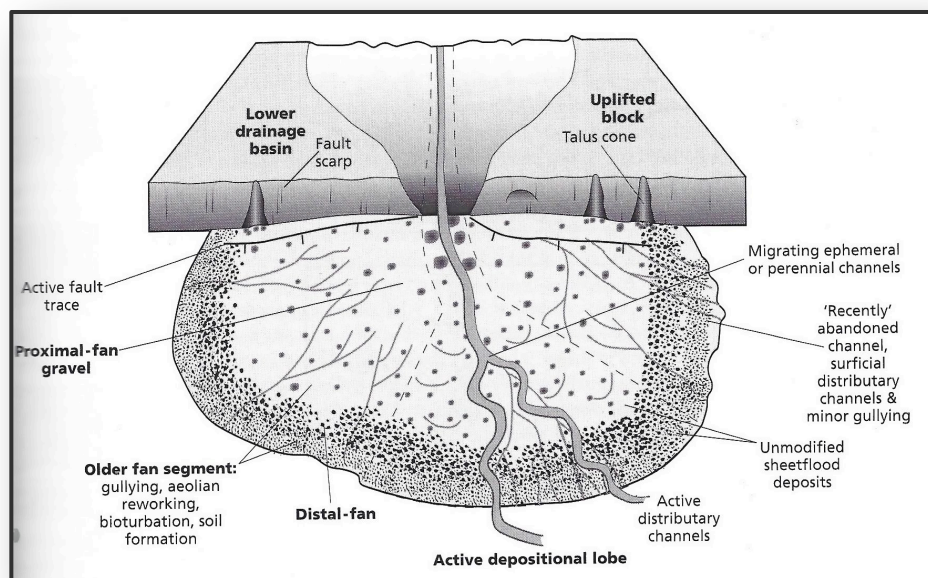Gilbert–type fan deltas are characterized by an abrupt discontinuity of the slope near the shoreface; the subsequent depositional submarine gradient can exceed 25°. Sediments which have been deposited at the top of the delta slopes together with frequent submarine failures' material can often be transported down the steep delta fronts as debris or flow avalanches (Fig. 6.24). These avalanche deposits move downwards to the lower part of the slope where they cease their motion as frictional forces overcome the internal driving forces (Leeder, 1999) and they accrete on the pre-existing slope, standing at their angle of repose. The foot of the delta slope is characterized by an abrupt or a gradational change to the deposits of the basin floor, which may feature lobes of re-sedimented coarse sediments (Postma & Roep, 1985, Fig. 6.25). Thickness is based on the local basin water depths, ranging from a few to many hundreds of meters while the fan shapes result from the variations in sediment supply, water depth, the relative sea-level changes and the tectonic movements.
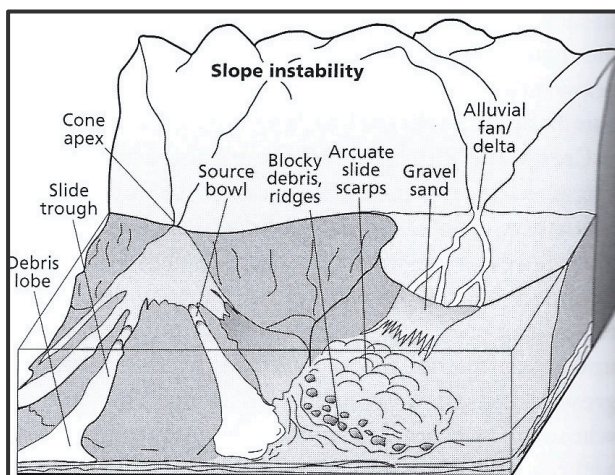
Figure 6.24 Schematic 3D view of slope instability features of Gilbert-type fan deltas. The left-hand fan delta has little subaerial surface expression, typical of very young fan deltas or those that develop on very steep slopes (Prior & Bornhold, 1990; Leeder, 1999).
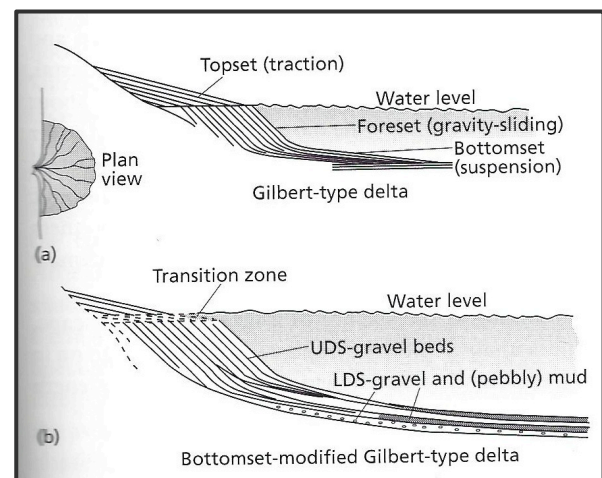
Figure 6.25 Illustration of a delta slope. The foot is characterized by an abrupt or a gradational change to the deposits of the basin floor, which may feature lobes of re-sedimented coarse sediments (Postma & Roep, 1985; Leeder, 1999)

The present-day exposed Gilbert-type fan deltas can be observed at altitudes higher than 300-400m above the sea level creating the intense morphology of the northwest Peloponnese. The new deltaic systems are currently being formed below the sea level in the south coastal zone of

the Gulf of Corinth, probably suggesting a third phase in the evolution of the Corinth Rift, according to Moretti et al. (2003) and Lykousis et al. (2007). The development of the alluvial fans towards the fault plane is evidence for continuous fault activity (Fig. 6.26).

The large submarine structures are directly related to the antecedent rivers of Foinikas and Volinaios (Paragraph 6.2). These relatively older rivers have constructed prominent fan deltas at the coastline of the currently active margin of the SW Gulf of Corinth (Fig. 6.26). Smaller younger streams, in contrast to the antecedent catchments are also being developed into the easily eroded Plio-Pleistocene sediments, constructing smaller fan deltas.
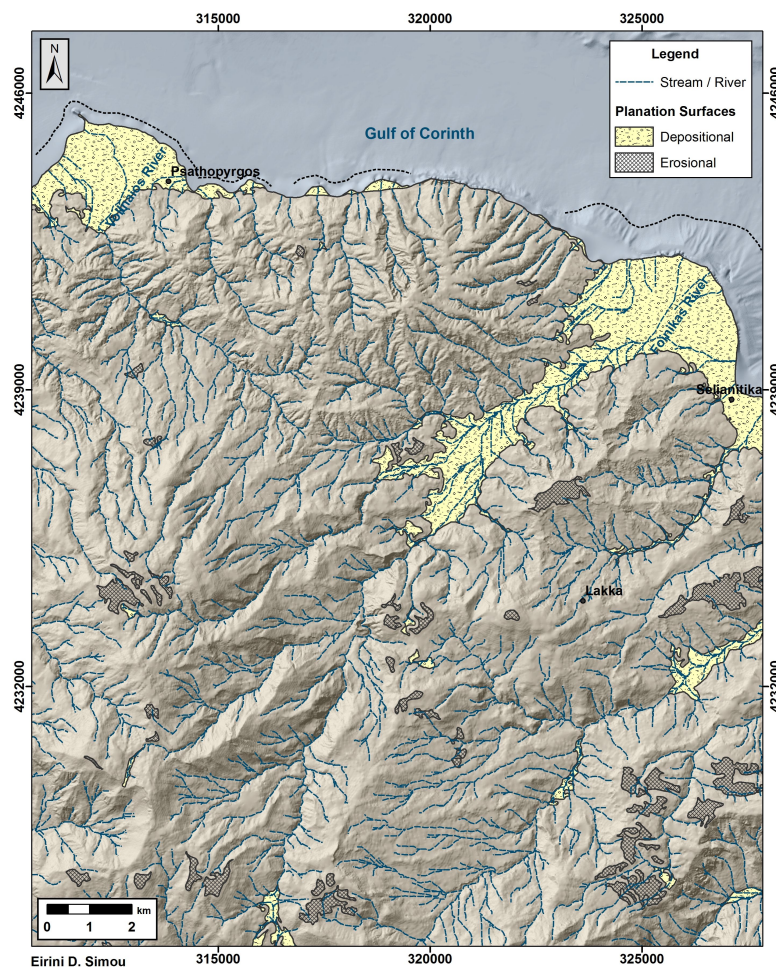
Figure 6.26 Planation Surfaces Distribution Map (in GGRS87). The prominent fan deltas at the coastline of the currently active margin of the SW Gulf of Corinth are directly related to the old, antecedent rivers of Foinikas and Volinaios while smaller fan deltas are being developed by smaller, younger streams between them. Dotted lines located offshore correspond to the submarine boundaries of the evolving fan delta sedimentation. The map is also presented in Appendix I.

The geometry of the Plio-Pleistocene sequences constructing the south margin of the western Gulf of Corinth has been significantly affected by the inception, development and migration northwards of the prevailing fault systems during the Corinth rift evolution.
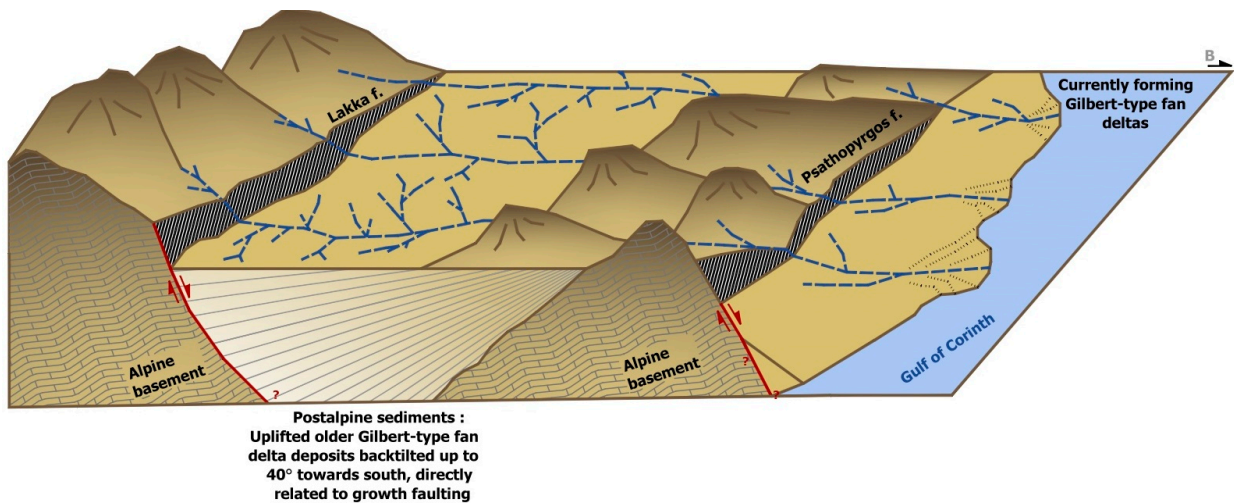
Figure 6.27 3D-block illustration of the study area showing post–alpine layer rotation variations as a result of syn-depositional faulting (growth faulting) near the active margin of a currently evolving sedimentary basin. Uplifted older Gilbert-type fan delta deposits are back-tilted up to 40º towards south. The following photos (Fig 6.28 & 6.29) show the differentiations in the bedding rotation (higher to the north, lower to the south close to Lakka fault) presenting evidence for growth faulting.

Figure 6.28 Horizontal to slightly inclined (up to 5º towards south) layers of the Plio-Pleistocene formations of the hanging-wall near the Lakka fault.

Figure 6.29 Plio-Pleistocene formations of the hanging-wall towards the Psathopyrgos fault zone, locally inclined up to 40º towards south (south of Kamares village, Achaia). Such inclined layers are also observed south of Rodini village (Fig.5.9).

The growth faulting, better presented in Fig. 6.27 – 6.29, is determined through the differential inclinations of the bedding within the fault block. The uplifted Gilbert-type fan delta deposits, exposed at the northern part of Peloponnese, are back-tilted from a few up to 40º towards south, influenced by the syn-depositional / syn-sedimentary of Lakka and Psathopyrgos extensional structures.

6.4 Morphotectonic Synthesis

The morphotectonic interpretation, which has been accomplished by the compilation of all the previously presented maps, has led to the construction of the Morphotectonic Map (Fig. 6.31), which illustrates the major and minor morphotectonic features of the project area. The defined elements have been totally extracted by their morphological impacts on the slope values, the geological setting and the drainage pattern and have been further evaluated in combination with fieldwork observations and the relative bibliographic references.

The overall morphology of the study area seems to be controlled mainly by the large-scale faults of Lakka and Psathopyrgos, which are clearly defined by the abrupt alternations of the morphological slope values (e.g. Fig. 6.30). These north dipping normal faults, trending E – W and SE – NW respectively are the most important structures in the southwestern part of the Gulf of Corinth as they are representative of the inception, growth and migration northwards of the Plio-Quaternary fault activity related to the Corinth rift evolution.
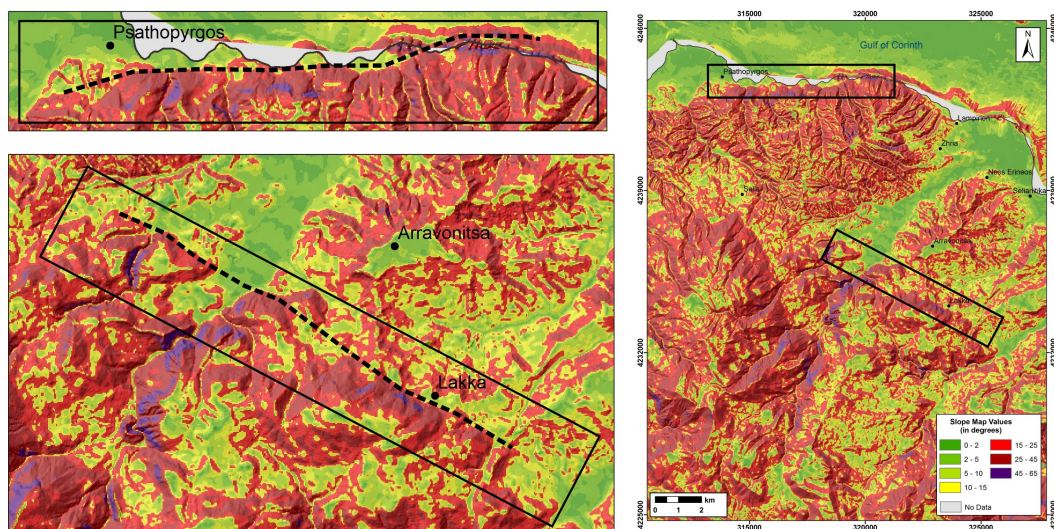
Figure 6.30 The Psathopyrgos and Lakka morphotectonic structures as determined from their influence on the slope values distribution. The right picture shows the position of these faults, bounding the Lakka fault block, and corresponds to the Slope Distribution Map of Fig. 6.9.
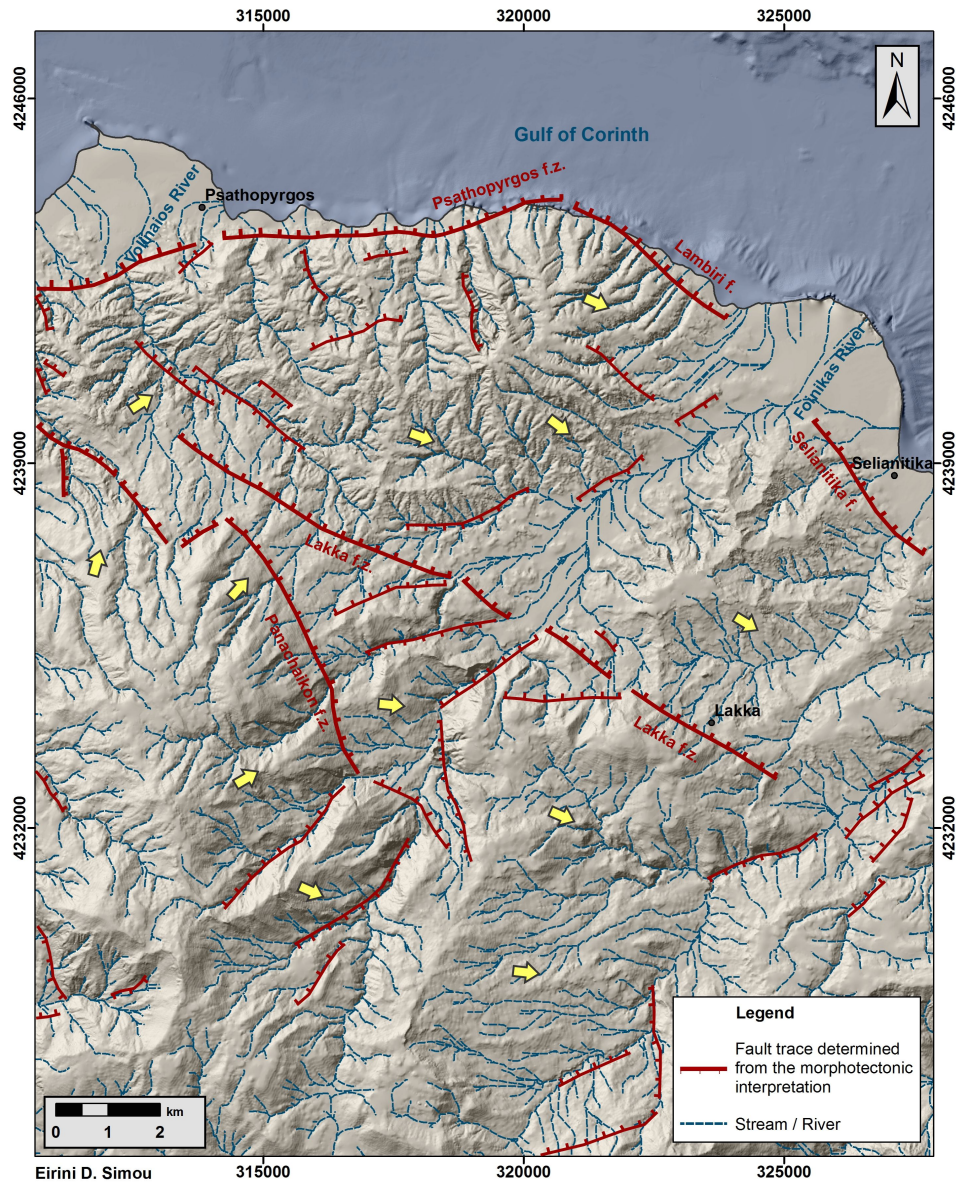
Figure 6.31 Morphotectonic Map (in GGRS87) presenting the major and minor tectonic structures in the study area. All the marked features have been defined by their morphological signatures on the slope values, the geological setting and the drainage pattern. Yellow arrows correspond to local tilting of fault blocks obtained entirely by drainage asymmetries. The map is also presented in Appendix I.

The SE – NW morphotectonic features towards the eastern part of the study area (mentioned as Lambiri and Selianitika faults on the Morphotectonic Map according to bibliographic references) also correspond to significant structures within the wider study area as they probably belong to the step over zone from Lakka fault block to West Eliki fault block. Their geomorphological development, enhanced by the evaluation of V_f geomorphic index, classifies them as individual tectonic segments less (but still) active than the Psathopyrgos fault. Panachaikon fault zone develops in a SE – NW direction and bounds the study area to the southwest.

79

The rest of the morphotectonic features presented on the map of Fig. 6.31, range in direction from N – S to NE – SW and NW - SE and correspond to secondary active / probably active fault structures which have been developed during the continuous Plio-Quaternary extensional tectonic deformation. These relatively minor tectonic elements are located along the deep incised streams and they have affected significantly the drainage geometry and evolution.

Except for the tectonic structures, evidence for local fault block tilting has been observed, expressed through drainage disorders. The relative analysis is presented in paragraph 6.2 and the results are illustrated on the Morphotectonic Map of Fig. 6.31.

7 Coastal Zone Instabilities

The tectonic and geomorphological variations, which have been extensively analysed in the previous paragraphs, are the controlling factors on the topographic relief. The southwestern margin of the Corinth Gulf, being tectonically and seismically active, provides a favourable setting for mass failure triggering.

Known past large-scale catastrophic events (e.g. Fig. 7.1, 7.2), located at the south margin of the Gulf of Corinth are related to significant sediment mass failures. Subsidence of ancient cities in historical times, such as Eliki and Voura in Egialia region, studied by Lykousis et al. (1997; 2005) or more recent case studies, such as the 1971 Panagopoula landslide (Sakellariou et al.,2001b; Lebourg et al., 2009) and the submarine landslides in Derveni area (March 2012), have increased the scientific interest related to these phenomena, which represent an ongoing hazard in the study area. As human needs and activities are growing, a comprehensive approach is necessary concerning the distribution and frequency of failures and the related geohazards (tsunamigenic potential).

Figure 7.1 The Panagopoula landslide (Achaia) occurred on April the 24th, 1971.

Figure 7.2 Coastal retreat in Derveni (Corinth) controlled by submarine landslides.

The erosional processes, in the framework of active extensional tectonics, are often being expressed not only by slow rates of grain-by-grain weathering and transportation but by instant landsliding events as well. Local lithology, intense seismic activity and high rates of sedimentation in the submarine region co-operate to form a high-energy geodynamic environment, enchasing the possibility of instabilities occurrence.

The fact that the highest rates of tectonic activity are concentrated at the southwestern Corinth rift where the Psathopyrgos fault zone is located, makes the landslide phenomena to be expected in the nearby shallow water and coastal environment, particularly in areas where slope values indicate a very narrow or absent continental shelf because of the fault surface existence.

Koukouvelas et al. (1997) attempted to present the clear linkage between active faults and landslide localization. According to their studies, the tectonically related instabilities can be separated into two types: (i) earthquake triggered slides during seismic events and (ii) slides related to steep fault-produced morphology and erosional factors. The second-type slides are distributed towards the fault plane as presented on Fig. 7.3. Small-scale, soil or rock, slides (Fig. 7.4) are usually located at the areas of maximum uplift in the central part of the fault plane while most of the sizable instabilities (e.g. Panagopoula landslide) occur at the ends of the exposed fault surface (Fig. 7.3).
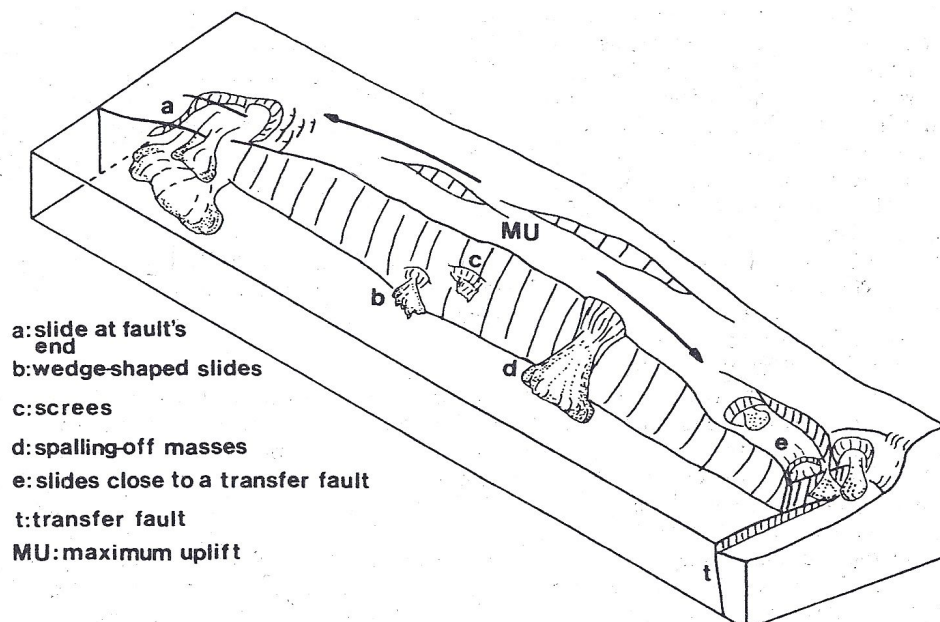
Figure 7.3 Morphological expressions of slide types along a fault trace of a normal fault (Koukouvelas & Doutsos, 1997).
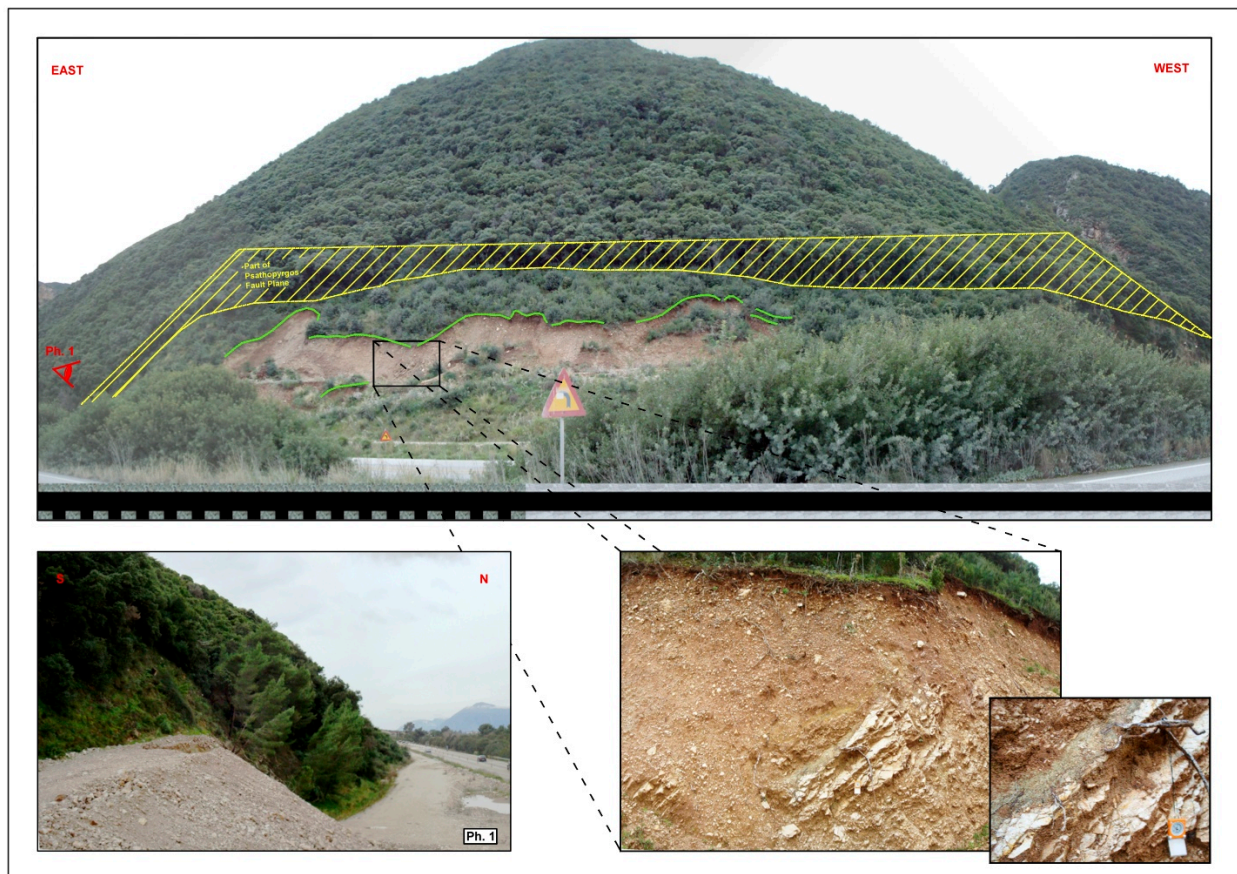
Figure 7.4 Small-scale failures related to the Psathopyrgos fault surface south of Rodini village, towards the Korinthos –Patra National Road. The yellow-marked area corresponds to a part of the Psathopyrgos fault plane. The green lines denote the landslide scarps. The bottom left pictures shows the landslide area looking from the east. The bottom right corner shows the soil nature of the materials in which the failures developed (deformed alpine limestones of the fault zone are revealed).

Small-scale instabilities are recorded in the study area in relation to the Psathopyrgos fault but are of minor importance as their consequences are expressed through limited mass movements onland that have not significant impact on the human environment. On the contrary, extensive landslides correspond to natural disasters, which may lead to property damage and loss of life. The Psathopyrgos fault zone has been related to large-scale mass movements in Panagopoula area, where landslide events have been controlled by the major tectonic feature.

The Panagopoula slope, located towards the eastern part of the Psathopyrgos fault, is characterized by gravitational instabilities for over 40 years, since April of 1971, when the main phenomenon occurred. At that date a great amount of failure masses interrupted the traffic as it moved rapidly downwards, covering the existing National Road and the railway lines. The main event has been followed by a several occasional instabilities (February 1983, November 1993, February 1994, February 1997).

The mean morphological slope in Panagopoula area dips northwards 25º to 30º from an altitude of approx. +300m straight down to the coast. Two north-flowing streams have influenced the nearby morphology:

i. The western one preserves high steep flanks, draining a large runoff area and feeding an extensive modern fan delta into the sea across a steep submarine escarpment.

ii. The eastern stream is related to gentle topographic relief, draining a smaller runoff area.

The Panagopoula landslide, covering approximately 197,000m^2, has affected the area between the two above-mentioned streams. Fieldwork observations combined with the morphotectonic analysis of the current study highlight that surface deformation is currently acting, affecting the topographic relief. The instabilities, occurring between the scree materials and the alpine basement, are linked to the geological setting and the active E – W trending normal fault of Psathopyrgos.

Sakellariou et al. (2001b) by systematic bathymetric and geophysical surveys of the submarine part of Panagopoula slope have confirmed that deformation was also observed in the marine environment expressed through downslope submarine sliding movements. Both the onshore and offshore parts of the Panagopoula slope are behaving and are being deformed as a single system, influenced by the north dipping Psathopyrgos fault plane, which acts as the main sliding surface. On the submarine slopes, the mass failures occur as creeping and slumping movements. The failure surfaces are mostly identified between the debris avalanche deposits and the underlying alpine basement.

Other studies that have been carried out this decade in the Gulf of Corinth region have proved that the submarine environment, in proximity to the study area, is generally characterized by highly unstable conditions and abundant slope failures, even at the eastern less active marginal slopes towards the West Eliki fault. The currently evolving fan deltas, which develop at the eastern end of the Psathopyrgos fault plane where tectonic activity is relatively reduced, undergo a variety of sediment failures like debris flows with significant reactivation processes (Lykousis et al., 2005; Lykousis et al., 2012). These retrogressive failures are extensive and, even they are not directly related to the fault plane, they may be destabilized by seismic shaking and lead to coastal hazards including extensive coastal retreat or slump-induced tsunamis.

Summarizing the above-mentioned data, fierce erosional processes, as a consequence of the continuous fault activity and the high rates of uplift, are responsible for the stress release and decompression of the steep morphological slopes. These, in conjunction with the high levels of seismicity (existing in the Gulf of Corinth region) are the main triggering factors in the activation of failure mechanisms. Large mass movements may develop due to slope weakening

and gradual reduction in rock strengthening subsequent to successive low-magnitude earthquake events. The main sliding surface usually starts on the fault scarp while the fault plane works as a weak surface on which the landslides may develop. In the current study area, the instabilities recorded on land are frequently mobilized by mass movements that occur in the submarine slopes of the coastal zone.

Landslides, which are located along active fault zones, suggest that the lithological and structural setting may be responsible for the pre-disposal of the slope to failure mechanisms but they not correspond to the main triggering factors. On the contrary, the development of large landslide events could be directly related to phases of intense tectonic activity.

The interpretation of the combined datasets in the study area shows that the southwestern margin of the Corinth Rift towards Psathopyrgos fault zone is characterized by intense coastal relief and a narrow, almost absent, continental shelf, which passes abruptly to steep submarine slopes. These steep slope values denote the effects of the most recent brittle deformation towards the Psathopyrgos fault plane and could be related to coastal and submarine instabilities and failures.

The high uplift rates and the rapid sedimentation that characterize the wider Psathopyrgos area, indicative of the regional high-energy terrestrial and submarine environment, are subsequently balanced by the transportation of the seafloor currents, especially where slope gradients decrease, disintegrating the probable slide deposits. Conversely, the nearby (easternmost) active -but older- tectonic structure of the West Eliki fault is related to less steep slopes in the marginal slopes of the basin. Canyons and gullies are extensive and sediment mass failures appear as retrogressive landslide scars identified near the headwalls. The mass movements evolving near the coastal and shallow marine areas may have a high tsunamigenic potential, which depends on the volumes of the mobilized materials. The 3-Dimensional qualitative analysis that was carried out for the needs of this study presents the interplay between ongoing active faulting and landslide distribution (Fig. 7.5, 7.6).
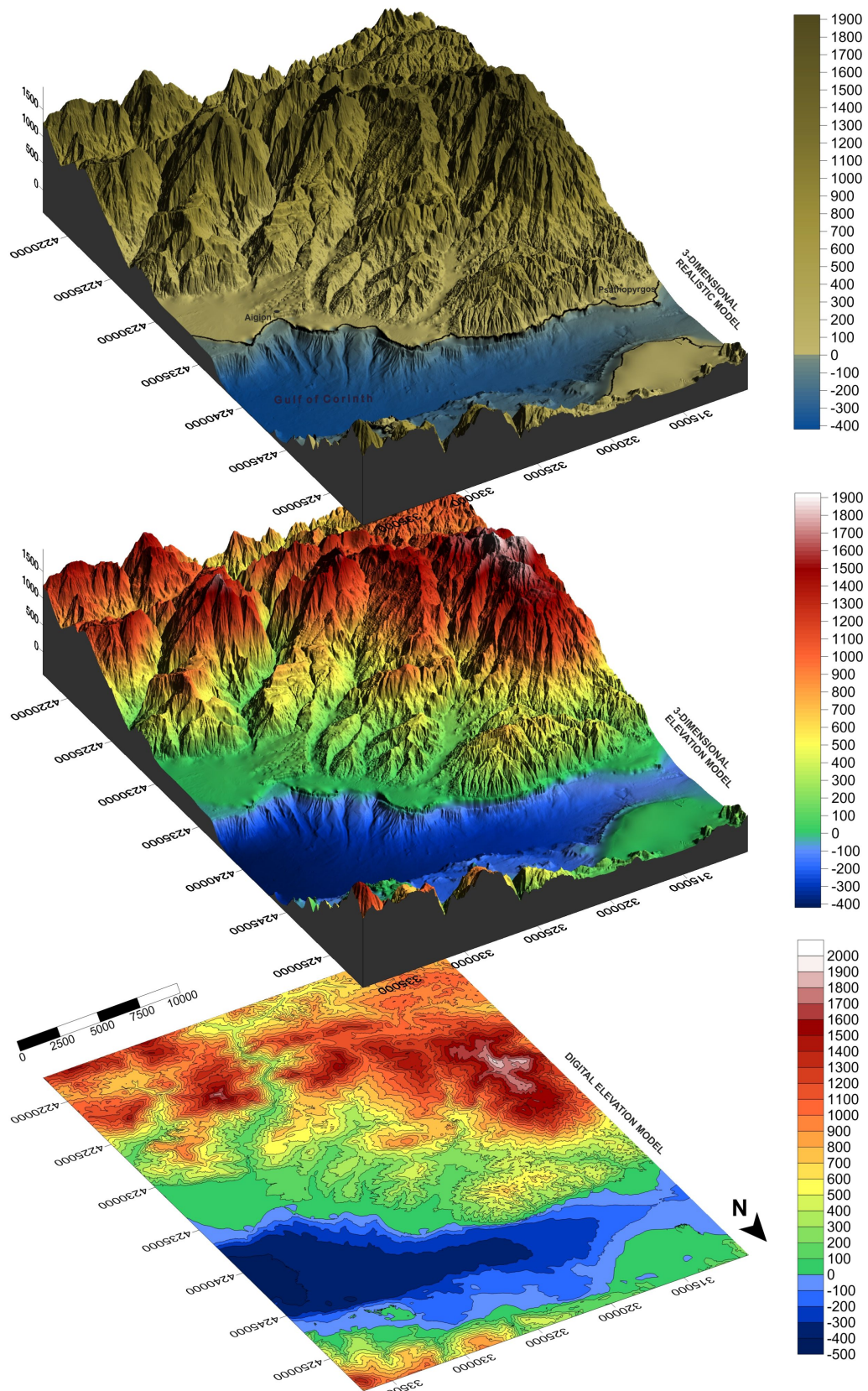
Figure 7.5 Digital Elevation Model (DEM), 3D Elevation Model and 3D Realistic Model of the combined marine & land surface data, presenting the morphology of the study area.
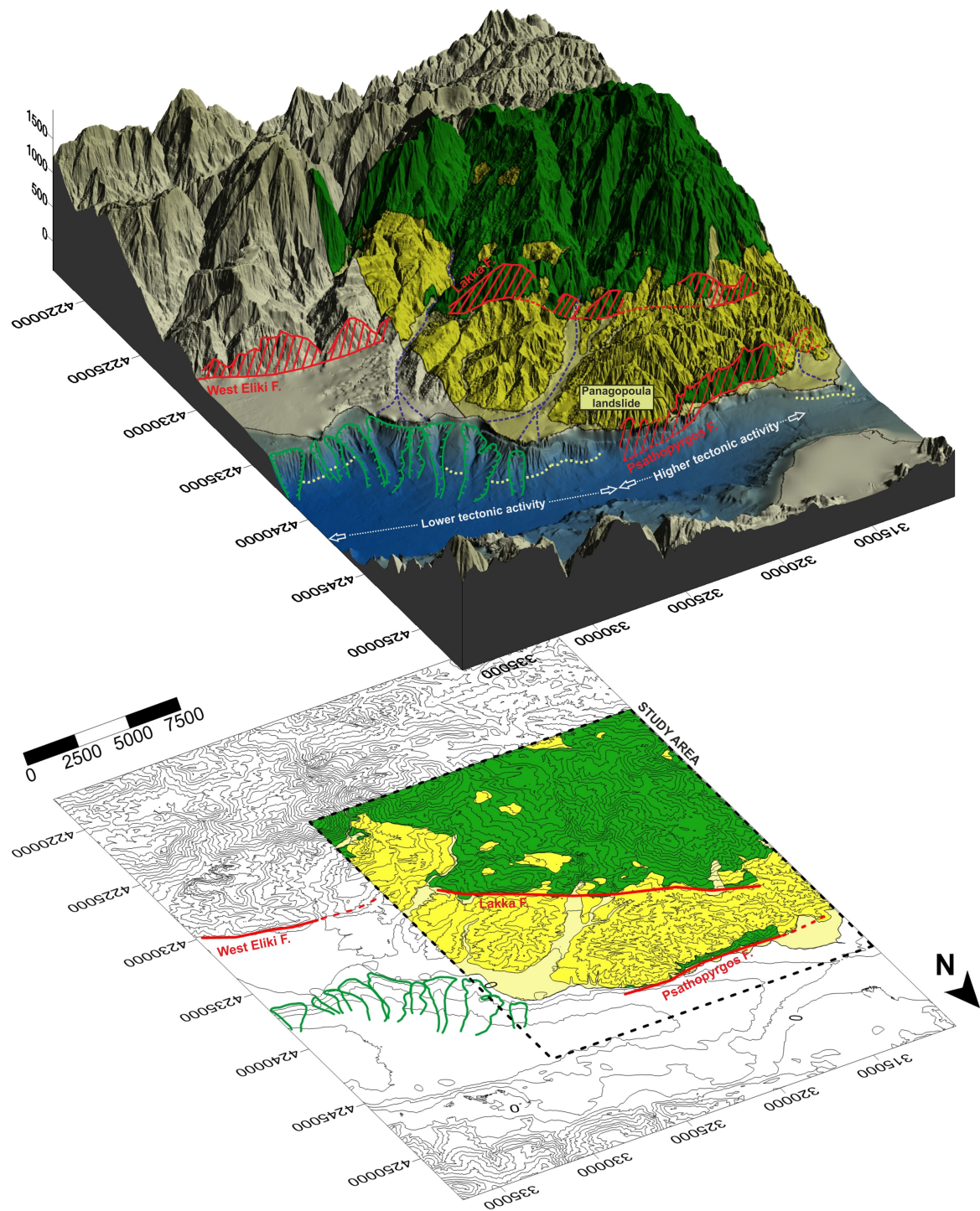
Figure 7.6 2D illustration and 3D model of the wider study area presenting the major fault planes (red lines and stripping) and the distribution of instabilities (green lines with ticks) in response to active faulting. The geological setting is applied to the narrow study area, corresponding to the Holocene and Plio-Pleistocene sediments (beige and yellow colours respectively) and the Pindos alpine basement (green colour). Ongoing sedimentation in the submarine environment is marked on the 3D model by the light yellow dotted lines.

8 Results of the study; Concluding Remarks

The studies of active tectonics, apart from their social-economic interest, follow a multi-disciplinary approach as they integrate data from structural geology, geomorphology, stratigraphy and seismology.

The tectonically active, currently evolving, landscapes result from a complex interplay between crustal and vertical movements, which act simultaneously with erosional and depositional processes. The Gulf of Corinth, the northern and most active part of the present-day Corinth Rift, constitutes a natural laboratory as it has been long identified as a site of major importance due to the continuous tectonic deformation.

Its western part is characterized by extensional deformation reaching approx. 14±2mm/yr, as documented by present-day GPS monitoring. The extremely high rates of seismicity, the continuous neotectonic activity mainly accommodated by the E-W trending Psathopyrgos fault, the exposed, well-preserved sedimentary sequences and the evidence of the intense geodynamic and geomorphological processes are only a few reasons for attempting a further morphotectonic study.

The intense neotectonic activity analysed with regard to the impacts of erosion and sedimentation on both the subaerial and submarine environment, has led to the comprehension and development of a qualitative model concerning the morphotectonics and the active geodynamic regime evolving towards the coastal zone of NW Peloponnese.

High-resolution multibeam bathymetry in combination with the available land surface data have contributed to submarine and subaerial morphological mapping. These, combined with the regional geological setting, have been used as a basis for the detection of the most recent tectonic structures and all those geomorphic features that indicate instabilities and mass failures

in the coastal zone probably triggered by the major tectonic structure of the study area, the Psathopyrgos fault.

The Lakka fault block, which corresponds to the current study area, is bounded by two significant east-west trending, north-dipping normal faults, the Psathopyrgos fault to the north and Lakka fault to the south. Laterally, it is bounded by the drainage divides of Foinikas river to the east (Selianitika village) and Volinaios river (Psathopyrgos village) to the west.

The whole study has been based on the quantitative and qualitative analysis of the topographic relief, the morphological slope values, the slopes' orientation, as well as the analysis of the drainage pattern and its disorders. The resulting Morphotectonic Map of the study area was carried out by means of the combined use of: (a) a merged Digital Elevation Model (DEM) for the subaerial and the submarine environment, (b) a Slope Distribution Map, (c) an Aspect Map and (d) a Drainage Pattern Map. Evaluation of the distribution of erosion as deep incision zones and the distribution of the planation surfaces in the study area have also contributed to more reliable results. The composition of the digital modelling in conjunction with the regional geological setting, allows the identification of the main morphological tectonic features that result from morphotectonic interpretation.

The study area, located in the NW Peloponnese, is mainly characterized by extensive occurrence of post-alpine deposits of various Plio-Quaternary phasies and alpine formations of Pindos nappe. The first formations correspond to older or currently evolving Gilbert-type fan delta deposits and indicate the high uplift rates of the south flanks of the Gulf of Corinth; the latter are Cretaceous limestone formations composing the pre-rift basement. The marine environment is characterized by tourbidites, debris avalanche deposits and the alpine bedrock.

The major, well-known tectonic structures corresponding to the Lakka fault block are:

– The Lakka fault: It represents a westward prolongation of the West Eliki fault bounding the study area to the south towards the Lakka village. The fault plane is oriented in an SSE - WNW direction (~110° to 130°), dipping 45° to 55° towards north. The fault plane is formed on Pindos limestones and well-preserved striations inclined towards northwest (~35°/345°) are distinct on fault plane. Debris materials have covered the fault slope toe.

– The Psathopyrgos E – W trending, north dipping fault: It is considered to be the presently active structure bordering the westernmost part of the Gulf of Corinth to the south. Its onshore geomorphic expression exceeds 15km in length. The steep coastal escarpment of the fault plane developing on the alpine bedrock, dipping approx. 40° - 65°, is exposed at the coastal zone. The Psathopyrgos fault has been correlated to high rates of the tectonic

activity, which is demonstrated by rapid uplift (in the order of ~0.7-0.8 mm/year) of the footwall.

The geomorphological signatures have affected topography allowing the configuration of active faulting in the study area. The morphological analysis was processed from the perspective of slope value distribution and the results are presented on the Slope Distribution map (Fig. 6.2). On this map, which was composed from the combined onshore and offshore datasets, the slope values (ranging between 0° - 65°) have been classified into seven classes aiming to indicate all those areas, both in the marine and the terrestrial environment, which are characterized by abrupt change of slope values, probably reflecting the position of active tectonic structures.

According to the classification of the slope values, the study area has been divided into three main areas: (a) The basinal area of the Gulf of Corinth with slope values ranging between 0° – 1°. (b) The coastal zone, further divided into two subareas with similar morphology. The first is comprised by moderately steep slopes of, locally, more than 25°. The second is by more gentle as slope values are in the order of 5° – 15. (c) The hilly – mountainous area of the footwall of Psathopyrgos fault, which is characterized by variable slope values indicating the maturity stage of the entire onshore area.

The combined datasets' slope value interpretation shows that the southwestern margin of the Gulf of Corinth is characterized by intense coastal relief which passes abruptly to the steep submarine slopes. These steep slope values clearly denote the effects of the most recent brittle deformation, which has occurred towards the currently active Psathopyrgos fault zone. Fierce erosional processes acting in the framework of active tectonics in correspondence to the lithological background do not allow the development of slopes generally steeper than 45°. The majority of the morphotectonic features, which have resulted from the interpretation of the Slope Distribution map, are expressed through morphological slopes in the order of 25°-45°.

Moreover, it should be highlighted that despite the fact that the slope values range between 0° to 65° in the wide study area (Fig. 6.2), the mean slope values turn out to be:

- 4° for the submarine region,
- 18° for the subaerial region and,
- 25° for the currently active region of Psathopyrgos fault, which is related to the higher rates of deformation.

Drainage basins, except for their contribution to the erosional processes, they assist in the morphotectonic interpretation through the localized disorders and asymmetries. Consequently, drainage analysis has been a necessary tool for the morphostructural synthesis as it contains

information about fault activity and evolution. The evaluation of the drainage pattern in the study area has been accomplished in the framework of the general geological setting.

The subaerial drainage system develops in a N – S to NE – SW direction and flows into the Gulf of Corinth. It consists of the:

- The fifth-order basin of Foinikas River. It bounds the study area to the west, covers an area of about 95 km^2 and extends approximately 20km towards south.

- The fourth-order basin of Volinaios River. It is the western boundary of the study area and the second largest basin (14km in length covering approx. 33km^2).

- The rest of the drainage basins, mainly defined by third-order and second-order streams, which cover significantly smaller in area, ranging from a few hundreds of m^2 up to 5 km^2. The orientation of each drainage basin, as well as the direction of the trunk streams and the number of the tributaries, varies mainly according to the position of the main controlling tectonic structures and the lithological background.

As far as the submarine drainage system is concerned, it is characterized by a simple pattern. The central part of the basin is dominated by a central E – W trending drainage runoff axis, exceeding 20km in length, accumulating the flow to the east, towards the deepest parts of the Gulf of Corinth (in this study the maximum depth is -420m).

Multiple submarine channels (up to 5km in length) cut transversely the continental slope, developing in a N–S direction towards the western and central part of the study area and in a NE – SW direction towards the eastern part (Foinikas river). These channels are straight and elongated with a few or no smaller crossing tributaries towards the active slope of Psathopyrgos. To the east (towards Foinikas river), where activity is less or temporarily ceased, submarine gullies develop that are considered as initial steps in the development of larger submarine canyons and more mature drainage networks related to less active regions.

Drainage disorders and asymmetries onland reveal the tectonic structures that have significant influence on the current topographic relief as a result of the interaction between uplift, tilting and the lithological background. The study area has been divided into 3 areas (Fig. 6.13) according to its drainage pattern characteristics. The first two areas correspond to younger drainage systems, related to the Psathopyrgos active fault. The third area, including Foinikas and Volinaios rivers, corresponds to antecedent drainage rivers sourced in pre-Neogene basement, affected by the less active Lakka fault structure.

Intense erosional processes are associated to extensive fluvial systems. The V_f geomorphic index, which was calculated for the needs of this study, discriminating between V-shaped and U-shaped flat-floored valleys, indicates whether streams are actively incising subjected to active

uplift, or they are eroding the landform laterally in response to lower rates of uplift (and consequently, activity) and relative tectonic quiescence. The evaluation of the V_f results shows that the western drainage basins (Drainage basins 1 to 14, Fig. 6.11) are in a high-energy geotectonic environment due to the Psathopyrgos fault. Towards west, tectonic activity seems to be decreased; the V_f values are probably indicating another individual tectonic segment or a step over zone to the West Eliki fault block.

As far as the sedimentation is concerned in the study area it is currently evolving below the sea level in the SW margins of the Gulf of Corinth. The large submarine structures are directly related to the antecedent rivers of Foinikas and Volinaios, which have constructed prominent fan deltas at the coastline. Smaller younger streams, in contrast to the antecedent catchments are also being developed into the easily eroded Plio-Pleistocene sediments, constructing smaller fan deltas. The older uplifted Gilbert-type fan delta deposits, exposed at the hills of NW Peloponnese, are currently being influenced by the fierce erosional processes. Controlled by the growth faulting of Lakka and Psathopyrgos extensional structures, they are presented back-tilted up to 40º towards south.

The synthesis of all the previously presented results obtained from the generated maps has led to the construction of the Morphotectonic Map (Fig. 6.31), which illustrates the morphotectonic features of the study area. Lakka and Psathopyrgos faults are clearly defined by the abrupt alternations of the morphological slope values (e.g. Fig. 6.30). They correspond to the most significant structures that have controlled the overall morphology of the study area and they are representative of the inception, growth and migration basinwards of the Plio-Quaternary fault activity related to the Corinth rift evolution. The SE – NW morphotectonic features towards the eastern part of the study area (mentioned as Lambiri and Selianitika faults on the Morphotectonic Map according to bibliographic references) also correspond to significant active structures. The rest of the morphotectonic features presented on the map of Fig. 6.31, range in direction from N – S to NE – SW and NW – SE. They are noticed along the deep incised streams and they have affected significantly the drainage geometry and evolution. In general, they correspond to secondary active or probably active fault structures that have been developed during the continuous Plio-Quaternary extensional tectonic deformation. Except for the morphotectonic features, the Morphotectonic Map presents evidence for local fault block tilting, entirely obtained by drainage asymmetries. The eastern part of the study area is characterized by tilting towards SE to ESE while the western part, southwards of Lakka and Panachaikon faults (Fig. 6.31) shows tilting towards NE. This differentiation could be explained by the existence of a ~N-S axis, located between these two areas, which causes the local disruption.

The erosional processes, in the framework of active faulting, are often being expressed not only by slow rates of grain-by-grain weathering and transportation through the fluvial systems but by instant mass failures as well. Local lithology combined with the steep slope values, the intense concentrated seismic activity and the high rates of sedimentation in the submarine region contribute to the formation of a high-energy geodynamic environment, enchasing the possibility of instabilities triggering.

The interpretation of the combined datasets in the study area shows that the southwestern margin of the Corinth Rift towards Psathopyrgos fault zone is characterized by intense coastal relief and a narrow, almost absent, continental shelf, which passes abruptly to steep submarine slopes. These steep slope values reflect the effects of the most recent brittle deformation towards the Psathopyrgos fault plane and are prone to coastal and submarine instabilities and failures. On the contrary, the easternmost less active tectonic structure of the West Eliki fault is related to less steep slopes in the margins of the basin. Canyons and gullies are extensive and sediment mass failures are identified near the headwalls as retrogressive landslide scars. The mass movements evolving near the coastal and shallow marine areas may lead to coastal hazards including extensive coastal retreat or slump-induced tsunamis depending on the volumes of the mobilized materials. As human needs and activities are growing, a special interest has been arisen concerning risk assessment and management, the results of this study summarised following the 3D model of the Gulf of Corinth (Fig. 7.5, 7.6) could be further evaluated, not only from a geological, but from a geohazard perspective as well

The clarification of the detailed geological conditions in the subaerial and the submarine environments, the understanding of the long-term neotectonic processes, the evaluation of the relevant geotechnical conditions, the estimation of erosion volumes and rates and the GPS velocity measurements interpretation in order to assess the deformation rates, are only a few suggestions for further investigation.

REFERENCES

Ambraseys, N., Jackson, J. (1990). Seismicity and associated strain of central Greece between 1890 and 1988, Geophys. J. Int., 101, 663-708.

Angelier, J. (1978). Tectonic evolution of the Hellenic Arc since the late Miocene, Tectonophysics 49, 23–36.

Angelier, J. (1979). Neotectonique de l Arc Egéen. Bull. Soc. géol. Nord, Publ. N° 3, 417.

Angelier, J., Lyberis, N., Le Pichon, X., Barrier, E., Huchon, P. (1982). The tectonic development of the Hellenic arc and the Sea of Crete: A synthesis. Tectonophysics, 86, 159-196.

Armijo, R., Meyer, B., King, G. C. P., Rigo, A., Papanastassiou, D. (1996). Quaternary evolution of the Corinth Rift and its implications for the Late Cenozoic evolution of the Aegean. Geophys. J. Int. 126, 11-53.

Bell, R.E. (2008). Tectonic evolution of the Corinth Rift, University of Southampton, School of Ocean and Earth Science, Doctoral Thesis, 227.

Bell, R.E., McNeill, L.C., Henstock T. J., Bull, J.M. (2011). Comparing extension on multiple time and depth scales in the Corinth Rift, Central Greece, Geophys. J. Int., 186, 463–470.

Bernard, P. et al., (1997). A low angle normal fault earthquake: the Ms=6.2, June 1995 Aigion earthquake (Greece), J. Seism., 1, 131–150.

Blair, T.C. & McPherson, J.G. (1994). Alluvial fans and their natural distinction from rivers based on morphology, hydraulic processes, sedimentary processes, and facies assemblages. Journal of Sedimentary Research, A64, 450–489.

Bourouis S., Cornet F.H. (2009). Microseismic activity and fluid fault interactions: Some results from the Corinth Rift Laboratory (CRL), Greece, Geophys. J. Int. vol. 178, 561- 580.

Briole, P., Rigo, A., Lyon-Caen, H., Ruegg, J., Papazissi, K., Mitsakaki, C., Balodimou, A., Vieis, G., Hatzfeld, D. & Deschamps, A. (2000), 'Active deformation of the Corinth rift, Greece: results from repeated Global Positioning System surveys between 1990 and 1995', Journal of Geophysical Research 105(B11), 25, 605–25, 625.

Brooks, M., Ferentinos, G. (1984). Tectonics and sedimentation in the Gulf of Corinth and the Zakynthos and Kefallinia channels, western Greece, Tectonophysics, 101, 25-54.

Buck, W.R. (1991). Models of continental lithospheric extension, Journal of Geophysical Research 96, 161–120.

Bull, W. B., McFadden, L.D. (1977). Tectonic geomorphology north and south of the Garlock fault, California. In: Doehering, D.O. (Ed.), Geomorphology in Arid Regions. Proceedings at the Eighth Annual Geomorphology Symposium. State University of New York, Binghamton, NY, 115–138.

Burbank, D.W., Anderson, R.S. (2012). Tectonic Geomorphology (second edition), Wiley – Blackwell.

Caress, D.W., Thomas, H., Kirkwood, W.J., McEwen, R., Henthorn, R., Clague, D.A., Paull, C.K., and Paduan, J. (2008). High-Resolution Multibeam, Sidescan, and Subbottom Surveys Using the MBARI AUV D. Allan B.

Clarke, P., Davies, R., England, P., Parsons, B., Billiris, H., Paradissis, D., Veis, G., Cross, P., Denys, P., Ashkenazi, V., Bingley, R., Kahle, H., Muller, M. & Briole, P. (1998). Crustal strain in central Greece from repeated GPS measurements in the interval 1989–1997, Geophysical Journal International 135, 195–214.

Clément, C. (2000). Imagerie sismique crustale de la subduction hellénnique et du golfe de Corinthe. Thèse de doctorat, Un. Paris VII, 175.

Collier, R., Leeder, M., Trout, M., Ferentinos, G., Lyberis, E. & Papatheodorou, G. (2000). High sediment yields and cool, wet winters: test of last glacial paleoclimates in the northern Mediterranean, Geology 28(11), 999–1002.

Corti, G., Bonini, M., Conticelli, S., Innocenti, F., Manetti, P. & Sokoutis, D. (2003). Analogue modelling of continental extension: a review focused on the relations between the patterns of deformation and the presence of magma, Earth Sciences Reviews 63(3), 169–247.

De Martini, P.M., Pantosti, D., Palyvos, N., Lemeille, F., McNeill, L. and Collier, R. (2002). Slip rates of the Aigion and Eliki faults from uplifted marine terraces, Corinth Gulf, Greece. In: EGS XXVII General Assembly, 4, Geophysical Research Abstract, Nice, France.

Doutsos, T., Kontopoulos, N., Poulimenos, G. (1988), The Corinth-Patras Rift as the initial stage of continental fragmentation behind an active island arc (Greece), Basin Research, 1, 177-190.

Doutsos, T. & Piper, D. (1990). Listric faulting, sedimentation, and morphological evolution of the Quaternary eastern Corinth rift, Greece; first stages of continental rifting, Geological Society of America Bulletin 102 (6), 812–829.

Doutsos, T., Poulimenos, G. (1992). Geometry and kinematics of active faults and their seismotectonic significance in the western Corinth-Patras rift (Greece), Journal of Structural Geology, 14 (6), 689-699.

Ferentinos, G., Papatheodorou, G., Collins, M.B. (1988). Sediment transport processes on an active submarine fault escarpment: Gulf of Korinth, Greece. Mar. Geol. 83, 43–61.

Flotte, N., Sorel, D., Mueller, C., Tensi, J. (2005). Along strike changes in the structural evolution over a brittle detachment fault: example of the Pleistocene Corinth–Patras rift (Greece). Tectonophysics 403, 77–94.

Ford, M., Rohais, S., Williams, E. A., Bourlange, S., Jousselin, D., Backert, N., et al. (2012). Tectono-sedimentary evolution of the western Corinth rift (Central Greece). Basin Research, 1–23.

Fossen, H. (2010). Structural Geology, Cambridge University Press, 463.

Ganas, A., Chousianitis, K., Batsi, E., Kolligri, M., Agalos, A., Chouliaras, G., Kalogeras, I., Makropoulos, K. (2013). The January 2010 Efpalion earthquakes at the western tip of the Gulf of Corinth, central Greece: earthquake interactions and blind normal faulting, Journal of Seismology 17, 465-484.

Ghisetti, F.C., Vezzani, L., Agosta, F., Sibson, R., Moretti, I. (2001). Tectonic setting and sedimentary evolution of the south - west margin of the Corinth Rift (Aigion-Xylocastro area). IFP Report no 562 11.

Goldsworthy, M., Jackson, J. (2000). Active normal fault evolution in Greece revealed by geomorphology and drainage patterns. Journal of the Geological Society, London, Vol. 157, pp. 967-981.

Goldsworthy, M., Jackson, J., Haines, J. (2002). The continuity of active fault systems in Greece, Geophys. J. Int., 148, 596-618.

Hatzfeld, D., Kementzetzidou, D., Karakostas, V., Ziazia, M., Nothard, S., Diagour- tas, D., Deschamps, A., Karakaisis, G., Papadimitriou, P., Scordilis, M., Smith, R., Voulgaris, N., Kiratzi, S., Makropoulos, K., Bouin, M. P. & Bernard, P. (1996), 'The Galaxidi earthquake of 18 November 1992: A possible asperity within the normal fault system of the Gulf of Corinth (Greece)', Bulletin of the Seismological Society of America 86, 1987–1991.

Heezen, B., Ewing, M., Leonard Johnson, G. (1966). The Gulf of Corinth floor, Deep Sea Research 13, 381–411.

Houghton, S., Roberts, G., Papanikolaou, I., McArthur, J. (2003). New 234U-230Th coral dates from the western Gulf of Corinth: Implications for extensional tectonics. Geophysical Research Letters, Vol. 30, No. 19.

Howard, A. D. (1967). Drainage analysis in geologic interpretation; a summation, AAPG Bulletin, v. 51, p. 2246-2259.

Jackson, J. A., J. Gagnepain, G. Houseman, G. C. P. King, P. Papadimitriou, C. Soufleris, Virieux, J. (1982), Seismicity, normal faulting, and the geomorphological development of the Gulf of Corinth (Greece): The Corinth earthquakes of February and March 1981, Earth Planet. Sci. Lett., 57, 377–397.

Jackson, J. and Leeder, M. (1994). Drainage systems and the development of normal faults: an example from Pleasant Valley, Nevada. J. Struct. Geol., 16: 1041-1059.

Jolivet, L. (2001). A comparison of geodetic and finite strain pattern in the Aegean, geodynamic implications, Earth and Planetary Science Letters 187, 95–104.

Karakostas, B. et al. (1994). The aftershock sequence and focal properties of the July, 1993 (Ms=5.4) Patras earthquake, Bull. Geol Soc. Greece, XXX/5, 167–174.

Keller, E.A., Pinter, N. (2002). Active Tectonics. Earthquakes, Uplift, and Landscape. Prentice Hall, New Jersey, 362.

Keraudren, B., Sorel, D. (1987). The terraces of Corinth (Greece): A detailed record of eustatic sea level variations during the last 500.000 years, Mar. Geol. 77, 99-107.

Koukouvelas, I. & Doutsos, T. (1997). The effects of active faults on the generation of landslides in NW Peloponnese. In: Engineering Geology and the Environment, Marinos, G. C., Koukis, G. C., Tsiabaos, S. G. C., (Eds), Proc. Int. Symp., A. A. Balkema, Rotterdam, 799-804.

Lebourg, T., El Bedoui, S., Hernandez, M. (2009). Control of slope deformations in high seismic area: Results from the Gulf of Corinth observatory site (Greece), Engineering Geology 108, 295-303.

Leeder, M. R., Jackson, J. A. (1993). The interaction between normal faulting and drainage in active extensional basins, with examples from western United States and central Greece. Basin Research, 5, 79-102.

Leeder, M.R. (1995). Continental rifts and proto-oceanic troughs, Tectonics of Sedimentary Basins (Eds Ingersoll, R.V. & Busby, C.J.). Blackwell Science, Oxford, 119–148.

Leeder, M. (1999). Sedimentology and Sedimentary Basins. From Turbulence to Tectonics. 592 pp. Oxford: Blackwell Science.

Leeder, M., Portman, C., Andrews, J., Collier, R., Finch, E., Gawthorpe, R., McNeill, L., Perez-Arlucea, M. & Rowe, P. (2005). Normal faulting and crustal deformation, Alkyonides Gulf and Perachora peninsula, eastern Gulf of Corinth rift, Greece, Journal of the Geological Society 162(3), 549–561.

Lykousis, V. (1990). Prodeltaic deposits. Seismic stratigraphy– sedimentology–slope stability. Unpublished PhD thesis, University of Patras (in Greek) 302 p.

Lykousis V., Papanikolaou D. & Sakellariou D. (1997). Geodynamically induced catastrophies of coastal ancient cities in Egialia, W. Korinthiakos Gulf, Greece. In: Marinos et al. (eds) "Engineering. Geology & Environment", V.3: 3197-3202, Balkema Pupl. Co. Amsterdam.

Lykousis V., Sakellariou D., Alexandri M., Nomikou E., Rousakis G. (2005). Slope failures and tsunamis in active margins: W.Corinth Gulf, Greece. 22nd IUGG International Tsunami Symposium, 286.

Lykousis V., Sakellariou D., Blandin J., Person R., Etiope G., Alexandri M., Nomikou P., Rousakis G. (2006). The ASSEM sea-bed observatory for long term multihazard monitoring: Gulf of Corinth experiment. Proceedings of the 8th Hellenic Symposium of Oceanography & Fishery, 151-154.

Lykousis, V., Sakellariou, D., Moretti, I. & Kaberi, H. (2007). Late Quaternary basin evolution of the Gulf of Corinth: Sequence stratigraphy, sedimentation, fault-slip and subsidence rates, Tectonophysics 440, 29–51.

Lykousis, V., Roussakis, G., Sakellariou, D. (2009). Slope failures and stability analysis of shallow water prodeltas in the active margins of Western Greece, northeastern Mediterranean Sea, Int. J. Earth Sci. (Geol Rundsch), 98, 807–822.

Lykousis V., Papatheodorou G., Sakellariou D., Nomikou P., Rousakis G. and Ferentinos G. (2012). Sedimentary processes in active rifts of the European continental margin: The Gulf of Corinth (NE Mediterranean). The Deep Sea and Subseafloor Frontiers Conference, 11-14 March 2012 Sitges, Spain

Makris, J., Papoulia, I., Karastathis, V., Ilinsky, D. (2003). Crustal structure of the Saronikos–Eastern Korinthiakos basin from wide apperture seismic data: evidence of thinned continental crust below the saronikos volcanic area. EGS–AGU–EUG Joint Assembly. Geoph. Res. Abstracts, vol. 5. Abstract Nr. EAE03-A04195.

Mariolakos, I., Papanikolaou, D. (1981). The Neogene basins of the Aegean arc from the paleogeographic and the geodynamic point of view, International Symposium on the Hellenic Arc and Trench System, Natl. Tech. Univ. of Athens, Athens.

McClusky, S.C. et al. (2000). Global Positiong System constraints on plate kinematics and dynamics in the eastern Mediterranean and Caucasus, J. Geophys, Res., 105, 5695-5719.

McKenzie, D. (1972). Active tectonics of the Mediterranean region, Geophys. J. R. Astron. Soc., 30, 109-185.

McKenzie, D. (1978a). Active tectonics of the Alpine – Himalayan belt: The Aegean Sea and surrounding regions, J. R. Astron. Soc., 55, 217-254.

McNeill, L., Cotterill, C., Henstock, T., Bull, J., Stefatos, A., Collier, R., Papatheoderou, G., Ferentinos, G. & Hicks, S. (2005a). Active faulting within the offshore western Gulf of Corinth,Greece: Implications for models of continental rift deformation, Geology 33, 241–244.

McNeill, L., Collier, R., De Martini, P., Pantosti, D. & D'Addezio, G. (2005b). Recent history of the Eastern Eliki fault, Gulf of Corinth: geomorphology, palaeo- seismology and impact on palaeoenvironments, Geophysical Journal International 161, 154–166.

Mercier, J., Sorel, D., Vergeli, P., Simeakis, K. (1989). Extensional tectonic regimes in the Aegean basins during the Cenozoic, Basin Res., 2, 49-71.

Moretti, I., Sakellariou, D., Lykousis, V. & Micarelli, L. (2003). The Gulf of Corinth: an active half graben?, Journal of Geodynamics 36, 323–340.

Moretti, I., Lykousis, V., Sakellariou, D., Reynaud, J-Y., Benziane, B. & Prinzhoffer, A. (2004). Sedimentation and subsidence rate in the Gulf of Corinth: what we learn from the Marion Dufresne's long piston coring, Comptes Rendus Geoscience 336, 291–299.

Myrianthis, M.L. (1984). Graben formation and associated seismicity in the Gulf of Korinth (Central Greece). In: Dixon, J.E., Robertson, A.H.F. (Eds.), The Geological Evolution of the Eastern Mediter- ranean. Geol. Soc. Sp. Publ., vol. 17, 701–707.

Nemec, W., Steel, R. J. (1988). Fan Deltas: Sedimentology and Tectonic Settings, Blackie, London.

Nichols, G.J., Uttamo, W. (2005). Sedimentation in a humid, interior, rift basin: the Cenozoic Li Basin, northern Thailand, Journal of the Geological Society, London, 162, 333–348.

Nichols, G. (2009). Sedimentology and Stratigraphy, Wiley-Blackwell, 419.

Nomikou, P., Alexandri M., Lykousis V., Sakellariou D., Ballas D. (2011). Swath Bathymetry and Morphological Slope Analysis of Corinth Gulf. 2nd INQUA-IGCP-567 International Workshop on Active Tectonics, Earthquake Geology, Archaeology and Engineering, Corinth, Greece.

Ori, G. (1989). Geologic history of the extensional basin of the Gulf of Corinth (?Miocene–Pleistocene), Greece, Geology 17, 918–921.

Palyvos, N., Pantosti, D., De Martini, P., Lemeille, F., Sorel, D. & Pavlopoulos, K. (2005). The Aigion-Neos Erineos coastal normal fault system (western Corinth Gulf Rift, Greece): Geomorphological signature, recent earthquake history, and evolution, Journal of Geophysical Research 110.

Palyvos N., Pantosti, D., Stamatopoulos, L., De Martini P. M. (2007). Geomorphological reconnaissance of the Psathopyrgos and Rion - Patras fault zones (Achaia, NW Peloponnesus), Bull. Geol. Soc. Greece, XXXX.

Palyvos, N., Mancini, M., Sorel, D., Lemeille, F., Pantosti, D., Julia, R., Triantafyllou, M. & De Martini, P.M. (2010). Geomorphological, stratigraphic and geochronological evidence of fast Pleistocene coastal uplift in the westernmost part of the Corinth Gulf Rift (Greece). Geol. Jour., 45, 78–104.

Palyvos, N., Mancini, M., Ford, M., Mayer N., Esu, D., Girotti, O., Urban, B. (2013). Western closure of the Corinth Rift: Stratigraphy and structure of the Lakka fault block. Geophysical Research Abstract, Vol. 15, EGU2013-5360, EGU General Assembly 2013.

Pantosti, D., De Martini, P.M., Koukouvelas, I.,Stamatopoulos, L., Pavlides, S., Palyvos, N., and Pucci, S. (2002). Paleoseismological trenching across the Eliki and Aigion faults (Gulf of Corinth, Greece). In: EGS XXVII General Assembly, 4, Geophysical Research Abstract, Nice, France.

Papadopoulos, G., Drakatos, G., Papanastassiou, D., Kalogeras, I., Stavrakakis, G. (2000). Preliminary results about the catastrophic earthquake of 7 September 1999 in Athens, Greece. Seismological Research Letters, 71, 318–329.

Papanikolaou, D. (1984). The three metamorphic belts of the Hellenides: A review and a kinematic interpretation, Geological Society of London, Special Publication, 17, 551-561.

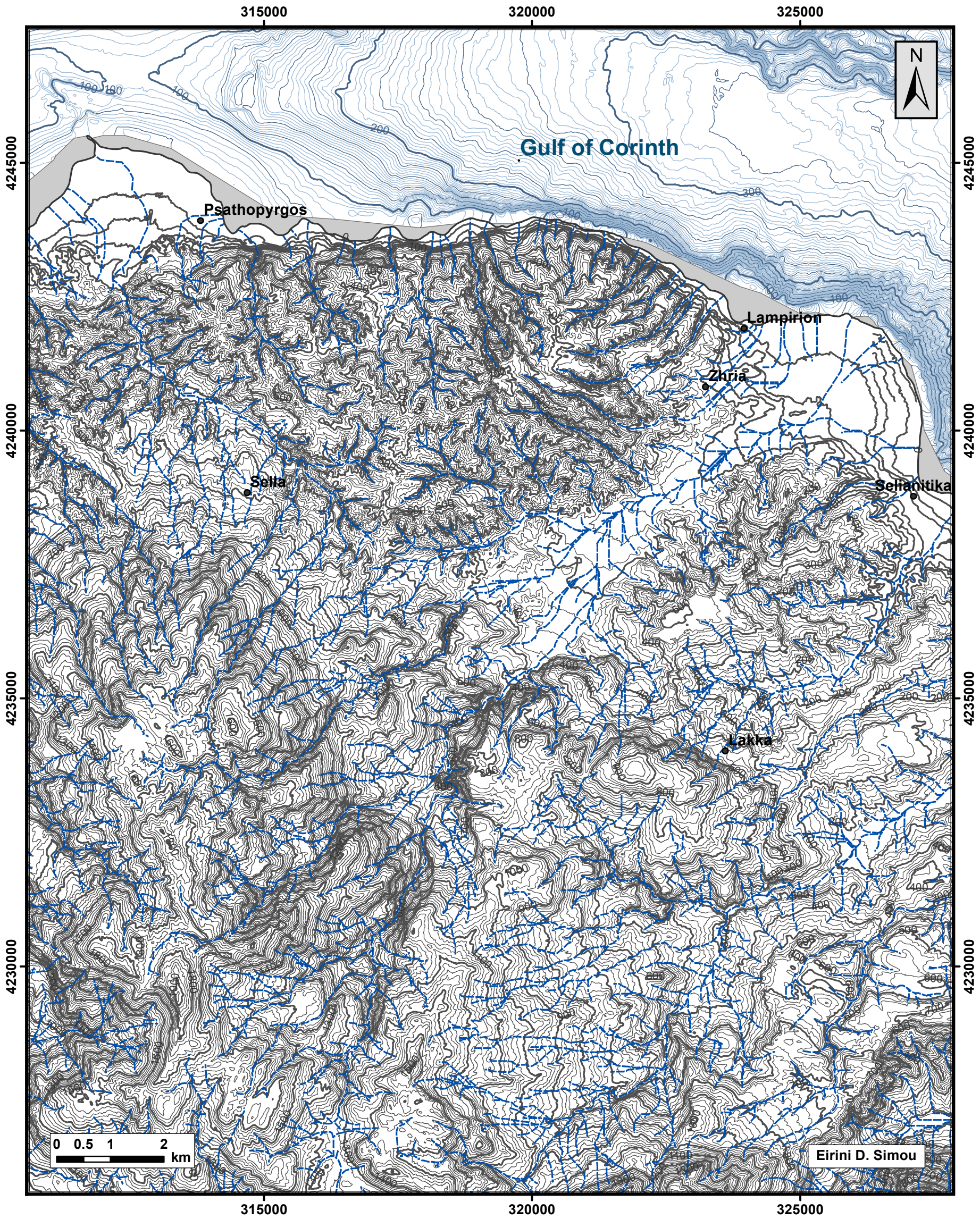Papanikolaou, D. (1993). Geotectonic evolution of the Aegean, Bull. Geol. Soc. Greece, XXVII, 33-48.

Papanikolaou. D., Panagopoulos, A. & Alexiadou, H. (2005). Landslides induced by active low angle normal faults: The case of Panagopoula landslide along the Psathopyrgos fault, western Corinth gulf, Greece. 14th Meeting Assoc. Eur. Geol, Soc., 19-23 September 2005, Torino, Abstracts p. 104.

Papanikolaou, D., Logos, E., Lozios, E., Sideris C. (1997a). Korinthos, in Neotectonic Map of Greece, scale 1:100.000, Earthquake Plann. and Prot. Organ., Athens.

Papanikolaou, D., Chronis, G., Lykousis, V., Sakellariou, D., Papoulia, I. (1997b). Neotectonic structure of the Western Gulf of Corinth and geodynamic phenomena of the Aigion earthquake. Proceedings of the 5th Hellenic Symposium of Oceanography & Fishery, Volume I (in Greek).

Papanikolaou, D., Alexandri, M., Nomikou, P., Ballas, D. (2002). Morphotectonic structure of the western part of the North Aegean Basin based on swath bathymetry. Marine Geology 190, 465-492.

Papanikolaou, D., Royden, L. (2007). Disruption of the Hellenic arc: Late Miocene extensional detachment faults and steep Pliocene – Quaternary normal faults – Or what happened at Corinth? Tectonics, Vol.26.

Pérez-Peña, J. V., Azor, A., Azañón, J. M., Keller, E. (2010). Active tectonics in the Sierra Nevada (Betic Cordillera, SE Spain): Insights from geomorphic indexes and drainage pattern analysis, Geomorphology 119, 74–87.

Perissoratis, C., Mitropoulos, D., Angelopoulos, I. (1984). The role of earthquakes in inducing sediment mass movements in the eastern Corinthiakos Gulf: an example from the February 24–March 4 activity. Mar. Geol. 55, 35–45.

Perissoratis, C., Piper, D. & Lykousis, V. (2000). Alternating marine and lacustrine sedimentation during the late Quaternary in the Gulf of Corinth rift basin, central Greece, Marine Geology 167, 391–411.

Postma, G. and Roep, Th.B., (1985). Resedimented conglomerates in the bottomset of a Gilbert-type gravel delta. J. Sediment. Petr., 55, 874-885.

Prior, D.B., Bornhold, B.D. (1990). The underwater development of Holocene fan deltas. In: Colella, A., Prior, D.B. (Eds.), Coarse- Grained Deltas, Spec. Publ. Internat. Assoc. Sedimentologists, vol. 10, pp. 75–90.

Roberts, S., Jackson, J. A. (1991). Active normal faulting in central Greece: An overview, in The Geometry of normal faults, Geol. Soc. Spec. Publ., 56, 125-142.

Roberts, G. P., Houghton, S. L., Underwood, C., Papanikolaou, I., Cowie, P. A., Van Calsteren, P., Wigley, T., Cooper, F. J., McArthur J. M. (2009). Localization of Quaternary slip rates in an active rift in 105 years: An example from central Greece constrained by 234U-230Th

coral dates from uplifted paleoshorelines, Journal of Geophysical Research, Vol. 114, B10406, doi:10.1029/2008JB005818.

Rohais, S., Eschard, R., Ford, M., Guillocheau, F. & Moretti, I. (2007). Stratigraphic architecture of the Plio-Pleistocene infill of the Corinth Rift: Implications for its structural evolution, Tectonophysics 440, 5–28.

Royden, L., Papanikolaou, D. (2011). Slab segmentation and late Cenozoic disruption of the Hellenic Arc. G3: Geochemistry – Geophysics – Geosystems, Vol. 12, No. 3, Q03010.

Sachpazi, M., Clement, C., Laigle, M., Hirn, A. & Roussos, N. (2003). 'Rift structure, evolution and earthquakes in the Gulf of Corinth, from reflection seismic images', Earth and Planetary Science Letters 216, 243–257.

Seger, M., Alexander, J. (1993). Distribution of Plio-Pleistocene and modern coarse-grained deltas south of the Gulf of Corinth, Greece. Int. Assoc. Sedimentol., Spec. Publ. 20, 37–48.

Sakellariou, D., Lykousis, V., Papanikolaou, D. (2001a). Active faulting in the Gulf of Corinth, Greece. 36th CIESM, Congress Proceedings 36, 43.

Sakellariou, D., Lykousis, V., Roussakis, G. (2001b). Slope failure phenomena along submarine active faulted slopes: Panagopoula area, Western Gulf of Corinth, Bull. of Geol. Soc., XXXIV/5, 1723-1731 (in Greek).

Seyitoglu, G. & Scott, B. C. (1996). 'The cause of N-S extensional tectonics in western Turkey: Tectonic escape vs back–arc spreading vs orogenic collapse', Journal of Geodynamics 22(1-2), 145–153.

Sokos, E., Zahradník, J., Kiratzi, A., Janský, J., Gallovicˇ, F., Novotny, O., Kostelecký, J., Serpetsidaki, A., Tselentis, G.A. (2012). The January 2010 Efpalio earthquake sequence in the western Corinth Gulf (Greece). Tectonophysics, 530-531, 299-309.

Stefatos, A., Papatheoodorou, G., Ferentinos, G., Leeder, M. & Collier, R. (2002). Seismic reflection imaging of active offshore faults in the Gulf of Corinth: their seismotectonic significance, Basin Research 14, 487–502.

Stemberk, J., Košťák, B. (2007). 3-D trend of aseismic creep along active faults in western part of the Gulf of Corinth, Greece, Acta Geodyn. Geomater., Vol. 4, No. 1 (145), 53-65.

Stewart, I. (1996). Holocene uplift and palaeoseismicity on the Eliki fault, western Gulf of Corinth, Annali di Geofisica 39, 575–588.

Stewart, I., Vita-Finzi, C. (1996). Coastal uplift on active normal faults: the Eliki Fault, Greece, Geophysical Research Letters 23, 1853–1856.

Strahler, A.N. (1952). Hypsometric (area-altitude) analysis of erosional topography. Geol. Soc. Am. Bull. 63, 1117–1142.

Strahler, A.N. (1957). Quantitative Analysis of Watershed Geomorphology, Transactions, American Geophysical Union, Vol. 38, No 6, 913-920.

Taymaz, T., Jackson, J. & McKenzie, D. (1991). Active tectonics of the north and central Aegean Sea, Geophysical Journal International 106, 433–490.

Tselentis G. A., Melis N. S. And Sokos E. (1994). The Patras (July 14, 1993; Ms=5.4) Earthquake Sequence. Bull.of Geol. Soc. Greece , Vol. 30 / 5.

Valkaniotis, S. (2009). Correlation between Neotectonic structures and Seismicity in the broader area of Gulf of Corinth (Central Greece). PhD Thesis, Aristotle University of Thessaloniki, Thessaloniki.

Westaway, R. (2002). The Quaternary evolution of the Gulf of Corinth, central Greece: coupling between surface processes and flow in the lower continental crust, Tectonophysics 348(4), 269–318.

Zelilidis, A. (2000). Drainage evolution in a rifted basin, Corinth graben, Greece, Geomorphology 35, 69–85.

Zelt, B. C., Taylor, B., Weiss, J. R., Goodliffe, A. M., Sachpazi, M. & Hirn, A. (2004). Streamer tomography velocity models for the Gulf of Corinth and Gulf of Itea, Greece, Geophysical Journal International 159(1), 333–346.

APPENDIX I : MAPS (Scale 1:75,000)

SYNTHETIC TOPOGRAPHIC MAP
SW Gulf of Corinth
(Scale 1:75,000)

N

315000 320000 325000

4245000

Gulf of Corinth

100
200
300

Psathopyrgos

Lampirion

Zhria

4240000

Selianitika

Sella

4235000

Lakka

4230000

0 0.5 1 2
km

Eirini D. Simou

315000 320000 325000

LEGEND

——— Isobath (Interval: 4m)

——— Contour (Interval: 20m)

– – – Streams / Rivers

▨ No data zone

Coordinate System: Greek Grid
Projection: Transverse Mercator
Datum: GGRS 1987

Multibeam Bathymetric Data, primarily
processed by P. Nomikou & M. Alexandri,
were collected by R/V AEGAEO (October
2002) for the Hellenic Centre for Marine
Reasearch (HCMR).

N

Peloponnese
Greece
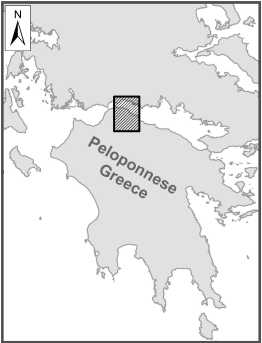
SIMPLIFIED GEOLOGICAL MAP
SW Gulf of Corinth
(Scale 1:75,000)

Gulf of Corinth

Volinaios River

Psathopyrgos

Lampirion

Zhria

Foinikas River

Neos Erineos

Selianitika

Sella

Arravonitsa

Lakka

Peloponnese
Greece

0 0.5 1 2
km

Eirini D. Simou
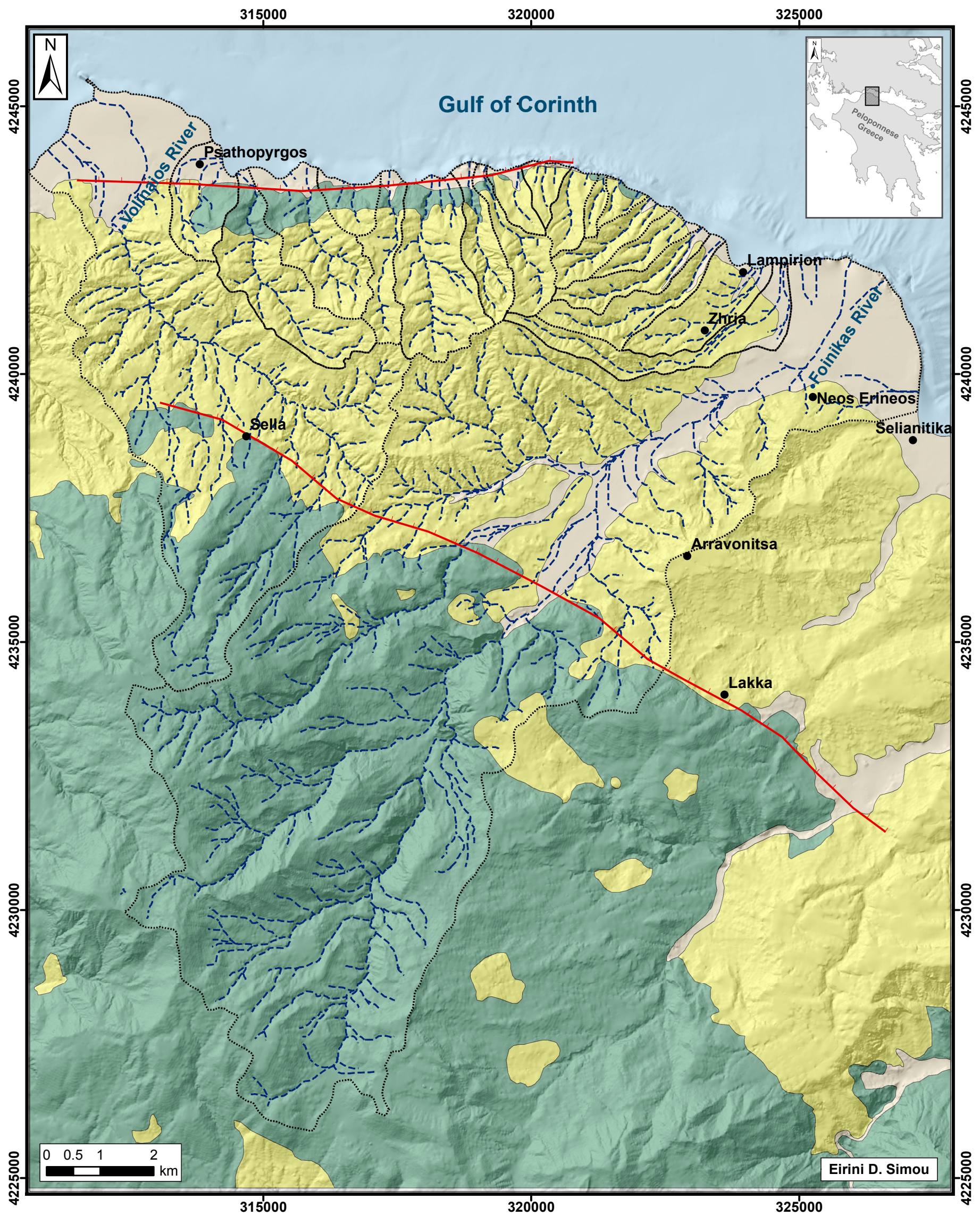
LEGEND

**Geological Formations
(simplified approach)**

Holocene Deposits

Postalpine Sediments

Alpine Basement

Main fault structures of
Psathopyrgos (towards north)
& Lakka (towards south),
bounding the Lakka fault block.

- - - - - Stream / River

· · · · · · Drainage Divide

Coordinate System: Greek Grid
Projection: Transverse Mercator
Datum: GGRS 1987

Multibeam Bathymetric Data, primarily
processed by P. Nomikou & M. Alexandri,
were collected by R/V AEGAEO (October
2002) for the Hellenic Centre for Marine
Reasearch (HCMR).

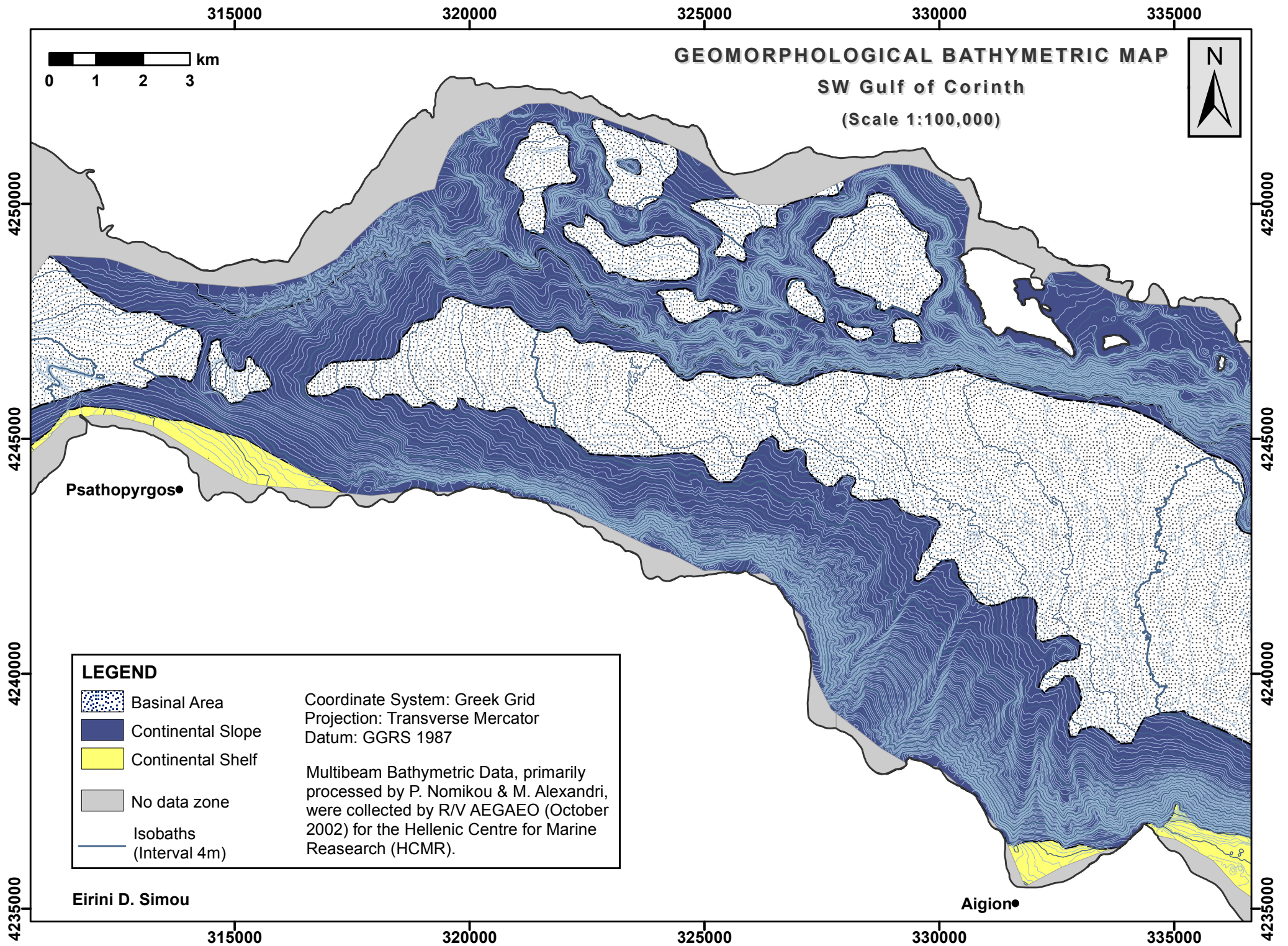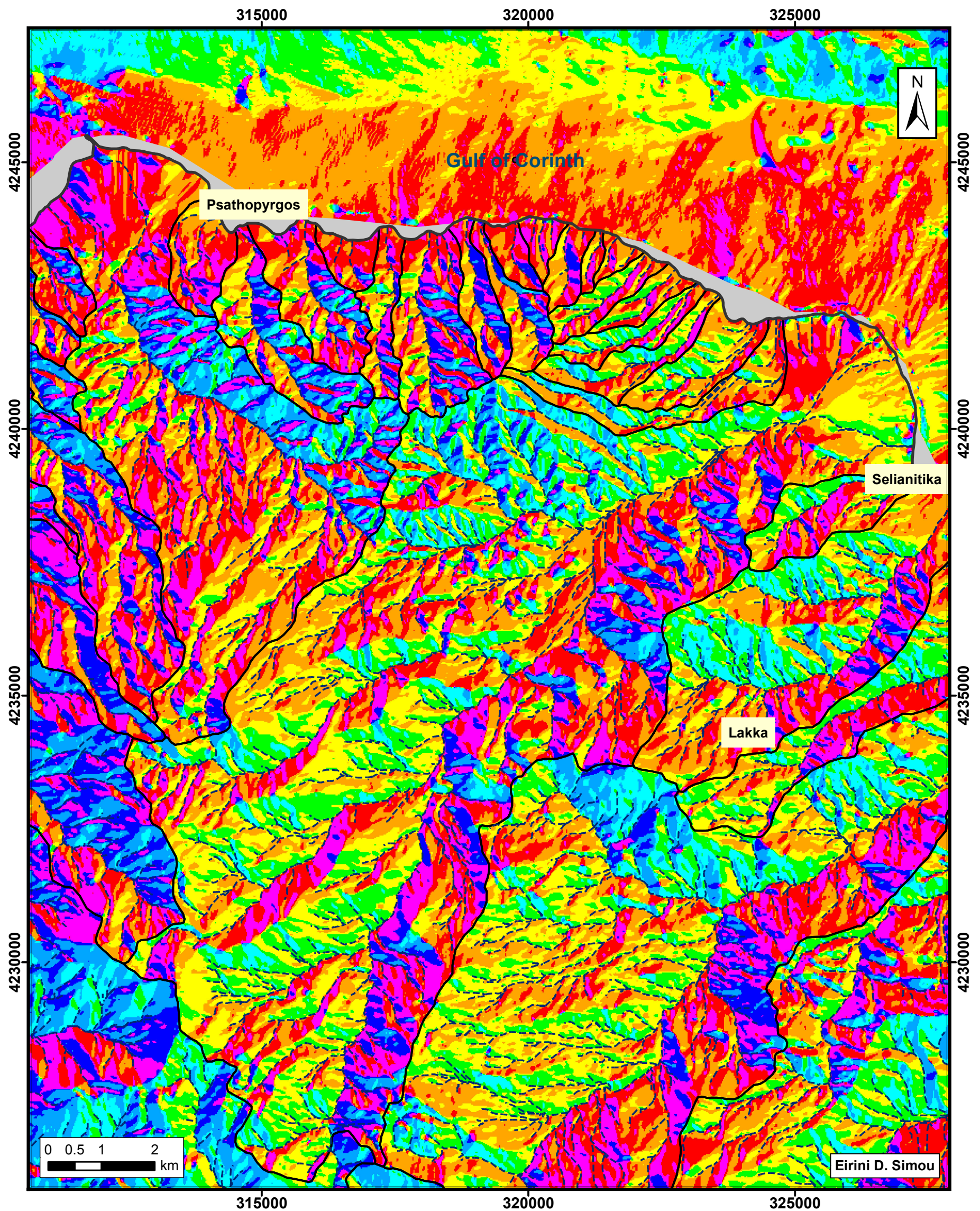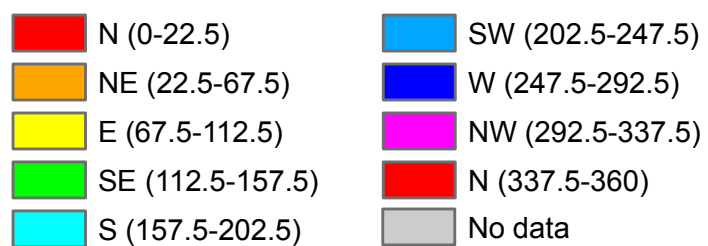# SLOPE DISTRIBUTION MAP
SW Gulf of Corinth
(Scale 1:75,000)

Gulf of Corinth

Psathopyrgos

Selianitika

Lakka

Eirini D. Simou
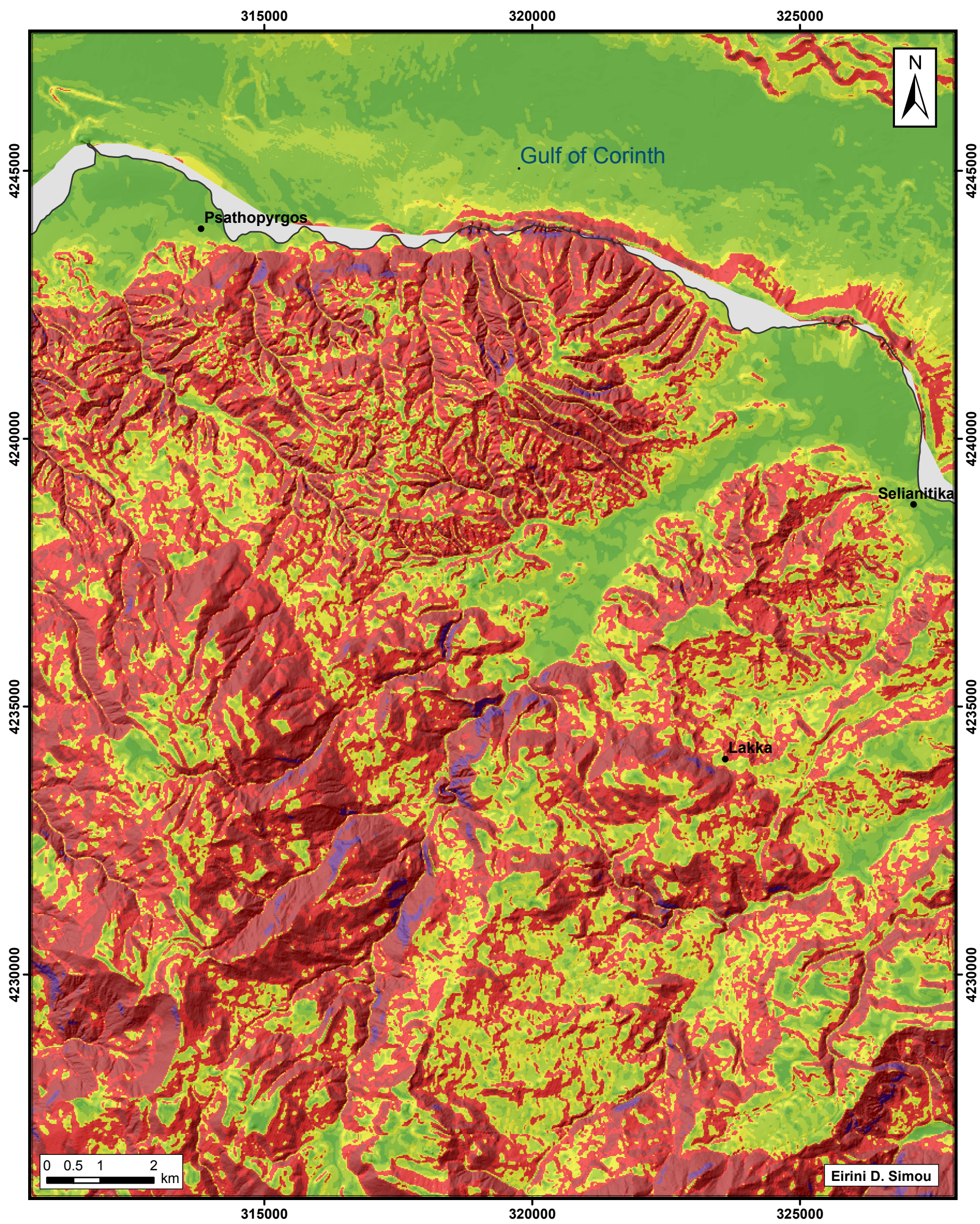
SLOPE MAP VALUES
(in degrees)

- 0 - 2
- 2 - 5
- 5 - 10
- 10 - 15
- 15 - 25
- 25 - 45
- 45 - 65
- No Data

Coordinate System: Greek Grid
Projection: Transverse Mercator
Datum: GGRS 1987

Multibeam Bathymetric Data, primarily
processed by P. Nomikou & M. Alexandri,
were collected by R/V AEGAEO (October
2002) for the Hellenic Centre for Marine
Reasearch (HCMR).

Peloponnese
Greece

GEOMORPHOLOGICAL BATHYMETRIC MAP
SW Gulf of Corinth
(Scale 1:100,000)

Psathopyrgos●

Aigion●

LEGEND

Basinal Area

Continental Slope

Continental Shelf

No data zone

Isobaths
(Interval 4m)

Coordinate System: Greek Grid
Projection: Transverse Mercator
Datum: GGRS 1987

Multibeam Bathymetric Data, primarily
processed by P. Nomikou & M. Alexandri,
were collected by R/V AEGAEO (October
2002) for the Hellenic Centre for Marine
Reasearch (HCMR).

Eirini D. Simou

ASPECT MAP
SW Gulf of Corinth
(Scale 1:75,000)

315000 320000 325000

4245000

Gulf of Corinth

Psathopyrgos

4240000

Selianitika

4235000

Lakka

4230000

Eirini D. Simou

0 0.5 1 2 km

315000 320000 325000

Aspect Map (values in degrees)

- N (0-22.5)
- NE (22.5-67.5)
- E (67.5-112.5)
- SE (112.5-157.5)
- S (157.5-202.5)
- SW (202.5-247.5)
- W (247.5-292.5)
- NW (292.5-337.5)
- N (337.5-360)
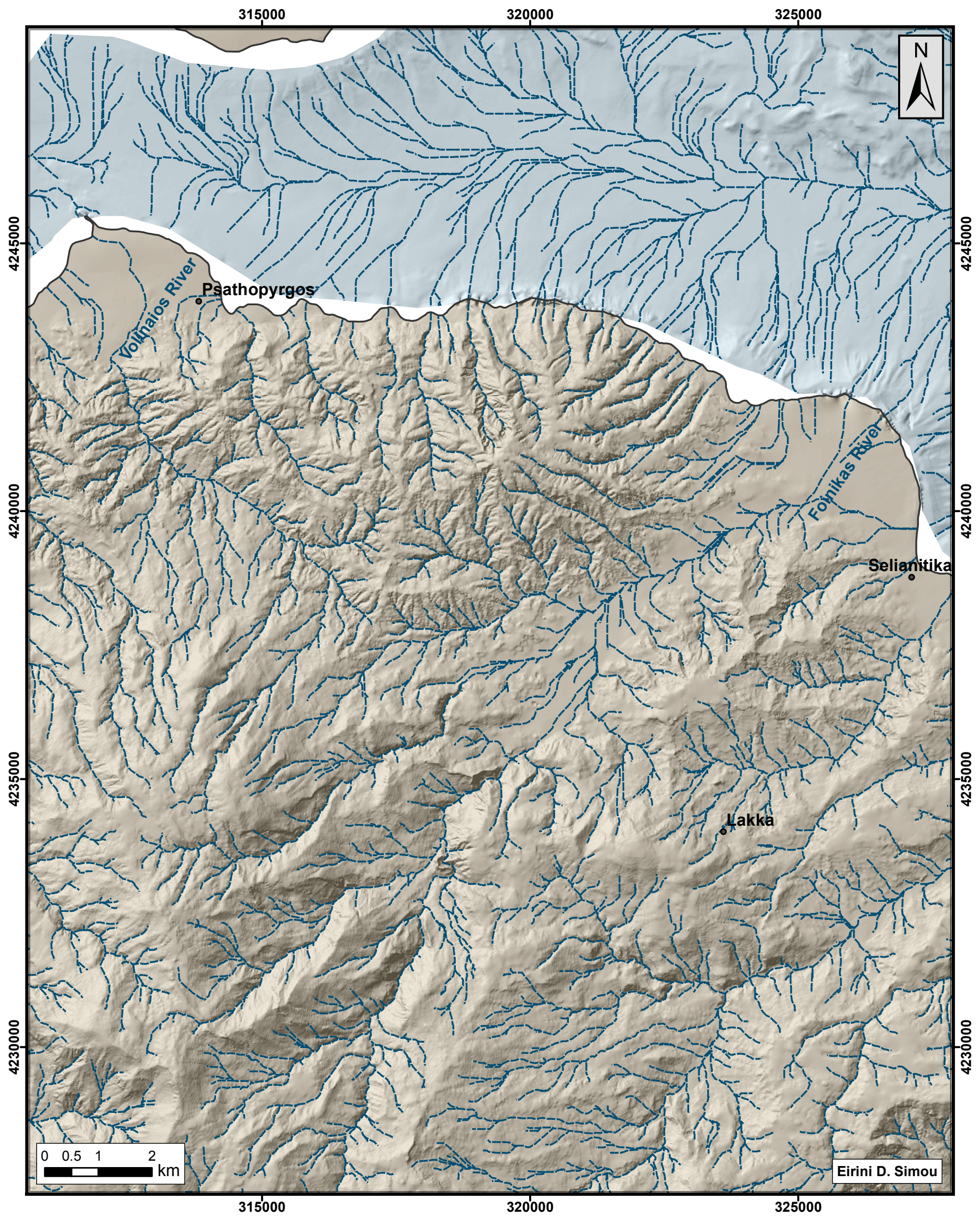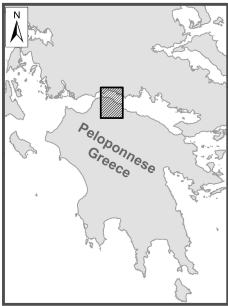- No data

- - - - - Rivers & Streams
———— Drainage divide

Coordinate System: Greek Grid
Projection: Transverse Mercator
Datum: GGRS 1987

Multibeam Bathymetric Data, primarily
processed by P. Nomikou & M. Alexandri,
were collected by R/V AEGAEO (October
2002) for the Hellenic Centre for Marine
Reasearch (HCMR).

Peloponnese
Greece
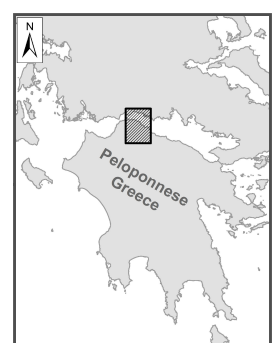
STREAM ORDER CLASSIFICATION MAP
SW Gulf of Corinth
(Scale 1:75,000)

Gulf of Corinth

Volinaios River

Foinikas River
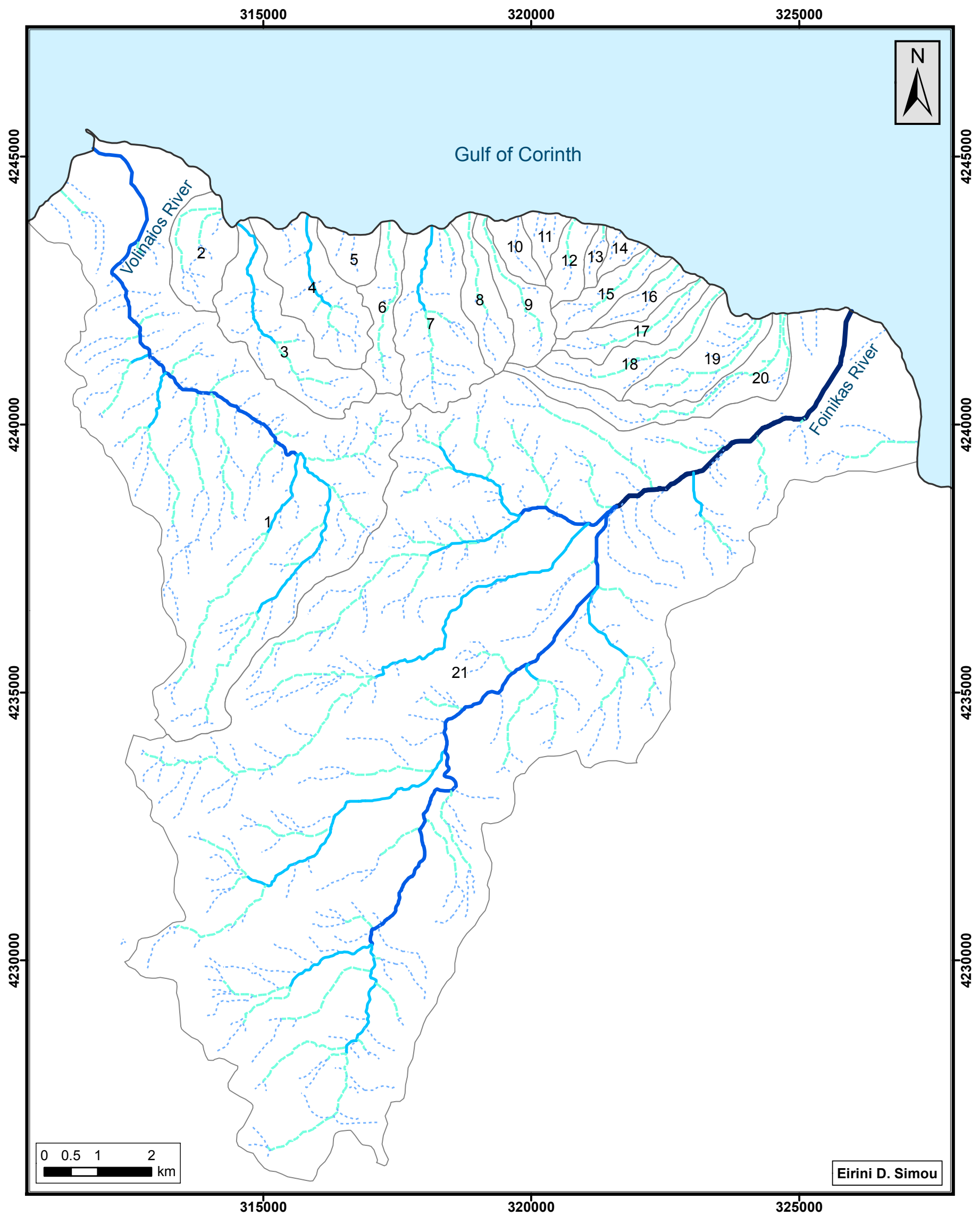
**Drainage Pattern Ordering
(Application of the Strahler
Stream Ordering Method)**

- - - - 1
- - - - 2
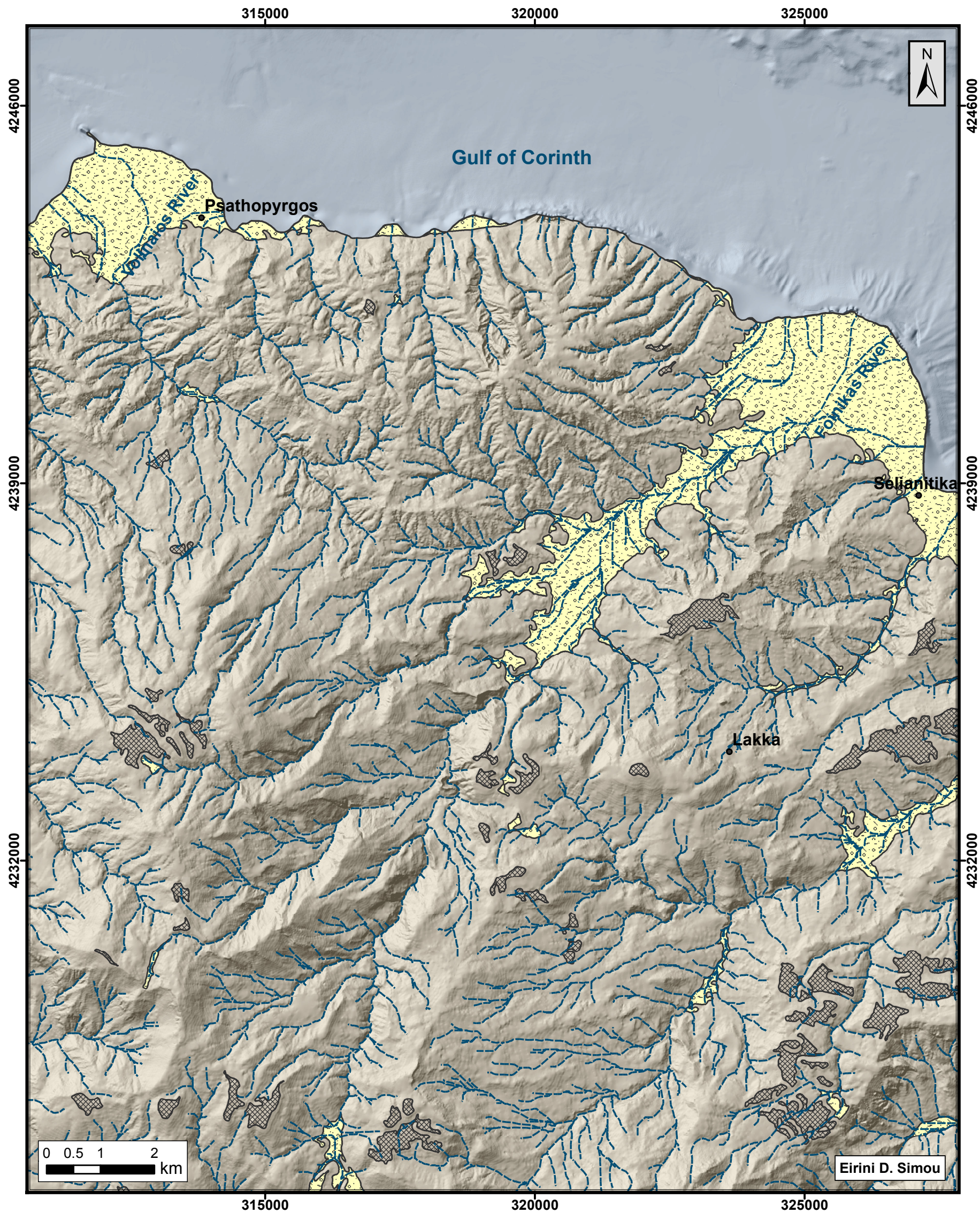──── 3
──── 4
──── 5
──── Drainage divide

Coordinate System: Greek Grid
Projection: Transverse Mercator
Datum: GGRS 1987

Multibeam Bathymetric Data, primarily
processed by P. Nomikou & M. Alexandri,
were collected by R/V AEGAEO (October
2002) for the Hellenic Centre for Marine
Reasearch (HCMR).

Eirini D. Simou

Peloponnese
Greece
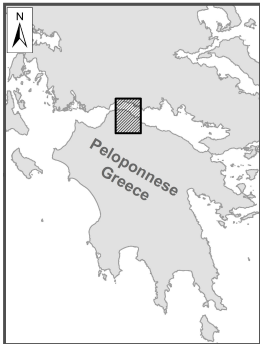
SUBAERIAL & SUBMARINE DRAINAGE MAP
SW Gulf of Corinth
(Scale 1:75,000)

315000 320000 325000

4245000

4245000

Voliniaos River

Psathopyrgos

4240000

Foinikas River

4240000

Selianitika

4235000

4235000

Lakka

4230000

4230000

315000 320000 325000

N

0 0.5 1 2 km

Eirini D. Simou

Legend

- – – – Subaerial & Submarine Drainage
- Land
- Sea
- No data zone

Coordinate System: Greek Grid
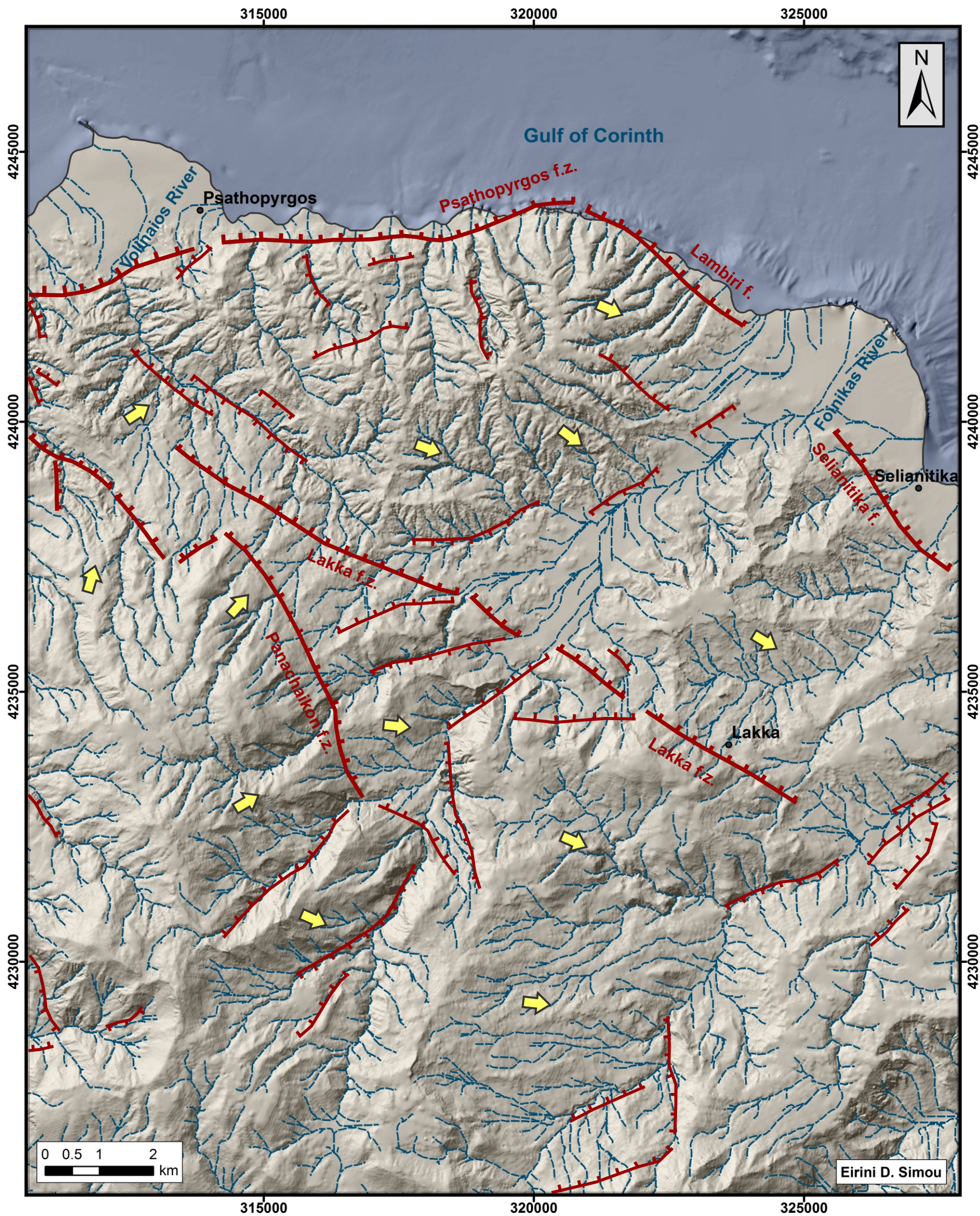Projection: Transverse Mercator
Datum: GGRS 1987

Multibeam Bathymetric Data, primarily
processed by P. Nomikou & M. Alexandri,
were collected by R/V AEGAEO (October
2002) for the Hellenic Centre for Marine
Reasearch (HCMR).

N

Peloponnese
Greece

PLANATION SURFACES DISTRIBUTION MAP
SW Gulf of Corinth
(Scale 1:75,000)

315000   320000   325000

4246000

Gulf of Corinth

Psathopyrgos

Velitsais River

Foinikas River

4239000

Selianitika

4232000

Lakka

0 0.5 1   2
km

Eirini D. Simou

315000   320000   325000

Legend

- - - - - Stream / River

Planation Surfaces

Depositional

Erosional

Coordinate System: Greek Grid
Projection: Transverse Mercator
Datum: GGRS 1987

Multibeam Bathymetric Data, primarily
processed by P. Nomikou & M. Alexandri,
were collected by R/V AEGAEO (October
2002) for the Hellenic Centre for Marine
Reasearch (HCMR).

N

Peloponnese
Greece
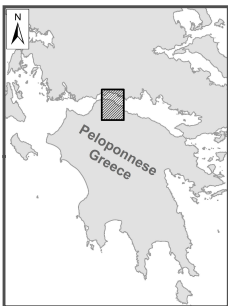
MORPHOTECTONIC MAP

S W   G u l f   o f   C o r i n t h

(Scale 1:75,000)

Gulf of Corinth

Psathopyrgos

Psathopyrgos f.z.

Lambiri f.

Voΐlnaios River

Foΐnikas River

Selianitika f.

Selianitika

Lakka f.z.

Panachaikon f.z.

Lakka

Lakka f.z.

315000 320000 325000

4245000 4240000 4235000 4230000

N

0 0.5 1 2 km

Eirini D. Simou

Legend

▬▬▬ Fault trace determined from the morphotectonic interpretation

- - - - Stream / River

Coordinate System: Greek Grid
Projection: Transverse Mercator
Datum: GGRS 1987

Multibeam Bathymetric Data, primarily processed by P. Nomikou & M. Alexandri, were collected by R/V AEGAEO (October 2002) for the Hellenic Centre for Marine Reasearch (HCMR).

Peloponnese
Greece
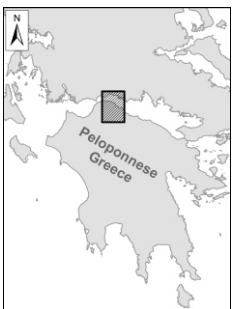
APPENDIX II : CALCULATIONS

Path No	V_{fw} (m)	E_{ld} (m) Elev Left Valley Side	E_{rd} (m) Elev Right Valley Side	E_{sd} (m) Elev valley floor (min)	V_f	Path Profile	Mean V_f
1.1	71	140.475	240.176	87.892	0.693		0.315
1.2	46	330.468	365.081	106.127	0.190		
1.3	23	451.673	462.412	126	0.069		
1.4	77	501.737	480.094	139.995	0.219		
1.5	74	561.212	441.67	179.574	0.230		

Path No	V_{fw} (m)	E_{ld} (m) Elev Left Valley Side	E_{rd} (m) Elev Right Valley Side	E_{sd} (m) Elev valley floor (min)	V_f	Path Profile	Mean V_f
1.6	162	503.381	440.54	193.304	0.581		
1.7	117	529.869	521.377	219.866	0.383		
1.8	93	692.249	480.725	247.776	0.275		
1.9	86	919.763	501.066	272.276	0.196		
2.1	38	189.008	372.468	157.19	0.308		0.321

Path No	V_{fw} (m)	E_{ld} (m) Elev Left Valley Side	E_{rd} (m) Elev Right Valley Side	E_{sd} (m) Elev valley floor (min)	V_f	Path Profile	Mean V_f
2.2	34	365.081	483.59	322.725	0.335		
3.1	29	318.65	259.219	95.267	0.150		0.217
3.2	20	467.463	384.326	238.204	0.107		
3.3	68	481.305	450.308	281.534	0.369		
3.4	13	442.303	461.455	318.795	0.098		

Path No	V_{fw} (m)	E_{ld} (m) Elev Left Valley Side	E_{rd} (m) Elev Right Valley Side	E_{sd} (m) Elev valley floor (min)	V_f	Path Profile	Mean V_f
3.5	23	466.389	405.041	347.692	0.261		
3.6	47	521.371	519.493	372.652	0.318		
4.1	124	334.056	93.738	60.557	0.809		0.328
4.2	31	421.078	362.177	150.137	0.128		
4.3	28	461.973	419.006	243.861	0.142		

Path No	V_fw (m)	E_ld (m) Elev Left Valley Side	E_rd (m) Elev Right Valley Side	E_sd (m) Elev valley floor (min)	V_f	Path Profile	Mean V_f
4.4	40	461.455	421.306	268.878	0.232		
5.1	35	93.738	118.554	37.762	0.512		0.377
5.2	18	362.177	420.621	317.152	0.242		
6.1	23	186.328	202.809	95.847	0.233		0.439
6.2	53	402.995	361.439	309.661	0.730		

Path No	V_fw (m)	E_ld (m) Elev Left Valley Side	E_rd (m) Elev Right Valley Side	E_sd (m) Elev valley floor (min)	V_f	Path Profile	Mean Vf
6.3	36	432.931	501.502	398.311	0.522		
6.4	27	565.613	580.746	473.602	0.271		
7.1	20	202.809	211.463	87.824	0.168		0.200
7.2	30	352.135	351.885	224.501	0.235		
7.3	45	385.375	445.169	272.526	0.315		

Path No	V_fw (m)	E_ld (m) Elev Left Valley Side	E_rd (m) Elev Right Valley Side	E_sd (m) Elev valley floor (min)	V_f	Path Profile	Mean V_f
7.4	21	501.502	507.228	300.994	0.103		
7.5	34	580.862	595.801	395.594	0.176		
8.1	28	211.463	244.082	110.793	0.239		0.187
8.2	21	351.885	364.129	197.066	0.130		
8.3	38	428.574	457.678	268.607	0.218		

Path No	V_{fw} (m)	E_{ld} (m) Elev Left Valley Side	E_{rd} (m) Elev Right Valley Side	E_{sd} (m) Elev valley floor (min)	V_f	Path Profile	Mean V_f
8.4	27	484.48	520.437	332.878	0.159		
9.1	9	244.082	196.302	179.514	0.221		0.243
9.2	20	364.129	354.841	255.884	0.193		
9.3	47	457.678	413.898	308.04	0.368		
9.4	40	522.531	484.671	366.741	0.292		

Path No	V_{fw} (m)	E_{ld} (m) Elev Left Valley Side	E_{rd} (m) Elev Right Valley Side	E_{sd} (m) Elev valley floor (min)	V_f	Path Profile	Mean V_f
9.5	17	579.362	501.039	419.64	0.141		
10.1	36	196.302	135.113	89.829	0.474		0.315
10.2	13	354.841	332.389	259.963	0.155		
11.1	34	184	205	135.113	0.573		0.665
11.2	39	332.389	300.371	264.927	0.758		

Path No	V_fw (m)	E_ld (m) Elev Left Valley Side	E_rd (m) Elev Right Valley Side	E_sd (m) Elev valley floor (min)	V_f	Path Profile	Mean V_f
12.1	28	197.847	222.659	107.921	0.274		0.278
12.2	34	300.371	286.842	172.885	0.282		
13.1	10	221.092	179.657	120.796	0.126		0.273
13.2	23	285.825	294.656	235.555	0.421		
14.1	12	179.657	183.242	121.221	0.199		0.199

Path No	V_fw (m)	E_ld (m) Elev Left Valley Side	E_rd (m) Elev Right Valley Side	E_sd (m) Elev valley floor (min)	V_f	Path Profile	Mean Vf
15.1	69	183.242	184	83.856	0.692		
15.2	47	301.197	285.719	171.23	0.385		0.481
15.3	43	370	397.661	266.436	0.366		
16.1	30	206.53	194.642	114.848	0.350		0.323
16.2	24	338.8	320.9	248.745	0.296		

Path No	V_{fw} (m)	E_{ld} (m) Elev Left Valley Side	E_{rd} (m) Elev Right Valley Side	E_{sd} (m) Elev valley floor (min)	V_f	Path Profile	Mean V_f
17.1	90	194.642	162	104.043	1.212		
17.2	51	281.634	262.367	167.94	0.490		0.795
17.3	71	336.102	280.548	221.444	0.817		
17.4	46	386.579	337.281	292.154	0.659		
18.1	40	175.426	160.861	79.086	0.449		1.106

Path No	V_{fw} (m)	E_{ld} (m) Elev Left Valley Side	E_{rd} (m) Elev Right Valley Side	E_{sd} (m) Elev valley floor (min)	V_f	Path Profile	Mean Vf
18.2	81	242.756	196.019	119.625	0.812		
18.3	54	258.284	222.731	173.51	0.806		
18.4	186	271.408	287.048	232.228	3.957		
18.5	28	371.645	480.563	298.701	0.220		
18.6	49	481.657	544.828	387.392	0.389		

Path No	Vfw (m)	Eld (m) Elev Left Valley Side	Erd (m) Elev Right Valley Side	Esd (m) Elev valley floor (min)	Vf	Path Profile	Mean Vf
19.1	120	224.138	204.117	146.598	1.777		1.777
20.1	64	443.019	204.117	146.598	0.362		0.408
20.2	41	500.845	509.309	385.593	0.343		
20.3	62	544.828	601.593	458.312	0.540		
20.4	28	571.859	640.33	533.708	0.387		

Path No	V_{fw} (m)	E_{ld} (m) Elev Left Valley Side	E_{rd} (m) Elev Right Valley Side	E_{sd} (m) Elev valley floor (min)	V_f	Path Profile	Mean V_f
21.1	716	242.361	407.18	101.013	3.200		
21.2	512	384.527	481.368	123.261	1.653		2.200
21.3	724	601.467	510.22	141.319	1.747		